AN INVESTIGATION OF THE USE OF FEEDBACK CONTROL TO RAISE THE FLUTTER SPEED OF AN AEROELASTIC SYSTEM

Thesis by

Harold S. Braham

In Partial Fulfillment of the Requirements

For the Degree of

Doctor of Philosophy

California Institute of Technology

Pasadena, California

1958

ACKNOWLEDGEMENTS

I wish to express my deepest appreciation to Dr. Gilbert D. McCann and Dr. C. H. Wilts for their help and encouragement during this study.

Dr. McCann suggested the project and was mainly responsible for initiating it and guiding it during its early phases.

Dr. Wilts repeatedly gave valuable suggestions, and was a true inspiration during the entire project.

Also, I would like to thank Miss Ann Graff for her patience with the author in typing this thesis.

ABSTRACT

This study deals with the possibility of raising the flutter speed of an aeroelastic system by feedback control. Emphasis is given to feedback control through a control surface driven by a powered actuator. It is shown that only for certain aeroelastic systems is it possible to significantly raise the flutter speed by this type of feedback control.

In addition, a second type of feedback control is considered, a jet reaction torquer acting on the wing itself. A marked increase in flutter speed is possible in essentially all aeroelastic systems with this form of control. Despite the fact that this type of controller requires more power than the control surface actuator, its use may be practical in many cases.

The question of the reliability of the feedback control used to raise flutter speed is becoming less important in this era of missiles where the entire system is controlled by automatic devices.

Part I discusses the basic problem. Parts II and III develop a general feedback theory. This theory, when applied to a specific aeroelastic system, permits ready determination of whether an increase in flutter speed is possible for that system. Parts IV and V consider numerical investigations of many systems using a control surface actuator. Analyses are made by both the general feedback theory and by analog computer, showing similar numerical results. Part VI considers the jet reaction torquer, and the increase in flutter speed that it can achieve. Conclusions are presented in Part VII.

TABLE OF CONTENTS

PART	TITLE	PAGE
I	BASIC TECHNIQUE OF FEEDBACK THROUGH A CONTROL SURFACE TO PREVENT FLUTTER	1
	1.1 Use of Powered Controls in a Simple Flap Servo or a Complex Autopilot	1
	1.2 Possibility of Using Feedback Control to Prevent Flutter	4
	1.3 Isolation of Rigid Body and Flutter Stabilizer Feedback Loops	5
II	CONDITIONS UNDER WHICH ANY UNSTABLE SYSTEM CAN BE STABILIZED BY FEEDBACK CONTROL	9
	2.1 Sufficiency Conditions for Stabilization of a General Feedback System	11
	2.2 Functional Form of Stabilizing Operator $L_2(s)$	19
	2.3 General Feedback Theory Applied to Servo Systems and Feedback Amplifiers which Invariably Contain Only Non-essential Zeros	25
	2.4 Possibility of Stabilization when Zeros are Essential (Non-minimum Phase)	31
III	COFACTORS OF AEROELASTIC MATRIX THAT DETERMINE WHETHER STABILIZATION IS POSSIBLE	43
	3.1 Three Degree of Freedom System	43
	3.2 Multi Degree of Freedom System	51
	3.3 Feedback Control Using Only β Information	54
	3.4 β Feedback as an Internal Loop in an α Feedback System	56

TABLE OF CONTENTS (Cont'd)

PART	TITLE	PAGE
IV	QUANTITATIVE INVESTIGATION OF THE POSSIBILITY OF STABILIZATION USING FEEDBACK THROUGH THE CONTROL SURFACE ACTUATOR (11 TEST CASES)	61
	4.1 Stability Cofactors of Three Degree of Freedom System	62
	4.2 Trends in Physical Quantities that Influence the Possibility of Stabilization by Feedback Control	87
	4.3 General Properties of the Zeros of $\Delta_{\beta\alpha}$ and $\Delta_{\beta\beta}$	91
	4.4 Investigation of the Stability Cofactors of a Uniform Wing, Approximated by a Three Degree of Freedom System	95
V	DETERMINATION OF THE WIDTH OF THE CONDITIONALLY STABLE BAND BY ROOT LOCUS DIAGRAMS AND BY THE ANALOG COMPUTER	106
	5.1 Use of Root Locus Diagrams to Determine the Band of Conditional Stability	107
	5.2 Analog Computer Determination of the Width of the Conditionally Stable Band	119
VI	ADDITIONAL TECHNIQUES OF STABILIZATION BY FEEDBACK CONTROL	122
	6.1 Stabilization by Jet Reaction Torquer	122
	6.2 Numerical Investigation of Stabilization by a Jet Reaction Torque on α	124
	6.3 Instrumentation Feasibility of a Jet Reaction Torquer	126
	6.4 Differences in the Two Types of Feedback Stabilization from a Physical Standpoint	127

TABLE OF CONTENTS (Cont'd)

PART	TITLE	PAGE
VII	CONCLUSIONS AND RECOMMENDATIONS FOR FURTHER STUDY	132
	7.1 Conclusions	132
	7.2 Recommendations for Further Study	134
REFERENCES		136
APPENDIX A.	DEMONSTRATION THAT THE CLOSED LOOP TRANSFER FUNCTION OF A FEEDBACK SYSTEM WITH MINIMUM PHASE BASIC ELEMENTS CONTAINS ONLY LEFT HALF PLANE ZEROS	137
APPENDIX B.	SERVO TORQUE IN h, α, β COORDINATE SYSTEM	143
APPENDIX C.	REPRESENTATION OF $\Delta_{\beta h}$, $\Delta_{\beta\alpha}$, $\Delta_{\beta\beta}$ OF A THREE DEGREE OF FREEDOM SYSTEM BY FIFTH DEGREE POLYNOMIAL IN S	146
APPENDIX D.	INVESTIGATION OF THE POLES OF Δ, $\Delta_{\beta\alpha}$, $\Delta_{\beta\beta}$, and $\Delta_{\alpha\alpha}$, AND THE ZEROS AT INFINITY	157
APPENDIX E.	TECHNIQUES OF REDUCING THE LAG IN G(s)	159

LIST OF SYMBOLS

a = location of e.a. aft of midchord, per unit of half chord

$[A]$ = aeroelastic force matrix $\equiv [A]_1 + [A]_2$

$[A]_1$ = structural force matrix

$[A]_2$ = aerodynamic force matrix

b = semi chord of wing plus control surface

b_c = semi chord of control surface

$B's$ = constants of three degree of freedom system defined in equation C.15

c = location of hinge aft of mid chord, per unit of half chord

c' = output of general feedback system

$C's$ = constants of three degree of freedom system defined in equation C.14

C_α = torsional spring constant of wing

C_β = torsional spring constant between wing and aileron

C_h = bending spring constant of wing at e.a.

$C(k)$ = Theodorsen function

D = aerodynamic quantity defined as $2\pi b\rho V^2 \ell$

e.a. = abbreviation for elastic axis

$[F]$ = external force vector

$G(s)$ = hydraulic servo transfer function, or torque per unit command

h = displacement of elastic axis, positive up

$H_h(s)$ = feedback stabilizer operator on h signal

$H_\alpha(s)$ = feedback stabilizer operator on α signal

$H_\beta(s)$ = feedback stabilizer operator on β signal

$H'(s)$ = modified feedback stabilizer defined in equations 3.13 and 5.2

I_α = moment of inertia of wing plus control surface about the e.a.

LIST OF SYMBOLS (Cont'd)

I_β = moment of inertia of control surface about the hinge

I_c = $I_\beta + (c-a)b\, S_\beta$

k = reduced frequency = $\frac{b\omega}{V}$

k_1 = constant factor in $L_1(s)$

k_2 = constant factor in $L_2(s)$

k_2' = constant factor in $L_2(s)$, for special case $L_2(s)$ is a derivative operator

k_1k_2 = constant factor in the loop gain of aeroelastic-servo system

k_d = dimensionless time constant = $\frac{b\omega_a}{V_d}$

K_1 = minimum stable value of k_1k_2 with feedback control

K_2 = maximum stable value of k_1k_2 with feedback control

K_5 = structural constant $\equiv 2b\,(x_r - \frac{1}{4})$

ℓ = length of the wing

L' = aerodynamic lift at e. a.

$L_1(s)$ = transfer function of general system to be stabilized

$L_2(s)$ = transfer function of general stabilizer

L = excess of poles over zeros in $L_1(s)$

m = mass of control surface

m' = mass per unit length of control surface

M = mass of wing plus control surface

M' = mass per unit length of wing plus control surface

n = $\frac{V_2 - V_1}{V_2}$

P_j = finite s plane poles of the loop gain

q' = $\frac{1}{2}\rho V^2 \ell$ = dynamic pressure times length

Q_a = aerodynamic moment on a about e. a.

Q_β = aerodynamic moment on β about hinge.

LIST OF SYMBOLS (Cont'd)

r = input to general feedback system

r_a = radius of gyration of wing plus control surface about e.a. $= \sqrt{\frac{I_a}{M}}$

r_β = radius of gyration of control surface about hinge $= \sqrt{\frac{I_\beta}{m}}$

R = excess of poles over zeros in $L_2(s)$

$R+L$ = excess of poles over zeros in $L_1(s)\ L_2(s)$

s = Laplace transform variable

$\bar{s}$ = dimensionless Laplace transform variable $\equiv \frac{s}{\omega_a}$

s_o = reference frequency $\equiv \frac{V}{2b}$

S_a = mass moment of wing plus control surface about the e.a.

S_a' = mass moment of wing plus control surface about the e.a. per unit length

S_β = mass moment of control surface about the hinge

t = time

T_1, T_3 = dimensionless time constants of Theodorsen function approximation which is a ratio of first degree polynomials

T_β = torque produced by control surface actuator

T_a = jet reaction torque on a

$U's$ = aerodynamic constants

V = velocity of air stream

V_o = maximum speed for which all zeros and poles of aeroelastic transfer function are in the left half s plane

V_1 = minimum speed for which both zeros and poles of aeroelastic transfer function are in the right half s plane

V_2 = minimum speed for which the conditionally stable zone of $k_1 k_2$ values is zero in width

V_d = divergence speed of the wing

$\bar{v}$ = dimensionless speed $\equiv \frac{V}{V_d}$

LIST OF SYMBOLS (Cont'd)

$[W]$ = matrix transforming h, α, β coordinates to h, α, γ

$[X]$ = displacement vector

x_α = location of c.g. of wing plus control surface, aft of e.a. $\equiv S_\alpha/M$

x_β = location of c.g. of control surface aft of hinge $\equiv S_\beta/m$

x_r = location of e.a. aft of leading edge per unit of <u>full</u> chord

Δx = cell length in finite difference approximation of wing

$[y]$ = displacement vector

Z_i = finite s plane zeros of the loop gain

$Z(s)$ = modified stabilizing cofactor using all three feedbacks defined in equation (3.6)

α = angle of rotation of wing positive nose upward

$\bar{\alpha}$ = angle of attack defined in equation C.5

α' = ratio of lead to lag time constant in servo lead network

β = relative angle of control surface positive nose upward = $\gamma - \alpha$

γ = absolute angle of control surface positive nose upward

δ = very small term representing the difference between a zero and pole located close together

Δ = determinant of aeroelastic matrix

Δ_{ij} = cofactor of i and j element in aeroelastic matrix

ε = input signal to powered actuator

ζ = damping factor of a root; equal to the ratio of the negative real part to the magnitude of the root

θ = bending angle of wing positive outboard upward

K = air to mass ratio = $\frac{\pi \rho b^2}{M/\ell}$

ρ = density of air

LIST OF SYMBOLS (Cont'd)

τ = time constant of servo lead network

ϕ_n = phase angle of infinite radius zeros which satisfy the condition of equation 2.6

ω = angular frequency, radians per sec.

ω_a = torsional frequency, $\sqrt{C_a/I_a}$

ω_h = bending frequency, $\sqrt{C_h/M}$

ω_β = frequency of aileron, $\sqrt{C_\beta/I_\beta}$

PART I

BASIC TECHNIQUE OF FEEDBACK THROUGH A CONTROL SURFACE TO PREVENT FLUTTER

1.1 Use of Powered Controls in a Simple Flap Servo or a Complex Autopilot

The use of a powered actuator to drive the control surface of an airplane or missile is now standard practice. A rudimentary physical picture of the essential features common to all such systems is shown in figure 1.1a. The associated block diagram considering the elastic properties of the wing is given in figure 1.1b. The coordinates h, α, and β are the vertical displacement, angle of rotation and relative aileron angle at a specific location along the wing.

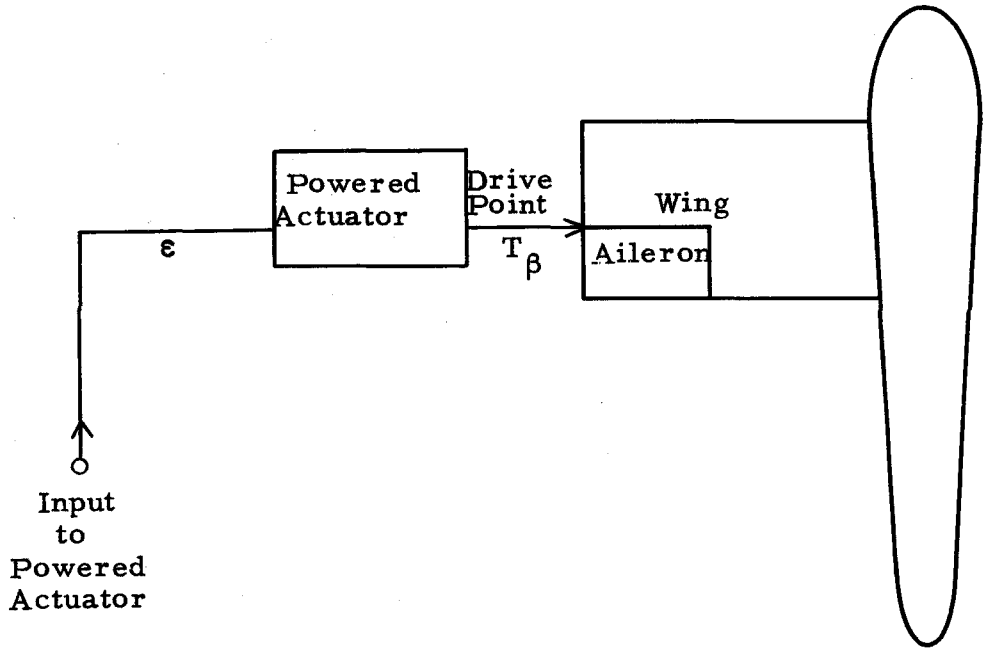

Plan View of Control Surface Driven by Powered Actuator

Figure 1.1a

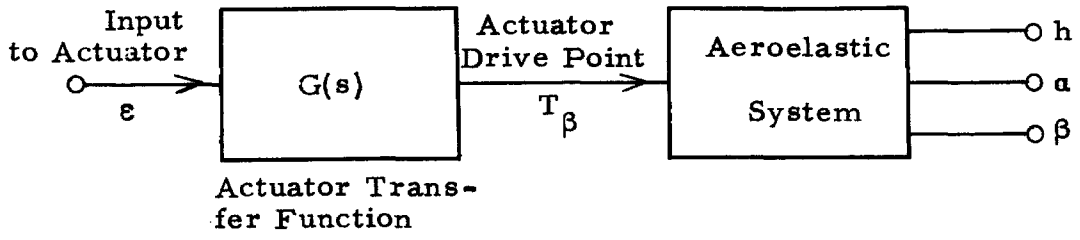

Block Diagram of System of Figure 1.1a

Figure 1.1b

The primary feature distinguishing the most complex of these systems from the simplest is the degree of information about aircraft motion fed back to the powered actuator input*. For example, a simple control may be used, in which the only data fed back to the actuator is the relative angle β of the control surface. This scheme is shown in figure 1.2.

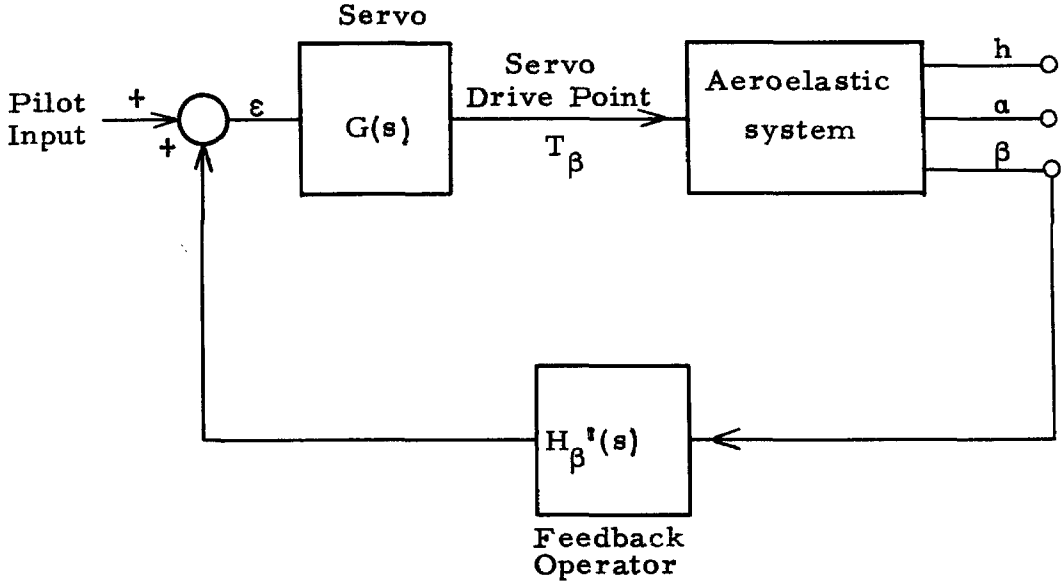

Simple Flap Servo Control

Figure 1.2

---

*In all cases, some primary input exists such as a command from the pilot, which the output ideally will follow.

On the other hand, a complete autopilot may be used. This usually feeds back quantities dependent on both α and h in addition to β, as shown in figure 1.3.

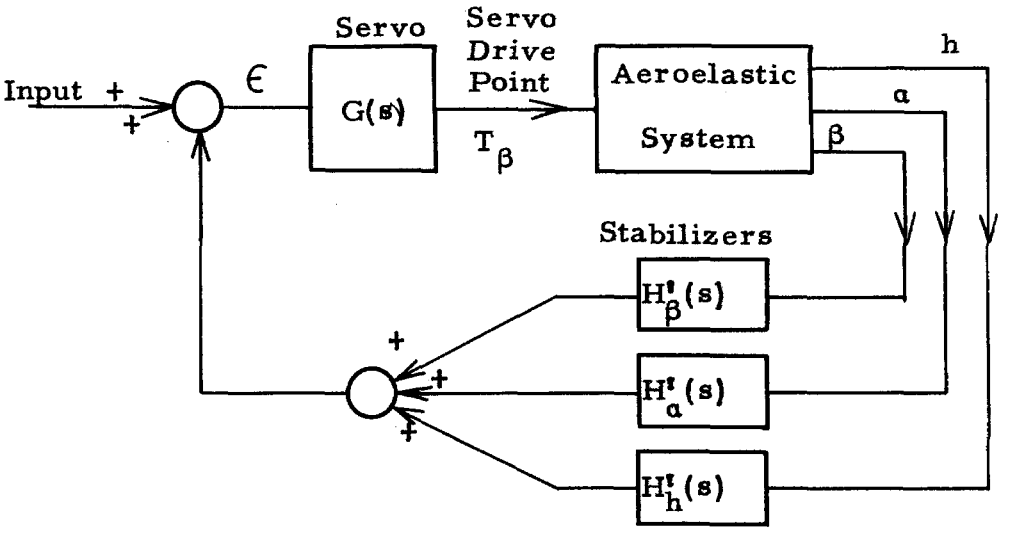

General Autopilot Control

Figure 1.3

For example, a typical use of an autopilot is the control of the vertical acceleration, $\ddot{h}$, of the aircraft. Thus $H^{\prime}_{h}(s)$ serves as the primary feedback. In addition the turning rate of the aircraft may be used for damping, requiring $H^{\prime}_{\alpha}(s)$ feedback. Also a flap servo control of the aileron is usually used as an internal loop, requiring $H^{\prime}_{\beta}(s)$ feedback. Thus all three feedbacks of figure 1.3 are used in a typical autopilot.

In the normal study of the autopilot loop of figure 1.3, one considers the aeroelastic system as a rigid body. This assumes infinite vibration frequencies for the structure. In most cases this is a valid approximation, since the structural modes of vibration of the wing are usually far above the required pass band of autopilot

frequencies. Typically, the lowest structural mode for a wing is somewhere between five and fifty cps depending on its size. This corresponds to about 30 to 300 radians/second. The response time of an autopilot is normally about one second, corresponding to a cutoff frequency of one radian/second. Thus the lowest vibration frequency of the structure is a factor of 30 to 300 above the autopilot pass band, thereby permitting the rigid body approximation.

1.2 Possibility of Using Feedback Control to Prevent Flutter

As just stated, the frequency pass band of the autopilot is usually well below the lowest structural mode frequency. Suppose, instead, one were to purposely extend the autopilot pass band above the first few structural mode frequencies. In particular, suppose the frequency response of the servo transfer function G(s), and the feedback operators $H_\beta^t(s)$, $H_a^t(s)$, $H_h^t(s)$ in figure 1.3 were maintained essentially constant throughout the range of these lowest structural modes. In that case, the autopilot loop would interact with the aeroelastic system and add an additional force to the aeroelastic* forces normally treated in flutter. This would cause the flutter speed to change from that of the aeroelastic system alone, increasing in some cases, while decreasing in others.

The purpose of this report is to synthesize appropriate $H_\beta^t(s)$, $H_a^t(s)$ and $H_h^t(s)$ operators for a fixed and specified servo and aeroelastic system, in order that the coupled aeroelastic

---

*These are the elastic and inertia forces of the structure and the aerodynamic forces.

servo system of figure 1.3 have a higher flutter speed than the aeroelastic system by itself. This represents a synthesis of the much discussed but little investigated possibility of raising the flutter speed of an aeroelastic system by feedback control.

The previous paragraphs tacitly assumed that it was feasible to maintain the frequency response of the servo operator, G(s), and the feedback and measurement operators, H(s), into the aeroelastic frequency band. This can certainly be accomplished even in the present state of the art. Hydraulic servos, the type invariably used, commonly have frequency responses flat up to 30 to 50 cps. In addition, the H(s) operator can consist partly of a lead network to compensate for lags in G(s), thereby in effect increasing the cutoff frequency of G(s). Similar compensation can be produced by H(s) on the transfer function of the measurement devices (gyros, accelerometers, etc). Thus it is certainly feasible to provide a frequency response for the G(s) and H(s) operators into the aeroelastic band*.

1.3 Isolation of Rigid Body and Flutter Stabilizer Feedback Loops

The last section indicated the main purpose of this study - to determine what functional form $H_\beta^t(s)$, $H_a^t(s)$ and $H_h^t(s)$ should take in order to raise the flutter speed. However in part 1.1 it was shown that the original purpose of these operators was the rigid body control of the airplane. The question naturally arises: is the functional form of these operators, determined from flutter

---

*Other techniques of raising the pass band of these operators are described in Appendix E.

prevention considerations, compatible with a satisfactory rigid body airplane control? For example, the flutter prevention considerations may dictate that $H'_\beta(s)$ be small. At the same time it may be true that the rigid body airplane control requires a large $H'_\beta(s)$ for tight aileron control. Hence the two objectives may require incompatible operators for $H'_\beta(s)$. This means each design of $H'_\beta(s)$, $H'_a(s)$ and $H'_h(s)$ that results from the flutter prevention synthesis must be checked against rigid body motion requirements, with no guarantee of compatibility. This certainly is an undesirable procedure.

A great simplification can be made, which essentially permits an isolation of the rigid body and flutter prevention realms of operation. Again this is predicated mainly on the wide frequency separation usually existing between the structural modes and the autopilot pass band actually needed for rigid body control. To accomplish this isolation, a separate set of stabilizers for flutter prevention $H_\beta(s)$, $H_a(s)$ and $H_h(s)$ is added in parallel with the rigid body stabilizers $H'_\beta(s)$, $H'_a(s)$ and $H'_h(s)$ of figure 1.3. To isolate the two feedbacks, a high pass filter is placed in cascade with the flutter prevention operators, while a low pass filter is placed in cascade with the normal autopilot operators. This scheme is shown in figure 1.4, where for simplicity only one $H'(s)$ operator is shown for the autopilot loop, and one $H(s)$ operator for the flutter prevention loop. The cutoff frequency of both the high pass and low pass filters should be located at the geometric mean of the needed autopilot pass band frequency and

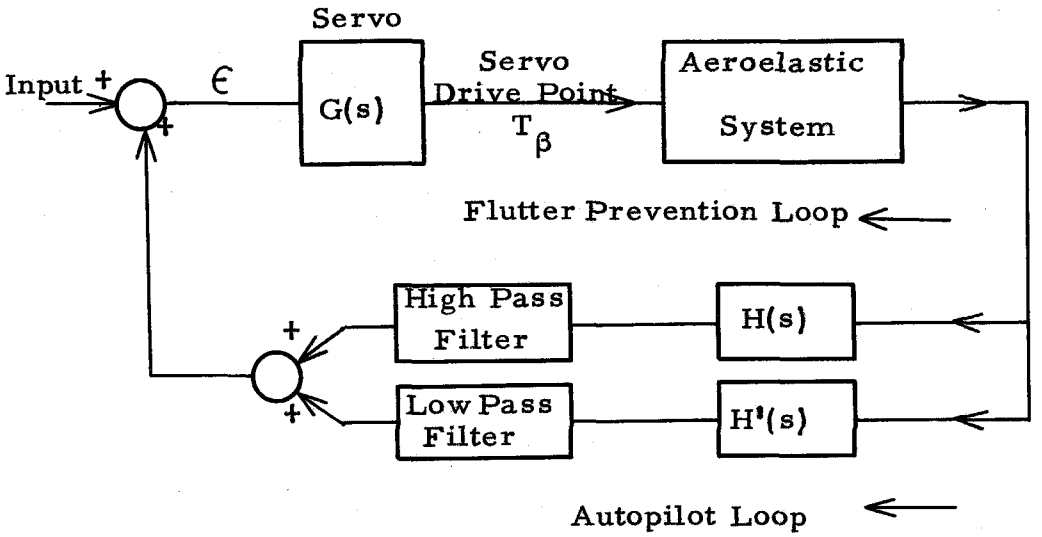

Flutter Prevention and Autopilot Loops Isolated by Filters

Figure 1.4

the aeroelastic structural mode frequency. The wide separation of these two frequencies permits almost complete elimination of that loop which is undesired at each frequency range of interest.

This isolation technique permits the analysis of each loop individually, while the second loop is completely ignored. For flutter prevention analysis, only that loop through the high pass filter need be examined. Furthermore one can neglect the high pass filter in analysis of the high pass loop, since it has essentially unity gain at the flutter frequencies. Thus the flutter prevention synthesis to be carried out in the remainder of this report reduces to an investigation of the block diagram of figure 1.5. The servo and aeroelastic transfer functions are considered fixed, but $H_\beta(s)$, $H_a(s)$ and $H_h(s)$ can be adjusted arbitrarily to achieve better flutter stability. No check on rigid body motion compatibility is necessary for any $H_\beta(s)$, $H_a(s)$ and $H_h(s)$ operators that arise from the synthesis.

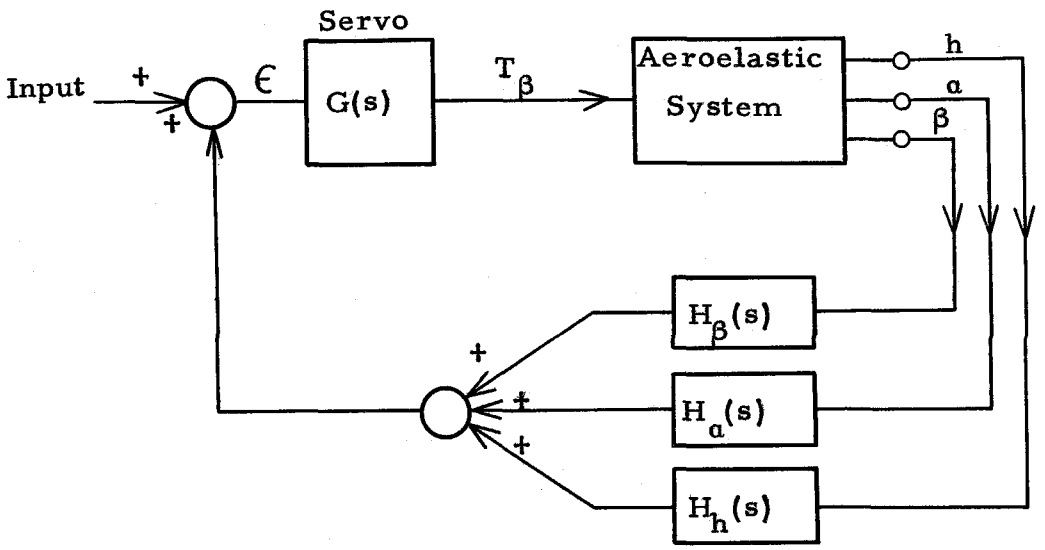

Flutter Prevention System Block Diagram

Figure 1.5

The preceding assumption of wide frequency separation of the needed autopilot pass band and the structural modes is not basic to the techniques to be developed in the remaining parts of this study. If the assumption is valid in a specific application, as it usually will be, then the two isolated loops of figure 1.4 can be used, and no check on compatibility of the flutter prevention loop on the autopilot loop is necessary. If, in special cases, the assumption is not valid and the frequency bands overlap, then only one loop such as figure 1.5 can be used. After determination of the H(s) operator necessary for flutter prevention, one must check the compatibility of this operator on the rigid body motion.

PART II

CONDITIONS UNDER WHICH ANY UNSTABLE SYSTEM CAN BE STABILIZED BY FEEDBACK CONTROL

A study of feedback around an aeroelastic system at speeds for which the aeroelastic system itself is unstable is now presented. The first step in this investigation is an answer to the following fundamental question. What conditions must a fixed and specified aeroelastic system satisfy in order to ensure the existence of some linear stabilizing operator which is capable of raising the flutter speed? The wording of the preceding question hints at the rather unusual situation existing for feedback control systems wherein the basic or fixed portion of the system is an aeroelastic system. Some, but not all, aeroelastic systems can be stabilized above the flutter speed by feedback control. In this part, the following phases of the problem are considered.

a) The conditions the aeroelastic system must satisfy to permit stabilization by feedback control at a given speed.

b) Determination of the functional form of a stabilizing operator which can achieve this stabilization.

The first phase, the conditions under which an unstable system can be stabilized by feedback control, is actually a fundamental question of general feedback theory. It is of interest not only in the present case where the fixed portion of the system is aeroelastic, but for systems where the fixed portion is mechanical, electrical, acoustical, etc. Unfortunately no theory has yet been developed to answer this question. The reason

for dearth of even an effort along these lines prior to this aeroelastic study is simple enough. It was not needed. As will be shown later, virtually all known feedback systems other than the aeroelastic ones fall into a rather restricted category, such that some feedback control operator always exists capable of stabilizing the basic system. For such systems the question of the existence of a stabilizing operator is trivial.

In this part a general feedback theory is developed, which is applicable to all feedback systems. The application of this theory to a particular aeroelastic system provides a ready answer to the question: can the aeroelastic system be stabilized by feedback control? Only in certain cases is the answer affirmative. The outgrowth of this general feedback theory is a mathematically rigorous, yet simple-to-apply, sufficiency condition. If this condition is satisfied by a fixed and specified but unstable system, then the existence of a stabilizing operator capable of stabilizing the composite system is assured. It is then shown by heuristic argument that for the special system of interest in this study, an aeroelastic system, the necessary condition for existence of a stabilizing feedback operator is, for all practical purposes, the same as this sufficiency condition. Hence a simple criterion is available for determination of whether stabilization of the aeroelastic system is possible. The determination of the functional form of the stabilizer follows as a natural consequence of the theory.

As might be expected the terminology of this general feedback theory is filled with concepts and techniques used by servo and feedback engineers. Free use is made of concepts such as

transfer functions, zeros and poles, root locus diagrams, etc. - concepts familiar to the feedback engineer. A person not well versed in feedback control theory should refer to a standard servo text such as reference 1.

2.1 Sufficiency Conditions for Stabilization of a General Feedback System

Consider a fixed specified system of transfer function $L_1(s)$ in figure 2.1, describing the relation between two arbitrary coordinates, r and c'.

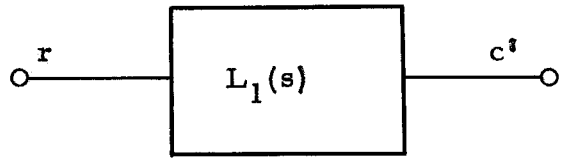

Transfer Function Between Arbitrary Coordinates of Basic System

Figure 2.1

If an aeroelastic system is under investigation, the input r may represent a torque T_β, and the output c' may represent the coordinate β of figure 1.2. $L_1(s)$* is completely described by the location of its zeros Z_i and poles P_j and by a gain factor k_1, as follows:

$$L_1(s) = k_1 \frac{\prod_{i=1}^{M-L} (s - Z_i)}{\prod_{j=1}^{M} (s - P_j)} \qquad (2.1)$$

---

*s represents the Laplace transform variable.

It is evident that the P_j represent the characteristic roots of the system, since the inverse Laplace transform $c'(t)$ contains terms of the form $e^{P_j t}$.

By assumption $L_1(s)$ of figure 2.1 describes an unstable system. Hence $L_2(s)$ is added as a possible stabilizing device, as shown in figure 2.2.

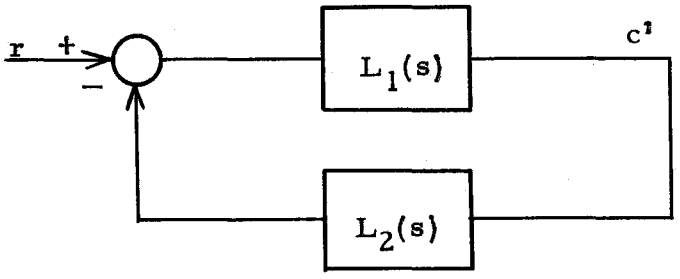

Stabilizing Device Added to Basic System

Figure 2.2

It is desired to find a functional form of $L_2(s)$, if one exists, which will make the characteristic roots of the composite system more stable than those of the original system. $L_2(s)$ can be written in a form similar to equation 2.1.

$$L_2(s) = k_2 \frac{\prod_{i=M+1-L}^{N-(R+L)} (s - Z_i)}{\prod_{j=M+1}^{N} (s - P_j)} \qquad (2.2)$$

Equation 2.1 explicitly indicates that the denominator of $L_1(s)$, of degree M, exceeds the numerator in degree by L. In similar fashion, equation 2.2 shows that the denominator of $L_2(s)$,

of degree N-M, exceeds the numerator by degree R. No restriction is made that either the poles or zeros of $L_1(s)$ lie in the left half of the s plane. Thus its poles P_j may be in the right half plane representing an unstable system. Also its zeros, Z_i, may likewise be in the right half plane. A special name is given to Z_i values in the right half plane in electrical engineering applications because of the significance of zeros of this type. They are called non-minimum phase zeros and are also of great significance in the present study. $L_2(s)$, of course, is to be chosen at the will of the designer to affect optimum stability.

In the remainder of this study, significance is attached to the half of the s plane in which the zeros and poles are located. Hence the following abbreviations will be used for left half plane and right half plane quantities - L.H.P., and R.H.P.

The characteristic equation of the system of figure 2.2 is found by the usual equation of feedback theory using equations 2.1 and 2.2.

$$1 - \text{Loop Gain} = 0 \tag{2.3}$$

or more specifically,

$$1 + L_1 L_2 = 0 \tag{2.4}$$

yielding,

$$1 + k_1 k_2 \frac{\prod_{i=1}^{N-(R+L)} (s - Z_i)}{\prod_{j=1}^{N} (s - P_j)} = 0 \tag{2.5}$$

The roots of equation 2.5 are the characteristic roots of the system with feedback. The constant k_1 is a fixed property of $L_1(s)$, but k_2 is a constant which can be varied to achieve stability. This constant k_2 (and hence the constant factor k_1k_2 of the loop gain) can be adjusted from zero to a large value for this purpose.

A clear graphical portrayal of how the characteristic roots vary as k_2 changes is furnished by root locus diagrams. The locations of the zeros and poles of the loop gain are important, since these are terminals of each root locus for the extreme values of ∞ and 0 for k_2. It is obvious from equation 2.5 that Z_i and P_j are the zeros and the poles of the loop gain in the finite portion of the s plane. In addition a zero of degree (R+L) exists at infinity, since the degree of the denominator of the loop gain exceeds the degree of the numerator by (R+L) in equation 2.5. More precisely one means that for values of s outside a circle of arbitrarily large radius in the s plane, the value of the loop gain becomes arbitrarily small, varying as $\frac{1}{s^{R+L}}$. The values of s approaching this circle are said to be zeros of the loop gain. Only those values of s approaching this circle in a specified direction may satisfy equation 2.5, and hence be terminal regions of a root locus. These (R+L) directions of approach or phase angle are given in equation 2.6.

$$\phi_n = \frac{\pi(1+2n)}{R+L} \quad \text{for } n = 0,\ 1,\ 2 \text{ --- } (R+L-1) \qquad (2.6)$$

These are of great importance in the remainder of the study and are referred to constantly. For brevity purposes, the following important shortened notation is adopted. Values of s which approach the arbitrarily large circle along these (R+L) directions of

equation 2.6, are referred to simply as the zeros at infinity of the loop gain. Figure 2.3 depicts the location of these (R+L) zeros at infinity for various values of (R+L)*.

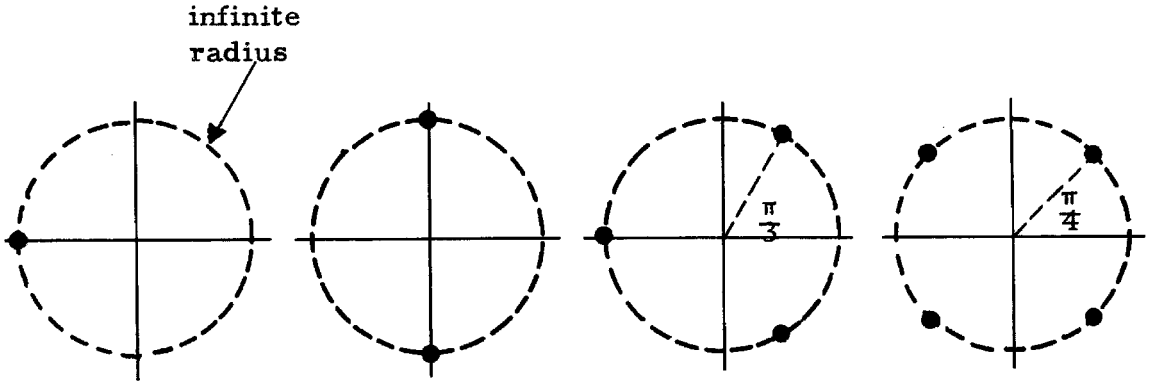

Zeros at Infinity in s Plane for Values of(R+L)
from 1 to 4
Figure 2.3

Note in figure 2.3 that no R.H.P. zeros exist at infinite radius for (R+L) < 2, but that some R.H.P. zeros exist for (R+L) > 2. A marginal condition exists for (R+L) = 2.

As a final preliminary it is convenient to define the terms

a) A non-essential zero (or pole) of $L_1(s)$.

b) An essential zero (or pole) of $L_1(s)$.

A non-essential zero (or pole) of $L_1(s)$ is defined as one that can be

---

*For physical systems (R+L) must be greater than zero, since a physical system must have zero "gain" at infinite frequency.

virtually removed from the loop gain by insertion of a suitable operator for $L_2(s)$ in equation 2.2. An essential zero or pole of $L_1(s)$ is one that cannot be so removed. An important conclusion to be proven next is that the zeros at infinity of $L_1(s)$, and the zeros and poles in the finite left half s plane are non-essential zeros or poles, while those in the finite right half s plane are essential.

To prove that the zeros of $L_1(s)$ at infinity are non-essential, one notes that R, the excess of poles over zeros of $L_2(s)$ is an adjustable number since $L_2(s)$ is adjustable. Hence (R+L), the number of zeros of the loop gain at infinity, is adjustable. (R+L) becomes smaller than L, the number of zeros at infinity in $L_1(s)$, if R assumes a negative value. The meaning of a negative value of R is simply that $L_2(s)$ has an excess of zeros over poles. In particular if

$$R = - \left| R \right| \tag{2.7}$$

then the number of zeros at infinity in the loop gain is reduced by $\left| R \right|$ from the number in $L_1(s)$. Furthermore, if R is given the following specific value,

$$R = - \left| L - 1 \right| \tag{2.8}$$

then the number of zeros at infinity in the loop gain is only 1, which becomes a L.H.P. zero at π radians, from figure 2.3*.

The proof that left half finite s plane zeros or poles of $L_1(s)$ are non-essential unlike those in the right half finite s plane is now demonstrated. Suppose $L_1(s)$ has a zero Z_i, manifested by a factor

---

*An answer will presently be given to the objection raised by the astute observer, who realizes that an excess of zeros over poles in $L_2(s)$ is physically unrealizable.

in $L_1(s)$:

$$(s - Z_i)$$

The only way that the zero Z_i can be removed from the loop gain is for $L_2(s)$ to be designed to contain an approximately cancelling factor,

$$\frac{1}{s - (Z_i+\delta)}$$

where δ is made as small as possible.

The sole difference between the actual loop gain and the ideal one for which there is perfect cancellation of Z_i, is that the actual loop gain has the additional ratio of factors

$$\frac{(s - Z_i)}{s - (Z_i+\delta)}$$

This produces an additional pole and zero of the loop gain very close to one another around Z_i. The combination gives rise to an additional root in the closed loop system of figure 2.2. For very small δ, as assumed, the value of this root is essentially Z_i for <u>any</u> value of k_1k_2, the loop gain constant. The time response term corresponding to this root is found by the usual inverse Laplace transform, and is proportional to

$$\delta\, e^{Z_i t}$$

At time t equal to zero, this term is proportional to δ, and hence has a very small value. For the case of Z_i in the left half finite s plane, the term becomes even smaller with time. Since this term is negligibly small over all time, the time response is virtually the same as the system with theoretically perfect cancellation,

and the zero Z_i may be said to be virtually removed. However if Z_i is in the right half finite s plane, the term grows with time and eventually becomes infinite even for a very small value of δ. Hence no cancellation of this type is possible for Z_i in the right half plane.

A similar argument holds if a pole of $L_1(s)$ instead of a zero were the factor under consideration. Thus the original premise is proved that left half finite s plane zeros and poles are non-essential, and right half finite s plane zeros and poles are essential.

The significant property of non-essential zeros of $L_1(s)$ is that all lie in the left half plane originally* or can be made to do so by the proper $L_2(s)$ operator**. The importance of having all zeros of the loop gain located in the left half s plane will soon be illustrated.

The sufficiency condition on $L_1(s)$ to ensure stabilization capability can now be stated and then proved.

Theorem 1

A sufficient condition on a specified unstable system, $L_1(s)$, to ensure existence of an $L_2(s)$ operator which can cause stability is that only non-essential zeros exist in $L_1(s)$. This means the finite zeros of $L_1(s)$ are in the left half s plane.

The proof of theorem 1 follows immediately from a consideration of the root loci of any system of the type of figure 2. 2.

---

*The finite magnitude ones.
**The ones at infinity.

For zero value of the constant factor of the loop gain, k_1k_2, the characteristic roots exist at the poles of the loop gain. At least one of these is unstable by definition, since these are the same roots as the system without feedback. As k_1k_2 is made very large, the roots approach arbitrarily close to the zeros of the loop gain. If all these zeros are in the left half s plane, then all roots are stable for large enough values of k_1k_2. Now if $L_1(s)$ has only non-essential zeros, an $L_2(s)$ operator must exist which can place all the zeros of the loop gain in the left half s plane as shown above. Thus if $L_1(s)$ has only non-essential zeros a stabilizing operator can always be found.

2.2 Functional Form of Stabilizing Operator $L_2(s)$

One form of $L_2(s)$ to achieve the stabilization is now described. It is somewhat ideal in form, but simple for illustration purposes. Given an $L_1(s)$ of the form of equation 2.1 where the zeros at infinity of $L_1(s)$ are L in number, one chooses the simplest form of $L_2(s)$ satisfying equation 2.8: a polynomial in s of degree (L - 1). Thus in equation 2.2, $L_2(s)$ takes the specific form:

$$L_2(s) = k_2 \prod_{i = M+1-L}^{M-1} (s - Z_i) \qquad (2.9)$$

For this condition, R + L = 1. Hence only one zero of the loop gain exists at infinity, this in the left half plane at π radians. Stated simply, $L_2(s)$ is made a polynomial in s of degree one less than the excess of poles over zeros in $L_1(s)$. Hence in the loop gain, the excess of poles over zeros is one.

The exact location of the Z_i values in equation 2.9 is not critical just so long as these lie in the left half plane. For k_2 designed adequately large so as to make k_1k_2 very large, the characteristic roots become essentially the zeros of $L_1(s)$ in the finite s plane, the zeros of $L_2(s)$ in equation 2.9, and the one of infinite magnitude at π radians. By assumption, all these are in the left half plane so that the system is stable.

The essential operation of the stabilizer in this example was to transform the finite plane characteristic roots of the system from the poles of $L_1(s)$ to the zeros of $L_1(s)$*. The stabilizer can be thought of as a device which can place the roots at either the zeros or poles of $L_1(s)$ wherever greater stability results. For the problem at hand at least one pole of $L_1(s)$ always is R.H.P. Hence the only possibility of stable operation is operation close to the zeros of $L_1(s)$, should they all be L.H.P. Thus the key factor in determining if stabilization is possible is the location of the finite s plane zeros of $L_1(s)$. If these are in the left half plane, stabilization is always possible.

A simple example is now presented where $L_1(s)$ contains three poles and no zeros, one pair of complex conjugate poles being in the R.H.P. According to the above theory, $L_2(s)$ should be designed as a second order polynomial in s, containing two zeros in the left half plane. The zeros and poles of $L_1(s)$ and $L_2(s)$ and the root loci of the composite system are shown in figure 2.4.

---

*Plus the zeros of $L_2(s)$ which are always designed to be L.H.P.

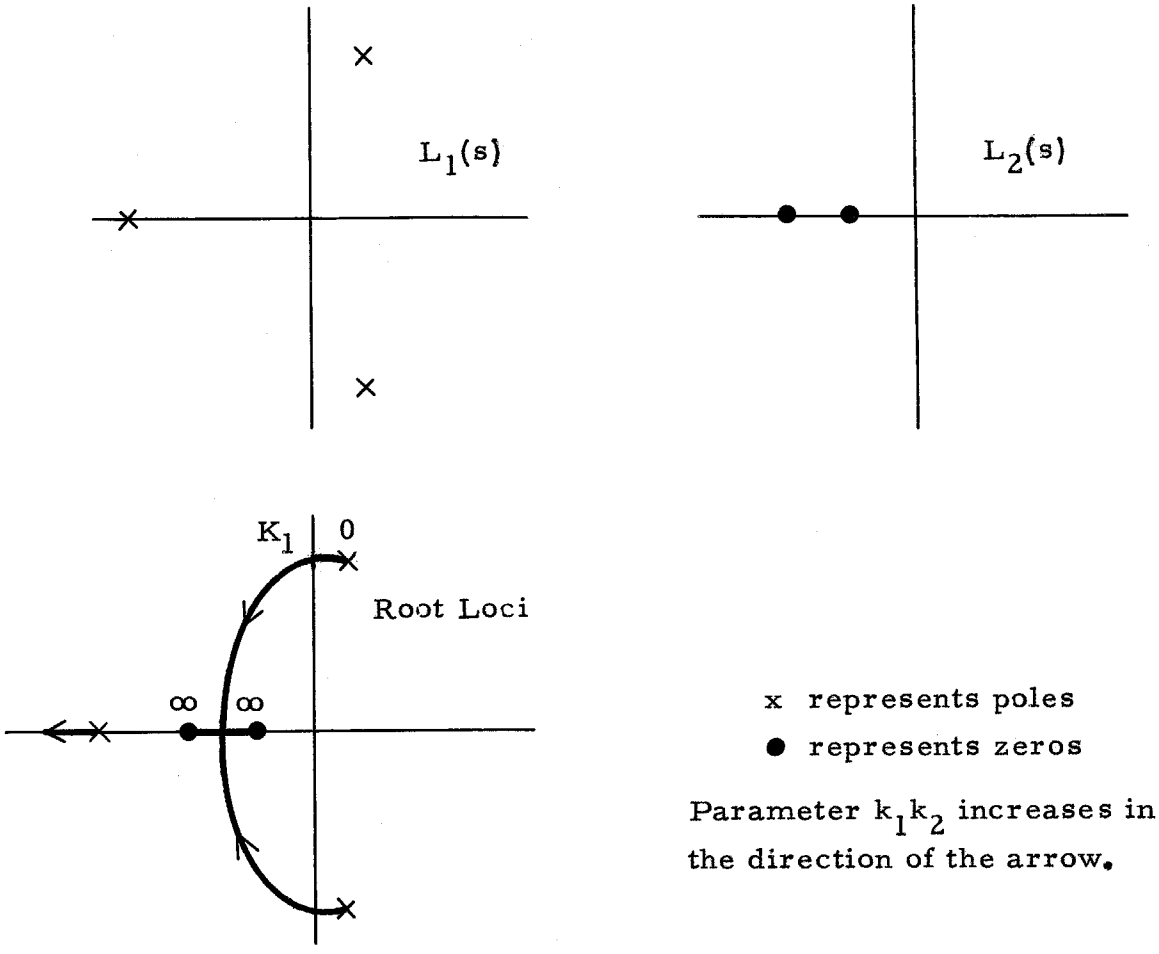

Zeros and Poles of a Typical $L_1(s)$ and $L_2(s)$, and Root Loci of Composite System

Figure 2.4

Any value of k_1k_2 between K_1 and infinity makes the composite system stable. Thus a range of values of k_1k_2 above some minimum exists capable of achieving stability. It is now evident that a limiting case of the use of the stabilizer was considered in the general discussion on page 20. There the roots approached the zeros of the loop gain for the specific value $k_1k_2 \rightarrow \infty$. Root locus diagrams

such as figure 2.4 show the general result that k_1k_2 need only exceed a certain critical value for stability.

As indicated previously, the functional form of the $L_2(s)$ stabilizer given by equation 2.9 is somewhat idealized. In practice the degree of the denominator of $L_2(s)$ must be equal to the degree of the numerator. Otherwise the stabilizer would have infinite gain at infinite frequency and might produce excessive noise even if it could be physically realized. In actual feedback practice an approximation to the stabilizing operator of this section is used. For every zero in $L_2(s)$, a corresponding pole is also introduced. However the magnitude of the pole is made large enough to produce negligible effect on the root loci for all values of k_1k_2 interest. Thus in servo practice, one does not actually use a zero term of the form

$$1 + \tau s$$

Instead, as an approximation, the following operator is used.

$$\frac{1 + \tau s}{1 + \frac{\tau s}{a'}} \qquad (2.10)$$

Or equivalently

$$a' \frac{s + \frac{1}{\tau}}{s + \frac{a'}{\tau}}$$

This is the familiar 'lead network' of servo theory. This operator produces a pole whose location on the negative real axis is a' times as large as the zero location, where a' is typically made 10 or more in magnitude. This far-removed pole has negligibly small effect on the root loci that existed without its presence. It does produce an additional root locus. If a' is made large,

this root may be made large in magnitude and very stable for essentially all gains k_1k_2 of interest. For very large, or infinite gain, of course, this root approaches the zero at infinity of $L_1(s)$, since the stabilizer of equation 2.10 does not truly change the zero at infinity of the loop gain from that of $L_1(s)$, but only apparently does so over the gains of interest.

These characteristics are shown in figure 2.5, where the system depicted in figure 2.4 is shown again, with the effect of the stabilizer of equation 2.10 added. For gains k_1k_2 up to say K_3, the system of figure 2.5c has essentially the same dynamic behavior of figure 2.5b, since the new root is very stable, and the old roots are essentially unchanged. For gains above K_3 the new root becomes increasingly less stable, until above K_4 it is unstable. Now K_4, the critical gain at which the root due to the pole of equation 2.10 becomes unstable, can be made as large as desired by making the pole or a' large. In the limit of $a' \to \infty$, K_4 approaches infinity, and the system becomes that of figure 2.5b. The maximum size of a' is mainly determined by equipment considerations. Since a' may be made very large, K_4 may be made very large, well above the actual gains used. Therefore the actual system of figure 2.5c can be made to perform essentially the same as figure 2.5b. Thus feedback practice, using stabilizers of the form of equation 2.10, is a very good approximation to the feedback theory of this part which considers ideal stabilizers. For simplicity the feedback theory of this part, which uses the

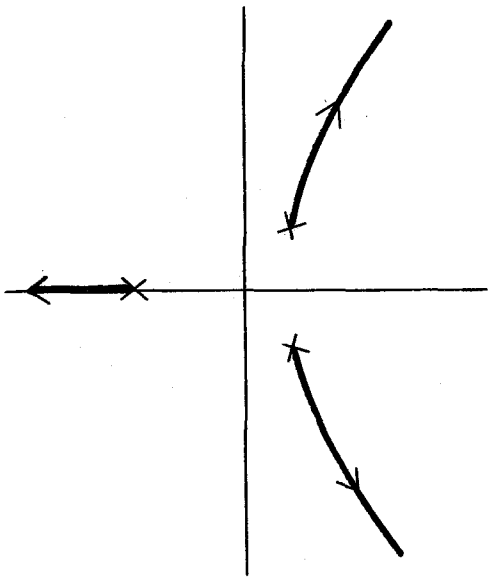

(a). Original System, $L_1(s)$.

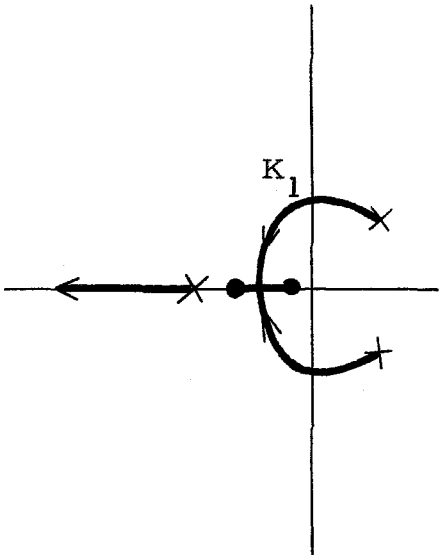

(b). System with Ideal Stabilizer of Double Lead Network.

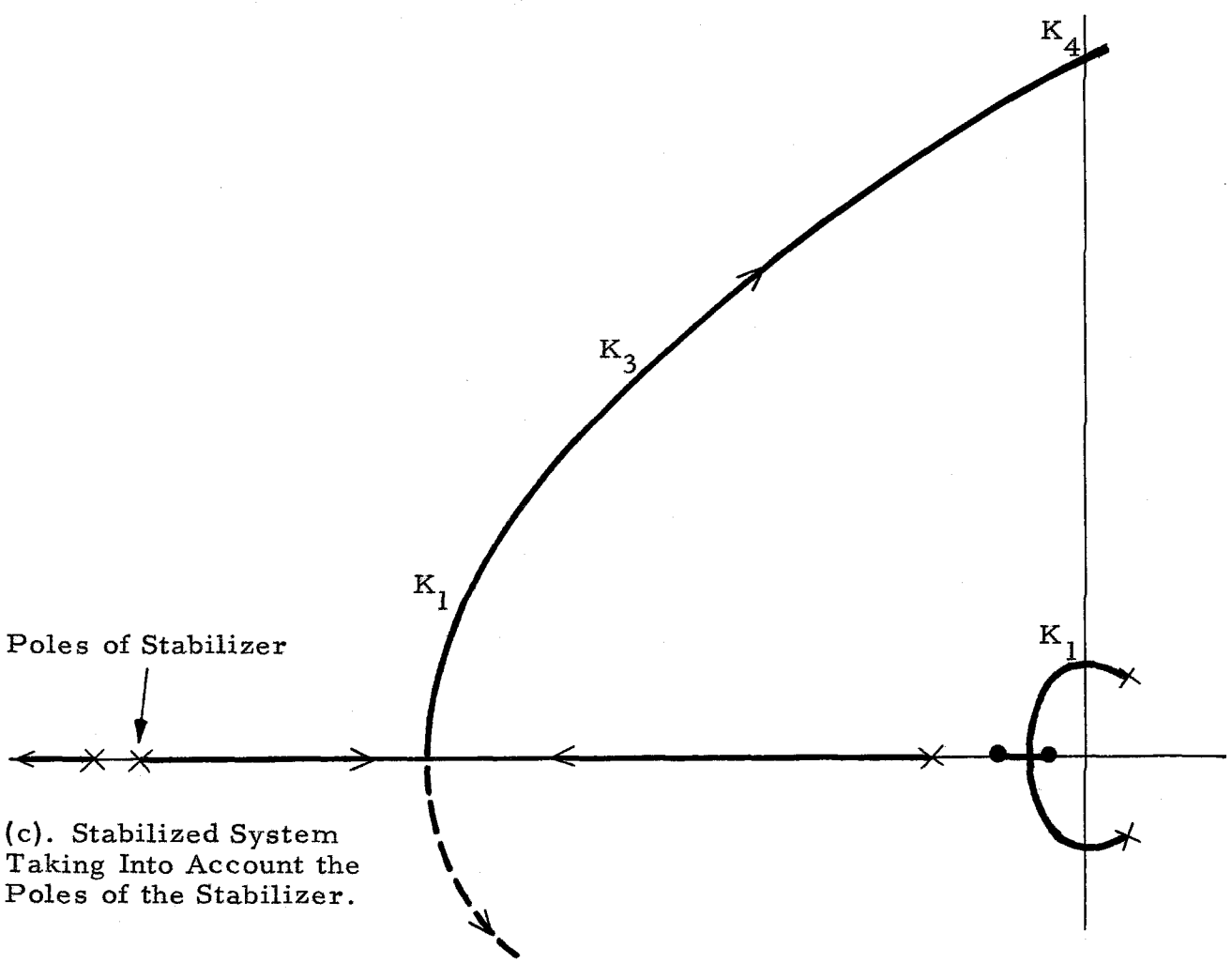

(c). Stabilized System Taking Into Account the Poles of the Stabilizer.

Root Loci of a Stabilized System with Ideal Stabilizer and Actual Stabilizer.

Figure 2.5.

ideal stabilizers of equation 2.9, will be employed in the remainder of this study. Actual feedback practice can approximate this performance to an arbitrarily close degree of accuracy.

2.3 General Feedback Theory Applied to Servo Systems and Feedback Amplifiers which Invariably Contain Only Non-Essential Zeros

Before applying this general feedback theory to the specific case of interest, an aeroelastic system, it is instructive to consider first the more restrictive case of servos, feedback amplifiers, and similar systems, comprising the vast majority of all systems that normally are considered as feedback systems. These systems invariably fall into the category treated in part 2.1 - those for which the closed loop transfer function contains only non-essential zeros. The underlying reason the zeros of such systems lie in the left half finite s plane is that such systems are virtually always made up of basic (non-feedback) elements each of which contains only left half plane zeros and poles in its transfer function. These are the so-called minimum phase operators of network theory. The complete feedback system for these servos, feedback amplifiers, etc. may consist of complicated interconnections of these basic elements in multi-loops such as shown in figure 2.6. The G's and the H's of figure 2.6 represent the transfer functions of the basic elements, and hence contain only L.H.P. zeros and poles.

Despite the complexity of the interconnections of a system as figure 2.6, or even more complicated ones, it is a fact that virtually without exception the closed loop transfer function of these systems (say from r to c') contains only non-essential or left half finite s plane zeros. This fact is demonstrated in Appendix A.

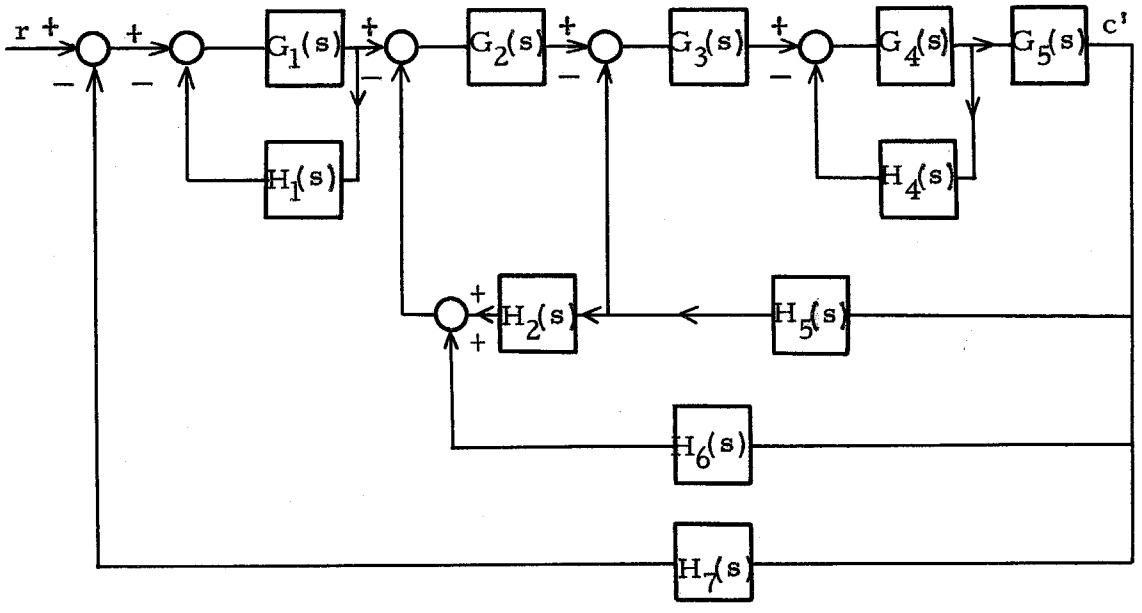

Multi-Loop Feedback System of Minimum Phase

Basic Elements

Figure 2.6

Thus if any unstable servo, feedback amplifier etc. is considered as the fixed $L_1(s)$ operator of figure 2.2, it follows from the preceding discussion and theorem 1, that there always exists a stabilizing operator $L_2(s)$ from c' back to r which can stabilize the system. Hence the following rule.

Rule 1

Virtually all servos, feedback amplifiers, etc. fall into the category of feedback systems containing only non-essential zeros, and hence can always be stabilized by feedback control.

From this viewpoint, most of servo theory is consolidated into a single aim of transplanting the infinite right half plane zeros of $L_1(s)$ into the left half plane, since the finite plane zeros already exist in the left half plane. As indicated in equation 2.9,

this is done ideally by making $L_2(s)$ a polynomial in s of degree (L-1), one less than the number of zeros of $L_1(s)$ at infinity.

For simple systems, the value of (L-1) may be 1, $L_2(s)$ becoming:

$$L_2(s) = k_2 (1 + \tau s) \tag{2.11}$$

A special case of this is,

$$\tau \rightarrow \infty$$
$$\text{and } k_2 \rightarrow \frac{k_2'}{\tau}$$

so that

$$L_2(s) = k_2' s \tag{2.12}$$

The $L_2(s)$ of equation 2.12 represents a perfect derivative device produced in practice by a tachometer feedback. The amount of stabilizer feedback, k_2 in equation 2.11 or k_2' in equation 2.12, is increased until the system is stabilized.

A somewhat simplified case is now considered of an $L_1(s)$ operator containing two R.H.P. poles and no zeros. Each type of feedback operator for $L_2(s)$ in equations 2.11 and 2.12 is shown in figure 2.7. The two infinite magnitude zeros of $L_1(s)$, of marginal location $\pm \pi/2$ radians, are converted to one L.H.P. zero in the loop gain at π radians in each case.

In both cases of figure 2.7 the system becomes stable for values of k_1k_2 greater than K_1*. The greater the gain k_1k_2, the

---

*Of course the value of K_1 in each system need not be the same.

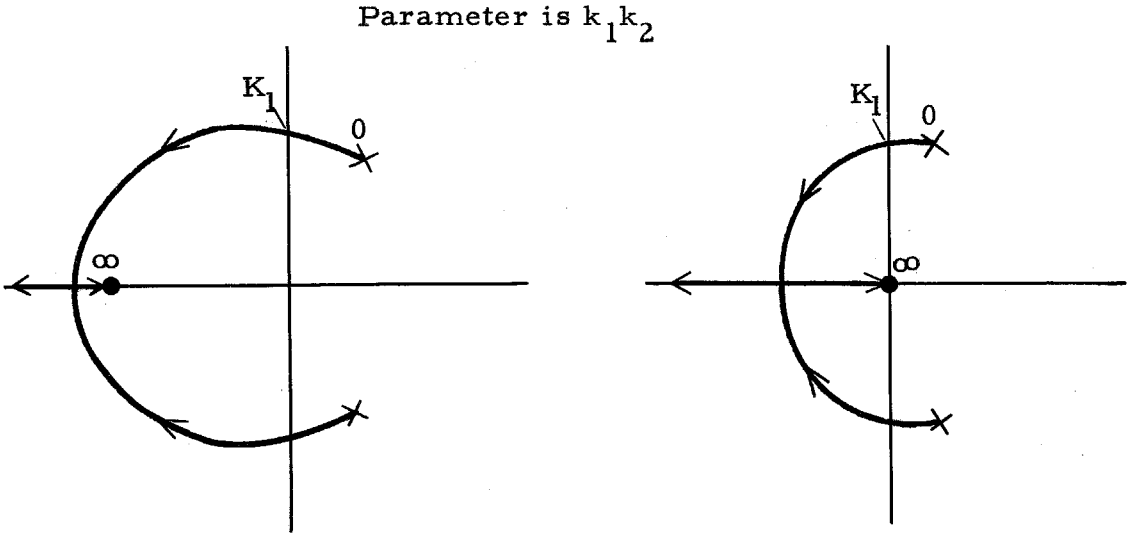

$L_2(s) = k_2 (1 + \tau s)$ a.

$L_2(s) = k_2' s$ b.

Stabilization of a Two Pole $L_1(s)$ Operator by

$$L_2(s) = k_2(1 + \tau s)$$
$$L_2(s) = k_2' s$$

Figure 2.7a, b

more positively damped the system becomes, a familiar result in servo systems using pure lead feedback (figure 2.7a), or tachometer feedback (figure 2.7b).

A final example of application of this general feedback theory to feedback systems with L.H.P. zeros is considered next. A realistic and very common case is chosen of an $L_1(s)$ operator having three poles and no zeros. According to equation 2.9 two zeros of $L_2(s)$ are needed for stabilization. The root loci are shown in figure 2.8, the same as figure 2.4. Again for values of k_1k_2 in excess of K_1, the system is stabilized.

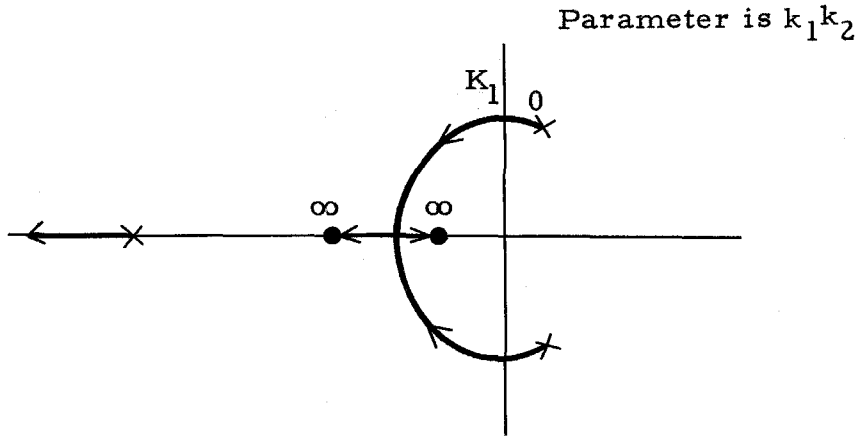

Root Loci for 3 Pole $L_1(s)$ and 2 Zero $L_2(s)$

Figure 2.8

A minor disparity between the feedback theory expressed above and normal feedback practice should be mentioned. Because of added complexity in instrumenting zero operators for $L_2(s)$ and because of the magnification in high frequency noise resulting, it is customary in feedback practice to use one less zero than indicated by equation 2.9. Thus the order of the zero in $L_2(s)$ is usually (L-2), thereby locating two infinite s plane zeros at $\pm \pi/2$ radians, rather than one at π radians. The roots which approach the infinite zeros at $\pm \pi/2$ are not as well damped as the one approaching the infinite zero at π radians in figures 2.4, 2.7 and 2.8. For illustration consider the classic problem in servo theory, the 3 pole $L_1(s)$ operator just considered. $L_2(s)$ becomes a single zero and figure 2.8 is now modified to figure 2.9.

This disparity between the general feedback theory of this part and actual feedback practice concerns only the degree of stabilization that need be incorporated into the system. This is

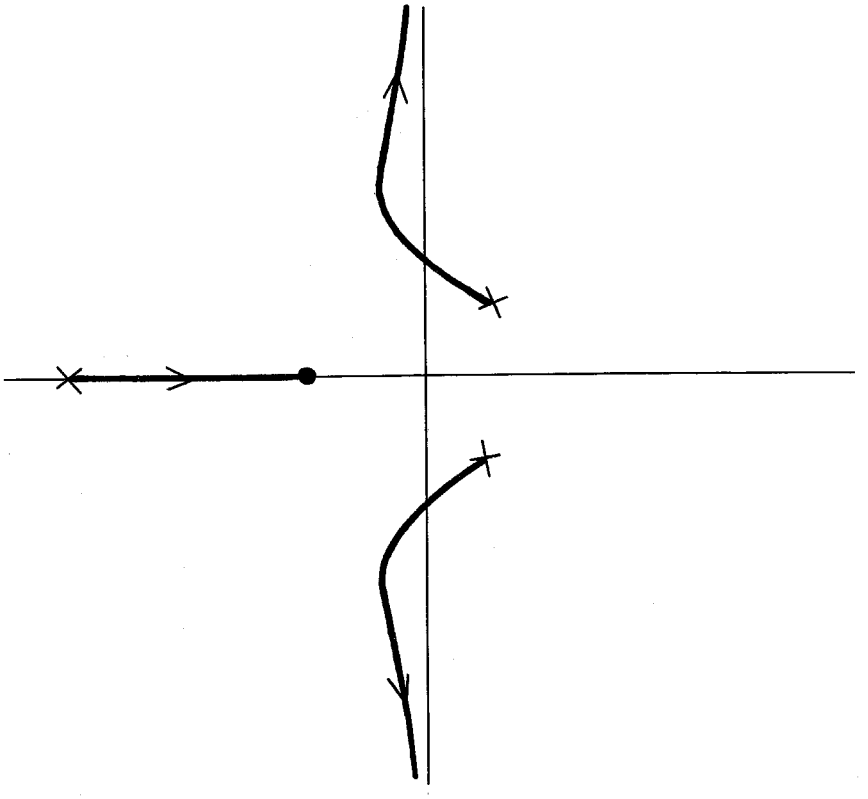

Root Loci for 3 Pole $L_1(s)$ Operator,

Single Zero $L_2(s)$ Operator

Figure 2.9

really a minor point since our major purpose is to determine whether stabilization is possible at all by feedback control. For those cases in which stabilization is possible, only as much damping as needed will be added in actual systems.

The more stringent requirement of the general feedback theory of this part, was introduced partly because of the conceptual ease in determining the stability of a root approaching π radians. For two roots approaching $\pm \pi/2$, as in actual feedback practice, the question arises - from which direction do the roots approach this marginal direction, from the left or right half plane? It takes

an actual root locus diagram such as figure 2.9 to answer this question, a difficulty avoided by the general feedback theory of this chapter. In actual practice the one less zero for $L_2(s)$ can be satisfactorily used in many cases, to provide the noise reduction and instrumentation simplicity mentioned above.

2.4 Possibility of Stabilization when Zeros are Essential (Non-Minimum Phase)

Part 2.3 showed that the known and investigated feedback control systems, such as servos, feedback amplifiers, etc., invariably have the zeros of the transfer function in the left half s plane. Rule 1 showed that such systems could always be stabilized by feedback control. In certain cases the transfer function of aeroelastic systems satisfy this condition of containing only non-essential zeros. For such cases the preceding theory of this part applies, and stabilization is readily achieved.

In many cases, however, the aeroelastic transfer function contains R.H.P. zeros. For these cases, there is no assurance that stabilization is possible. To ascertain the conditions, if any exist, under which stabilization is possible, the general feedback theory is extended to the case of essential or non-minimum phase zeros.

The first characteristic noted about such systems is that stabilization, if possible, is the so-called conditional stability of servo theory. That is, the system can be stabilized by feedback control only for values of the loop gain constant k_1k_2 above a certain lower limit K_1, and below a certain upper limit, K_2.

$$K_1 < k_1k_2 < K_2 \qquad (2.13)$$

This statement is easily proved. For k_1k_2 equal to zero, the characteristic roots exist at the poles of the loop gain, while for k_1k_2 equal to infinity, the roots exist at the zeros. By assumption, both a R. H. P. zero and pole exist, so that for either very small or very large gain, the system is unstable.

Equation 2.13 shows that for systems with essential zeros, the band of stable values of k_1k_2 is finite since K_2 is finite. In contrast, part 2.2 showed that for systems with all zeros non-essential, K_2 becomes infinite and the band of values of k_1k_2 becomes semi-infinite. Physically this means for systems with R. H. P. zeros, there is a chance of adding an excess of feedback which may destabilize, a non-existent possibility with systems of only L. H. P. zeros. Hence the width of the stability band of k_1k_2 becomes the important characteristic for systems with essential zeros.

Since the ultimate purpose of this study is to investigate the use of feedback control to stabilize <u>actual</u> aeroelastic systems, one cannot consider stabilization possible if the stable band of k_1k_2 is too narrow. To take an extreme example, if K_2, the maximum stable value of k_1k_2 in equation 2.13, were to exceed K_1, the minimum stable value, by only one per cent, certainly stabilization would be possible mathematically. In practice, however, it would be impossible, since the aerodynamic and other aeroelastic parameters would have to be known and controlled to that unrealizable degree of accuracy. A good measure of the width of the stable band of k_1k_2 values is the ratio K_2/K_1.

One more step needs to be taken before a clear picture can be formed of the characteristics of the stable region of $k_1 k_2$ values for systems with essential zeros. Consider a special case, one in which both a zero and pole exist far from the imaginary axis in the right half s plane. This is a limiting case of aeroelastic systems for speeds above flutter. Above the first speed at which both a zero and pole are in the right half plane, small speed increments cause both to move markedly into the R. H. P. This fact will be illustrated later in the numerical study cases of figures 4.2 and 4.3*.

Two type root locus possibilities exist for this case of a zero and pole far out in the right half plane. Either the same one, or different loci, connect the right half plane pole and zero. These two cases are illustrated in figure 2.10.

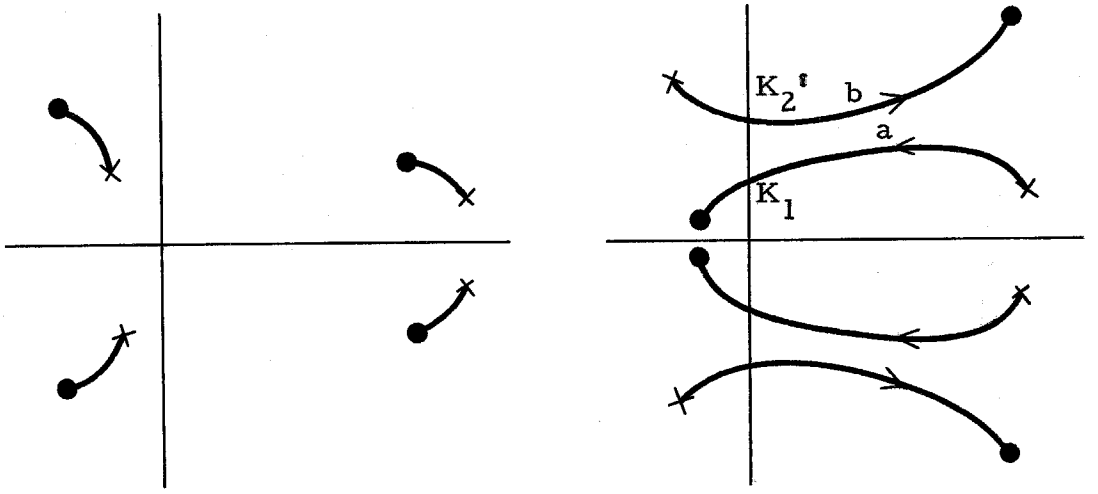

Root Loci when a Zero and Pole Exist Far Out

In the Right Half Plane

Figure 2.10

---

*Also, for speeds far above divergence, a real root moves far into the right half plane.

Figure 2.10a usually results when the distance in the right half s plane between zero and pole is small compared to their distance from the zeros and poles in the left half plane*. Figure 2.10b usually occurs when the R.H.P. pole and zero are far apart. It will now be shown by heuristic argument that, for both cases in figure 2.10, no value of k_1k_2 exists capable of stabilizing the system.

Obviously this statement is true in figure 2.10a since an entire locus exists in the right half plane. The addition of a stabilizing lead network or pure zero operator such as given by equations 2.10 and 2.11 will not change this right half plane locus appreciably. This can be seen by actually sketching the effect of these operators on the root loci of figure 2.10. It can also be seen by considering the analogy of a root locus to an electric line of flux. In this analogy a pole is equivalent to a unit positive line charge, and a zero equivalent to a unit negative line charge. In figure 2.10a, the pole and zero are close together as stated. Hence the plus and minus charges in the analogy are close together. The electric field and hence the root locus between these two cannot be modified appreciably by electric charges located in the far away left half plane, which is the interpretation of stabilizing zeros and poles located there. Thus a system as figure 2.10a cannot be stabilized.

The root on the locus marked a in figure 2.10b is stable only for $k_1k_2 > K_1$. However the root on locus b is stable only for $k_1k_2 < K_2'$. For system stability both roots must be stable or

---

*This can be readily seen by considering the analogy between a root locus and an electrostatic line of flux described in reference 2.

$$K_1 < k_1 k_2 < K_2' \tag{2.14}$$

Now distance along any locus from the pole to the zero is a monotonically increasing measure of the value of $k_1 k_2$. From this fact it can be seen by inspection of figure 2.10b that for the case under study - a pole and zero located far out in the right half plane - K_1 must be large and K_2' small. Since this is contrary to the inequality of equation 2.14, no stabilization is possible. The physical interpretation of this result is that the gain $k_1 k_2$ must be large to stabilize the root on locus a, and small to stabilize the root on locus b. These two requirements are inconsistent, and instability of one or the other root must result.

The range of values of $k_1 k_2$ for which stability results becomes zero for this assumed case of a zero and pole located far out in the right half plane. No stabilization is possible for either of the only two possible situations that can exist in figure 2.10b. The numerical examples of parts IV and V will illustrate that this is the condition that exists in aeroelastic systems for adequate speeds above that at which a zero and pole first move into the right half plane.

One can now sketch a qualitative boundary of stable values of $k_1 k_2$ versus speed valid for aeroelastic systems in general. The distinction between various systems exists only in the associated numerical values. Figure 2.11 a and b shows the situation for the two possible generic cases. In figure 2.11a the pole is the quantity to cross into the right half s plane at the lower speed, while in figure 2.11b the zero crosses first. In both cases all zeros and

poles lie in the left half plane below this speed, V_o.

By simple extension of the theory of part 2.3, it can be proved rigorously that a suitable stabilizing operator can achieve stability below the speed V_o for <u>all</u> positive values of k_1k_2. The plausibility of this statement is seen, since the limits of k_1k_2 equal to zero and infinity locate the characteristic roots at the poles and zeros respectively, by assumption in the left half plane. Because of this, the designation is given - the infinite stable range.

From speeds V_o to V_1 in figure 2.11, either a pole or a zero, but not both, move into the right half plane. For the former case (figure 2.11a) a limit on the stable lowest value of k_1k_2 exists, since zero value places a characteristic root at the R.H.P. pole. For the latter case (figure 2.11b) a limit on the stable highest value of k_1k_2 exists, since an infinite value locates a characteristic root at the R.H.P. zero. Hence either a lower or upper limit of k_1k_2 exists, but not both. Thus the significant ratio K_2/K_1 is infinite over this range in both cases. Hence this range is called the semi-infinite stable range.

Above speed V_1 both a R.H.P. zero and pole exist. It is obvious from the discussion of the last paragraph that an infinite value of k_1k_2 locates a root on the R.H.P. zero, while zero value locates it on the R.H.P. pole. Hence both a lower and upper limit exists for stable k_1k_2 values. As the speed increases above V_1, the zero in figure 2.11a (or pole in figure 2.11b) which has just become R.H.P. at speed V_1, moves further into the right half plane. The stable band of k_1k_2 reduces as this occurs until finally above

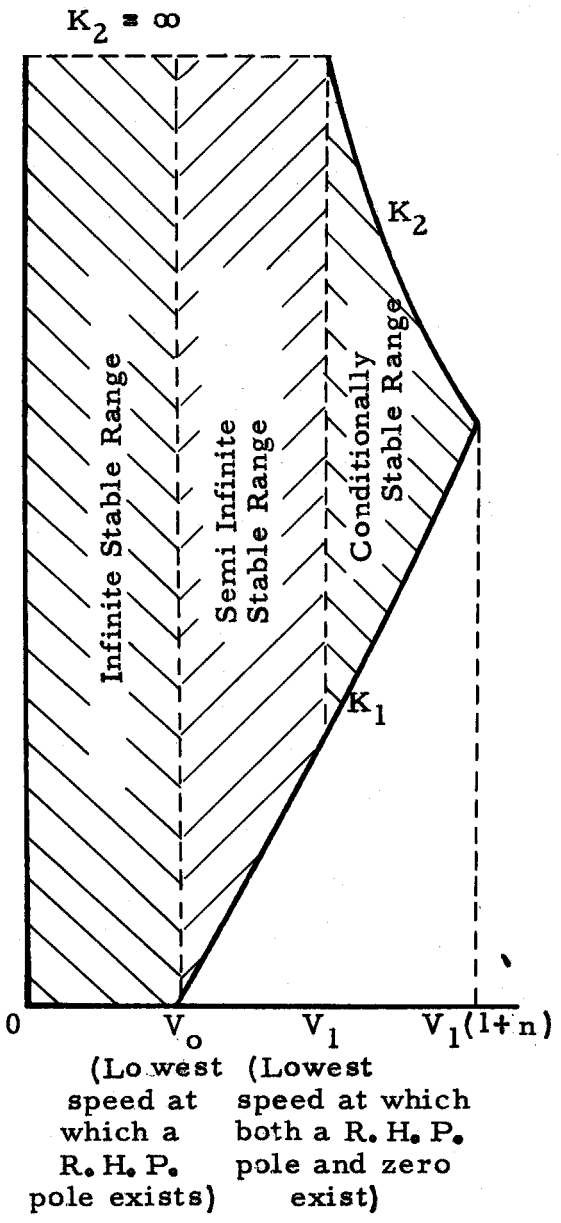

(a)

Case a R. H. P. Pole exists at the lower speed

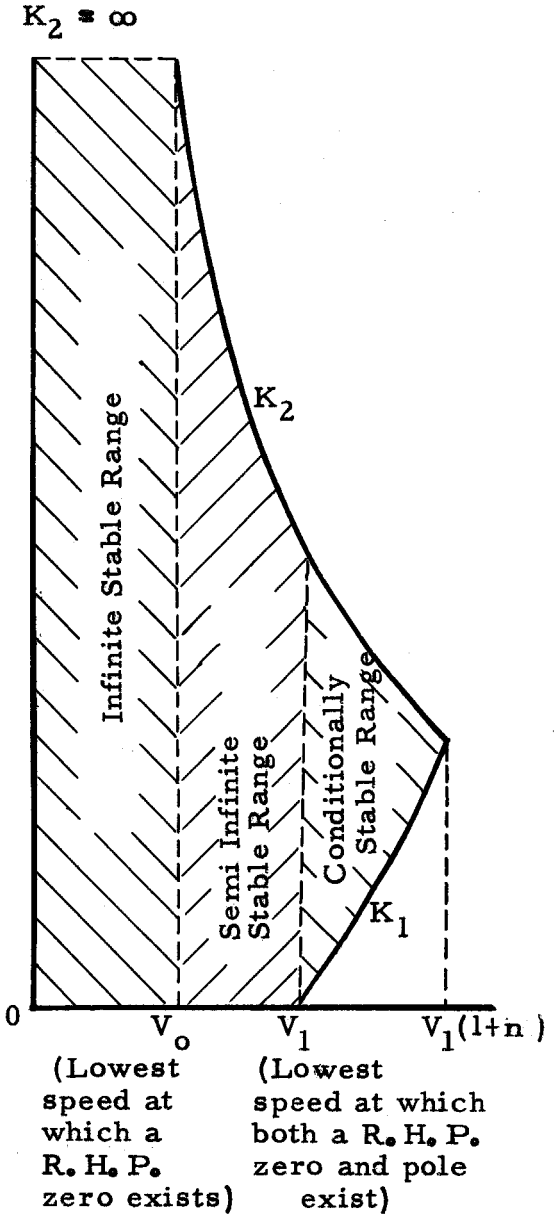

(b)

Case a R. H. P. Zero exists at the lower speed

Stable Boundary of $k_1 k_2$ Versus Speed

Figure 2.11

some speed $(1 + n)\ V_1$, it becomes essentially zero in width, the situation depicted previously in figure 2.10. The root locus of this troublesome root, illustrating the narrowing-with-speed of the stable band of k_1k_2 values in the s plane, is shown in figure 2.12. It is worthwhile to remember the previously mentioned fact that distance along the locus is a monotonic function of k_1k_2. This helps in forming ready mental pictures of the stable range of k_1k_2 values from the diagram.

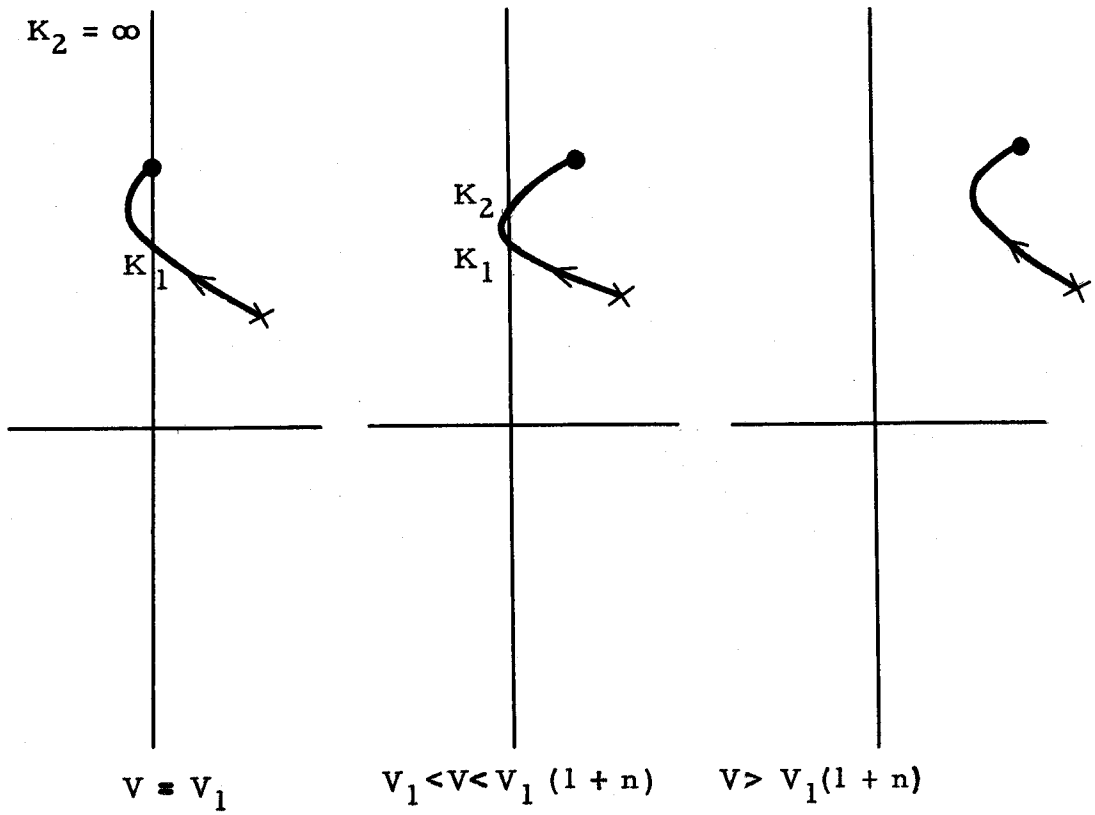

Variation of the Stable Range of k_1k_2 with Speed as Seen from the Root Locus Diagram

Figure 2.12

Figure 2.11 really summarizes in compact form the entire general theory of this part applied to aeroelastic systems. Below a speed V_1, where either all the zeros or all the poles are L.H.P., the ratio of stable k_1k_2 values, $\frac{K_2}{K_1}$, is infinite. Hence with nominal k_1k_2 operation somewhere in the middle of this range, stability is still achieved even if the system parameters, such as the aeroelastic gain are not known accurately. The feedback almost always represents a definite trend in both cases, a monotonically stabilizing effect in figure 2.11a, a monotonically destabilizing effect in figure 2.11b. Obviously a large feedback, and hence a large k_1k_2 value, should be used in the first case, while small or zero feedback should be used in the second case. Despite large variations in system parameters, manifested by large percentage changes in K_1 and K_2 at any speed, stabilization will still result for such operation because of the infinite width of the stability band*. This semi-infinite stable range is really the case studied in detail in parts 2.1, 2.2 and 2.3.

Above speed V_1 both zeros and poles lie in the right half plane and a finite band of stable k_1k_2 values exist up to a speed $V_1(1+n)$. This highest speed exceeds the maximum speed of the semi-infinite stable range by n, when expressed in per unit of V_1. Mathematically, conditional stability is possible over this range. However only a small part of the conditionally stable range would even be considered as usable in an actual system. This is true because the ratio of K_2 to K_1 is not very large (perhaps 2 or less)

---

*Below the speed V_1, one extreme value K_1 or K_2 is infinite when measured on a logarithmic scale, as is the ratio of K_2/K_1 on an absolute scale.

over most of the conditionally stable zone as will be shown in the numerical examples of part V. The great uncertainty of system parameters might easily throw the operation of the actual system outside this narrow stable zone of k_1k_2 values, even when the calculations concerning the ideal or nominal system predicted stability.

To illustrate this point one notes that in ordinary servo systems, where the system parameters are much better known than in aeroelastic servo systems, an adequately broad stable range of system loop gain is required*. Typical operation is at the center of the stable band, a factor of two being a typical minimum value separating the nominal operating point from both the lower and upper stable values of loop gain. Thus the ratio of K_2/K_1 becomes 4 for such systems. In aeroelastic servo systems, the parameters are many more and not known so well, requiring a much broader band of nominally stable k_1k_2 values. Errors in test measurement of structural constants such as location of the c.g., manufacturing tolerances, and approximations** made in any analytical study are all sources which make the actual system deviate from the nominal one studied analytically. This greatly increased uncertainty concerning actual system performance requires a much larger factor between the nominal operating point, and each stable extreme K_1 and K_2, than the aforementioned value of 2 of a typical servo. A

---

*This is expressible in such terms as gain margin.

**These are many indeed, such as the aerodynamic ones of incompressible flow, strip theory, center of pressure at the quarter chord, usually made in subsonic aerodynamics. Also structural approximations are made, such as the concept of an elastic axis, neglect of bending moment of inertia, etc. Last, but not least, is the finite difference approximation of a continuous system.

figure of 4 is probably in no way overly safe. This means a ratio of K_2/K_1 of 16. Hence a practical quantitative rule might be given as follows.

Rule 2

Only those portions of the conditionally stable zone for which K_2/K_1 is say 16 or more, can be used to achieve practical stabilization by feedback control. The nominal operating point of k_1k_2 in this zone is then a factor of 4 removed from the K_1 and K_2 stable extremes.

The next question one naturally asks concerns the application of rule 2 to numerical examples. How much speed increase over V_1 does this usable portion of the conditionally stable region represent? If this is negligibly small (say less than 5%), as it is in all the cases to be examined in part V, then for all practical purposes the speed range over which adequate stabilization is possible may be said, with sufficient accuracy, to exist only up to speed V_1 in figure 2.11. This represents speeds at which either all the zeros, or all the poles, are L. H. P. Since the speed regime for which the aeroelastic system is unstable is the one under investigation, by assumption at least one pole is R. H. P. Thus the necessary condition for practical stability above the aeroelastic flutter speed is that the zeros of the aeroelastic transfer function lie in the left half plane. But this is precisely the sufficiency condition of theorem 1. Hence the following important rule.

Rule 3

For all practical purposes both the necessary and sufficient condition for increase in flutter speed by feedback control is that the zeros of the aeroelastic transfer function lie in the left half

plane. The technique of achieving the functional form of the stabilizing operator is given in part 2.2.

A word is in order concerning the numerical results of part V which was used above. This result shows that the usable portion of the conditionally stable zone is very small compared to speed V_1. In part V it is shown for the systems studied, that the maximum value of the conditionally stable zone is typically only 5% to 25% in excess of V_1. Furthermore the speeds which satisfy rule 2, or $K_2/K_1 > 16$, invariably cover only a small fraction of the conditionally stable range (less than 10%). The last two results show that the maximum usable speed of the conditionally stable range is typically only .5% to 2.5% greater than V_1. This is negligible and the maximum usable speed may be said to be V_1, with adequate accuracy for our purposes.

PART III

COFACTORS OF AEROELASTIC MATRIX THAT DETERMINE WHETHER STABILIZATION IS POSSIBLE

Part II developed a general feedback theory. This theory was applied to aeroelastic servo systems in a speed regime above the aeroelastic flutter speed. The question as to whether stabilization was possible at these speeds, was reduced to an investigation of the zeros of the aeroelastic transfer function. For stability to be possible at any speed above flutter, it was shown these zeros must all be in the left half s plane. In this part, explicit expressions for the aeroelastic transfer function are derived, in order to obtain the expressions constituting these zeros. In the next part, the numerical results of application to test cases are described.

To emphasize the basic factors involved without a maze of detail, the three degree of freedom system is considered first. After this the multi-degree of freedom system with distributed properties is treated.

3.1 Three Degree of Freedom System

Figure 3.1 is a block diagram pertinent to the three degree of freedom system, where the three coordinates of the wing, h, α, and β are explicitly shown.

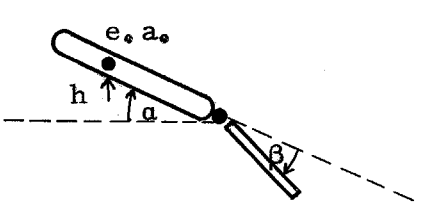

Three Degree of Freedom System

Figure 3.1

It is shown in appendix B that the servo force, a torque of magnitude T_β, acting between the control surface and the wing, can be treated as an external torque of the same magnitude acting only on the β coordinate. Thus the aeroelastic force matrix, [A], can be written as follows, treating T_β as the only external force.

$$\begin{bmatrix} 0 \\ 0 \\ T_\beta \end{bmatrix} = \begin{bmatrix} A_{hh} & A_{h\alpha} & A_{h\beta} \\ A_{\alpha h} & A_{\alpha\alpha} & A_{\alpha\beta} \\ A_{\beta h} & A_{\beta\alpha} & A_{\beta\beta} \end{bmatrix} \begin{bmatrix} h \\ \alpha \\ \beta \end{bmatrix} \tag{3.1}$$

The A's represent the elastic and mass properties of the structure and the aerodynamic forces, all functions of s.

The coordinates h, α, and β resulting from the external force T_β are easily found from equation 3.1.

$$\begin{aligned} h &= \frac{\Delta_{\beta h}}{\Delta} T_\beta \\ \alpha &= \frac{\Delta_{\beta\alpha}}{\Delta} T_\beta \\ \beta &= \frac{\Delta_{\beta\beta}}{\Delta} T_\beta \end{aligned} \tag{3.2}$$

where

$$\begin{aligned} \Delta &\equiv \text{determinant of A matrix of equation 3.1} \\ \Delta_{\beta h} &\equiv \text{cofactor of } \beta\text{-h element of } \Delta \\ \Delta_{\beta\alpha} &\equiv \text{cofactor of } \beta\text{-}\alpha \text{ element of } \Delta \\ \Delta_{\beta\beta} &\equiv \text{cofactor of } \beta\text{-}\beta \text{ element of } \Delta \end{aligned} \tag{3.3}$$

Note that $\Delta_{\beta\beta}$ is also the characteristic determinant of the system when β is restrained to zero motion. The significance of this property of $\Delta_{\beta\beta}$ is illustrated in part 3.3.

The transfer functions of equation 3.2 can be employed in figure 1.5 to give the following more specific block diagram.

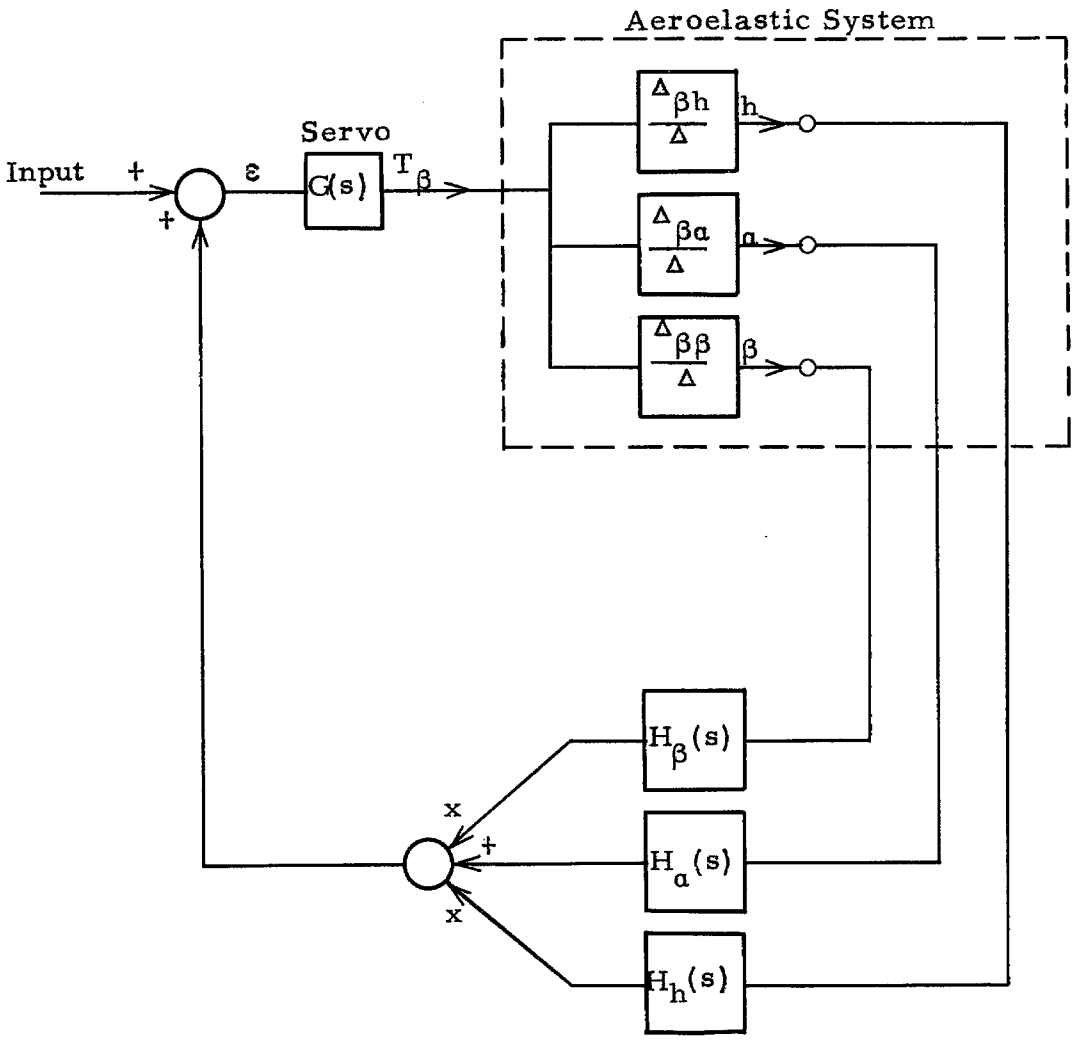

Block Diagram of Three Degree of Freedom

Aeroelastic System, Stabilizers and Servo

Figure 3.2

In the notation of part II, the fixed system or $L_1(s)$, is made up of the aeroelastic operators $\frac{\Delta_{\beta h}}{\Delta}$, $\frac{\Delta_{\beta a}}{\Delta}$, $\frac{\Delta_{\beta\beta}}{\Delta}$, and the servo G(s). The operators $H_h(s)$, $H_a(s)$, and $H_\beta(s)$ can be varied at the will of the designer to achieve optimum stability.

The characteristic equation of figure 3.2 is found using the standard feedback relation

$$1 - \text{Loop Gain} = 0 \tag{3.3}$$

or more explicitly

$$1 - \frac{G\left[\Delta_{\beta h} H_h + \Delta_{\beta a} H_a + \Delta_{\beta\beta} H_\beta\right]}{\Delta} = 0 \tag{3.4}$$

In equation 3.4 the dependence on s is implied.

It is instructive to compare equation 3.4 with the relation of the general feedback system, equation 2.5*. Obviously the poles, P_j, of equation 2.5 are equivalent to the zeros of Δ in equation 3.4, the characteristic roots without the servo. Also the zeros Z_i are equivalent to the roots of the following expression from equation 3.4.

$$G\left[\Delta_{\beta h} H_h + \Delta_{\beta a} H_a + \Delta_{\beta\beta} H_\beta\right] = 0 \tag{3.5}$$

According to rule 3 of part II, the location of the zeros of equation 3.5, at any speed at which the aeroelastic system is unstable, determines whether stabilization is possible. If the zeros

---

*In the discussion to follow, those zeros and poles of the loop gain are ignored which result from poles of the numerator and demoninator, respectively, of equation 3.4. These will invariably be in the left half plane, and hence not important for our present purpose. This fact is demonstrated in appendix D.

are all in the left half s plane, or non-essential zeros, then stabilization can be achieved. The zeros of the servo operator, G(s), will invariably be in the left half plane, since it falls under the classification of a feedback system of minimum phase elements as defined in part 2.3*. These L.H.P. zeros are of no importance for our present purpose. Therefore, the function to be investigated for significant zeros reduces from equation 3.5 to equation 3.6.

$$Z(s) = \Delta_{\beta h} H_h + \Delta_{\beta a} H_a + \Delta_{\beta\beta} H_\beta = 0 \tag{3.6}$$

Thus the question of the possibility of stabilization by feedback control reduces to the criterion of rule 4.

Rule 4

Stabilization of an unstable aeroelastic system is feasible if, and only if, the zeros of Z(s) of equation 3.6 lie in the left half plane.

The major problem of the synthesis, therefore, is to determine whether a suitable combination of H_h, H_a, and H_β exists, so as to make Z(s) contain only left half plane zeros, thereby permitting stabilization.

It is easily seen that if any one of the operators,

$$\Delta_{\beta h}$$

or

$$\Delta_{\beta a} \tag{3.7}$$

or

$$\Delta_{\beta\beta}$$

---

*The form of the transfer function of typical hydraulic actuators is given in reference 3, equation 46.

contains only left half plane zeros, then Z(s) can be made to have only left half plane zeros. For example if $\Delta_{\beta h}$ has only left half plane zeros, then an obvious stabilization technique is to make

$$H_a = H_\beta = 0 \tag{3.8}$$

Under this condition, equation 3.6 becomes

$$Z(s) = \Delta_{\beta h} H_h \tag{3.9}$$

Z(s) would then have only left half plane zeros, because $\Delta_{\beta h}$ has this property.

Therefore, if any one of the three operators of equation 3.7 contains only left half plane zeros, Z(s) can be made to have only non-essential zeros, and stabilization is possible.

The next consideration is the case where all three operators contain right half plane zeros. Can a non-essential Z(s) operator be yet constructed by a <u>combination</u> of H_h, H_a, and H_β stabilizers? It turns out the answer to this question is negative for all practical purposes. This will now be demonstrated, relying on the theory of part II.

Consider first a Z(s) combination of two operators, H_a, H_h. Equation 3.6 becomes

$$Z(s) = \Delta_{\beta h} H_h + \Delta_{\beta a} H_a = 0 \tag{3.10}$$

By assumption, $\Delta_{\beta h}$ and $\Delta_{\beta a}$ contain right half plane zeros.

Equation 3.10 may be written,

$$Z(s) = \Delta_{\beta h} H_h \left[1 + \frac{\Delta_{\beta a}}{\Delta_{\beta h}} \frac{H_a}{H_h} \right] \tag{3.11}$$

The zeros of $\Delta_{\beta h} H_h$ are not zeros of equation 3.10 since by definition H_a is not identically zero. Thus the factor $\Delta_{\beta h} H_h$ does not contain zeros of equation 3.11 and may be divided out.

The zeros of equation 3.11 become those of,

$$Z'(s) = (1 + \frac{\Delta_{\beta a}}{\Delta_{\beta h}} H') = 0 \tag{3.12}$$

where

$$H' = \frac{H_a}{H_\beta} \tag{3.13}$$

The original synthesis problem expressed in rule 4, has been reduced to an equivalent one of investigating $Z'(s)$ of equation 3.12 for left half plane zeros. It is to be remembered that R.H.P. zeros occur in both $\Delta_{\beta a}$ and $\Delta_{\beta h}$ by assumption.

To investigate equation 3.12, it is noted the same form exists as equation 2.5, the basic equation for the theory of part II. Hence the theory of part II relevant to equation 2.5 can be applied here. The statement that both $\Delta_{\beta a}$ and $\Delta_{\beta h}$ of equation 3.12 contain right half plane zeros, is equivalent in equation 2.5 to both zeros, Z_i, and poles, P_j, of the loop gain being in the right half plane. The theory of part II required that for such a situation, some roots of equation 2.5 must exist in the right half plane, for all practical purposes. Hence for the corresponding function here, $Z'(s)$ of equation 3.12, some right half plane zeros must exist irrespective of the H' operator. The same applies to $Z(s)$ of equation 3.10, as originally stated.

A simple extension is used to prove the same result for the general three operator case of equation 3.6. This can be written

$$Z(s) = \Delta_{\beta\beta} H_\beta \left[1 + \frac{\Delta_{\beta h} H_h + \Delta_{\beta a} H_a}{\Delta_{\beta\beta} H_\beta} \right] = 0 \qquad (3.14)$$

By the same argument as above, the factor $\Delta_{\beta\beta} H_\beta$ can be dropped yielding,

$$Z'(s) = 1 + \frac{\Delta_{\beta h} H_h + \Delta_{\beta a} H_a}{\Delta_{\beta\beta} H_\beta} = 0 \qquad (3.15)$$

For $Z'(s)$ of equation 3.15 to have all left half plane zeros, the theory of part II requires the numerator of the ratio of factors, or the following expression, to likewise have all left half plane zeros.

$$Z''(s) = \Delta_{\beta h} H_h + \Delta_{\beta a} H_a = 0 \qquad (3.16)$$

However $Z''(s)$ of equation 3.16 is exactly equation 3.10 of the two feedback case, which has been shown to contain right half plane zeros. Therefore $Z'(s)$ of equation 3.15, and hence $Z(s)$ of equation 3.6, has right half plane zeros.

A very important conclusion is deduced from the preceding discussion. In order that $Z(s)$ of equation 3.6 have only left half plane zeros, and hence for stabilization to be possible, at least one of the operators $\Delta_{\beta h}$, $\Delta_{\beta a}$ or $\Delta_{\beta\beta}$ must likewise contain only left half plane zeros. If all these operators contain right half plane

zeros, it does no good to use combinations of $\Delta_{\beta h}$, $\Delta_{\beta a}$, and $\Delta_{\beta\beta}$, weighted by H_h, H_a and H_β, in an attempt to make Z(s) contain only left half plane zeros. Thus the entire synthesis can be carried out by examining $\Delta_{\beta h}$, $\Delta_{\beta a}$ and $\Delta_{\beta\beta}$ individually. The operator which contains only left half plane zeros up to the highest speed, determines the highest speed for which stabilization is possible. Feedback of only that coordinate suffices to achieve this stabilization. This conclusion is explicitly stated in rule 5.

Rule 5

Maximum flutter speed is achieved by use of only one stabilizing operator in figure 3.2, H_h, H_a or H_β. This speed is determined by investigating $\Delta_{\beta h}$, $\Delta_{\beta a}$, and $\Delta_{\beta\beta}$ and noting the first speed at which all three have R.H.P. zeros. The particular coordinate feedback to achieve this is determined by the cofactor whose zeros are L.H.P. below that speed.

3.2 Multi-Degree of Freedom System

The extension to the multi-degree of freedom system necessary to represent the distributed properties of the wing is very simple. The N cell finite difference approximation is shown below

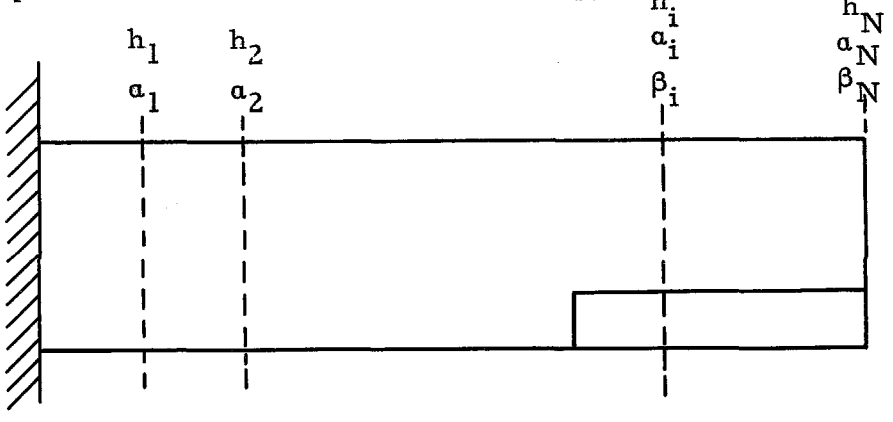

Finite Difference Approximation to Distributed Wing Plus Control Surface

Figure 3.3

The servo torque which acts at some point on the control surface in the ℓ^{th} cell is treated as a generalized force on β_ℓ. An obvious extension of figure 3.2 to handle the multi-degree of freedom system of figure 3.3 is shown in figure 3.4.

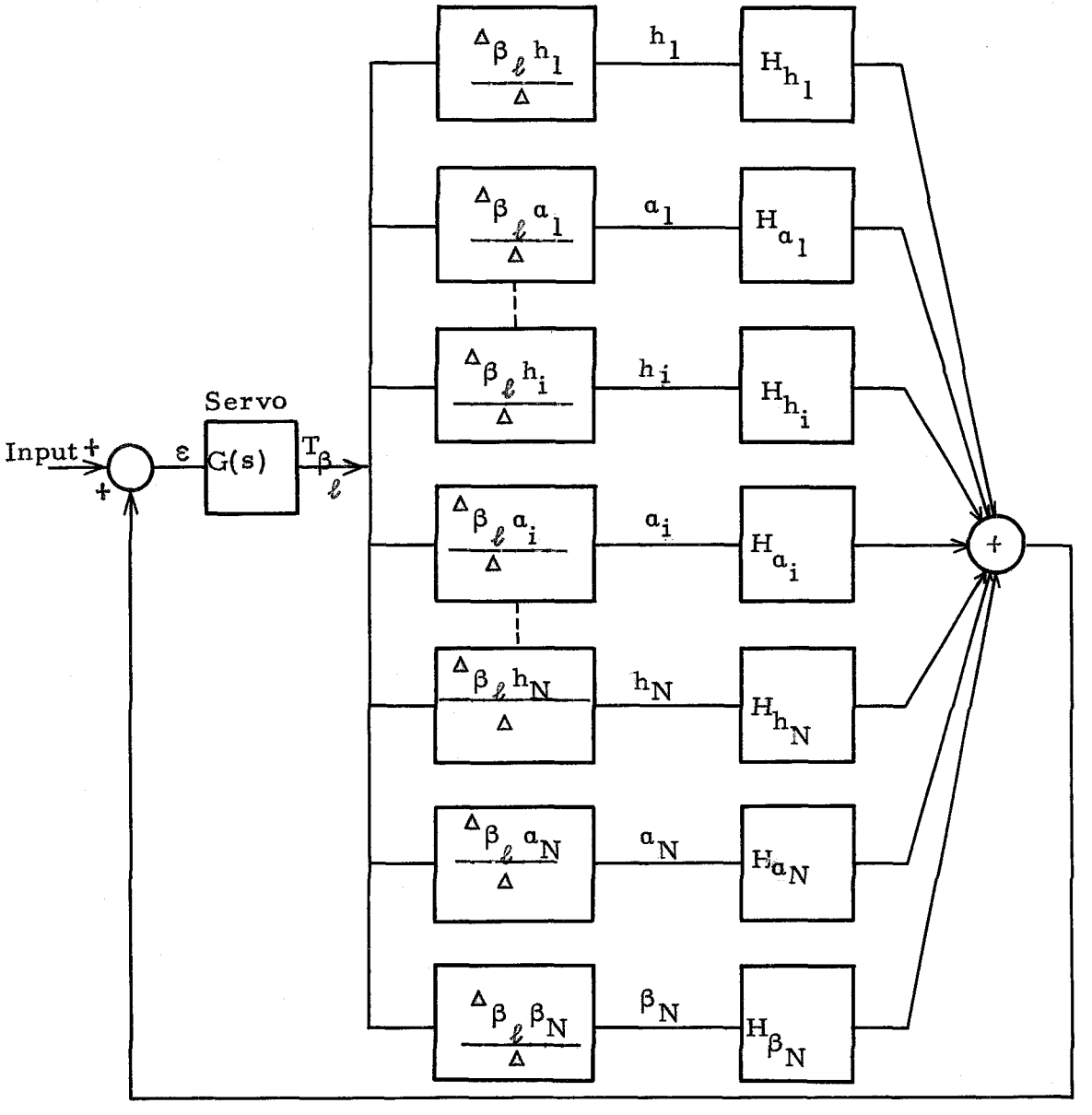

Block Diagram of Multi-Degree of Freedom

Aeroelastic Servo System

Figure 3.4

The possibility of using feedback of h, α or β at any station is represented in figure 3.4. Equation 3.4 is generalized to

$$1 - \frac{G}{\Delta}\left[\Delta_{\beta_\ell h_1} H_{h_1} + \Delta_{\beta_\ell \alpha_1} H_{\alpha_1} + \cdots + \Delta_{\beta_\ell h_N} H_{h_N} + \Delta_{\beta_\ell \alpha_N} H_{\alpha_N} + \Delta_{\beta_\ell \beta_N} H_{\beta_N}\right] = 0 \qquad (3.17)$$

A similar argument to that in part 3.1 for the three coordinate case shows that optimum stabilization is achieved by feedback of only one coordinate, the coordinate x such that $\Delta_{\beta_\ell x}$ has no right half plane zeros up to the highest speed. For the three degree of freedom system, the synthesis reduced to an examination of the zeros of all cofactors in the β row of the aeroelastic matrix of equation 3.1, namely, $\Delta_{\beta h}$, $\Delta_{\beta\alpha}$, $\Delta_{\beta\beta}$. For the multi-degree of freedom system, all the cofactors in the β_ℓ row need be examined, that is $\Delta_{\beta_\ell y}$ for all y coordinates. While in theory the location of the drive point cell, the ℓ^{th} cell, may be considered variable, in practice this is essentially fixed in location. Certainly the control surface is always outboard, and usually the servo drive point on the control surface is determined from other considerations. Therefore $\Delta_{\beta_\ell y}$ need be investigated only for a fixed, specified value of ℓ.

It seems reasonable to expect that the y coordinates at the same ℓ^{th} cell will yield the true or near true optimum $\Delta_{\beta_\ell x}$. This follows since these coordinates bear the most correlation to the β drive point. Also these outboard coordinates are quite significant in the flutter mode shapes, usually first torsion or bending. Thus in practice only three cofactors probably need be investigated for location of zeros - $\Delta_{\beta_\ell h_\ell}$, $\Delta_{\beta_\ell \alpha_\ell}$, $\Delta_{\beta_\ell \beta_\ell}$, where ℓ is the drive

point cell. Hence the synthesis of a possible stabilizing operator for the multi-degree of freedom system is the same in form as the single degree of freedom system: the examination of the cofactors of the h, α, and β columns for the β row, the ℓ^{th} cell applying for the distributed system.

3.3 Feedback Control Using Only β Information

Before investigating the numerical cases to be taken up in part IV, it is simple, yet illuminating, to investigate in general the case in which only β feedback is used in figure 3.2 or 3.4. The preceding theory of part III showed that stability could be achieved for this case at all speeds for which $\Delta_{\beta\beta}$ had L.H.P. zeros. Now $\Delta_{\beta\beta}$ unlike the other stabilizing cofactors $\Delta_{\beta h}$, and $\Delta_{\beta\alpha}$, has important physical significance. Examination of equation 3.1* shows that $\Delta_{\beta\beta}$ represents the characteristic determinant of the system if β is constrained to zero motion. The statement that β feedback control can stabilize up to the speed at which a R.H.P. zero of $\Delta_{\beta\beta}$ exists, can thus be interpreted as meaning that speed at which the wing with locked control surface becomes unstable. For the actual airplane with distributed properties, this speed becomes the speed at which flutter occurs, when one locks the finite difference cell on the control surface at which the servo drives. However locking the drive point cell on the aileron is closely akin to locking the entire aileron, especially for cases in which the aileron does not constitute a major percentage of the wing span. Thus the

---

*Or the more general n by n matrix for an n degree of freedom system.

following theorem.

Theorem 2

Feedback of only the β coordinate can be used to stabilize for all speeds up to the flutter speed that occurs when the servo drive point of the control surface is locked. This is usually essentially the same speed as the flutter speed of the original wing without aileron.

In modern day supersonic airplanes the hinge line is pushed forward to almost coincide with the leading edge of the control surface. As is well known*, aileron flutter can occur for such cases well below the flutter speed of the locked aileron. Typical three degree of freedom systems examined in the literature show the following numerical results. In the system studied in reference 5, the unrestrained aileron flutter speed was only 0.18 that of the locked aileron. In reference 4, the system studied had a free aileron flutter speed of 0.46 that of the locked aileron. The flap servo, or β feedback, can eliminate all such aileron flutter, and raise the flutter speed to that of the locked aileron even when the structural restraint on β is zero or small.

Since the flutter speed of the locked aileron is invariably higher than that of the unrestrained or lightly restrained aileron** the investigation in part IV will consider possible improvement produced by α and h feedback relative to the flutter speed with the

---

*Reference 7.
**Illustrated by experience of many numerical cases besides those cited.

aileron locked. Stated in terms of the theory of this part, $\Delta_{\beta\beta}$ invariably has only L. H. P. zeros for speeds greater than that at which R. H. P. zeros occur in Δ. Hence, one need investigate $\Delta_{\beta\beta}$, $\Delta_{\beta\alpha}$ and $\Delta_{\beta h}$, but <u>not</u> Δ, to find the maximum practical flutter speed for the aeroelastic-servo system.

3.4 <u>β Feedback as an Internal Loop in an α Feedback System</u>

The theory of parts 3.1 and 3.3 showed that feedback of either α motion alone, or h motion alone, suffices to give the best possible stabilization above the flutter speed of the basic wing. It will be shown by numerical example in part IV that in the cases studied, and very probably in all systems, h motion feedback is incapable of yielding a stable system. Hence feedback of α motion alone will provide the best possible stabilization.

Though α feedback alone is required above the basic wing flutter speed, β feedback will be used in addition to α feedback in actual systems. The use of β feedback is intended to remove, at least in part, two undesirable characteristics of the aeroelastic servo loop of figure 3.2 which exist when only α feedback is used.

1) a removal of the lags due to the actuator operator, G(s).
2) a removal of the effect of non-linearities of G(s) which arise from valve saturation*.

To illustrate this effect of β feedback, figure 3.2 is redrawn, first without any feedback, and then with α and β feedbacks in figures 3.5a and b.

---

*See reference 3, page 9, for a physical description. Also reference 5, Section X, for a mathematical description of how one treats the saturation.

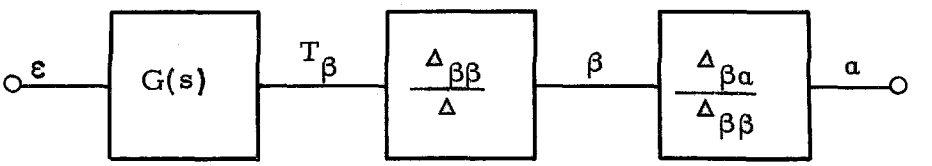

a) No Feedback

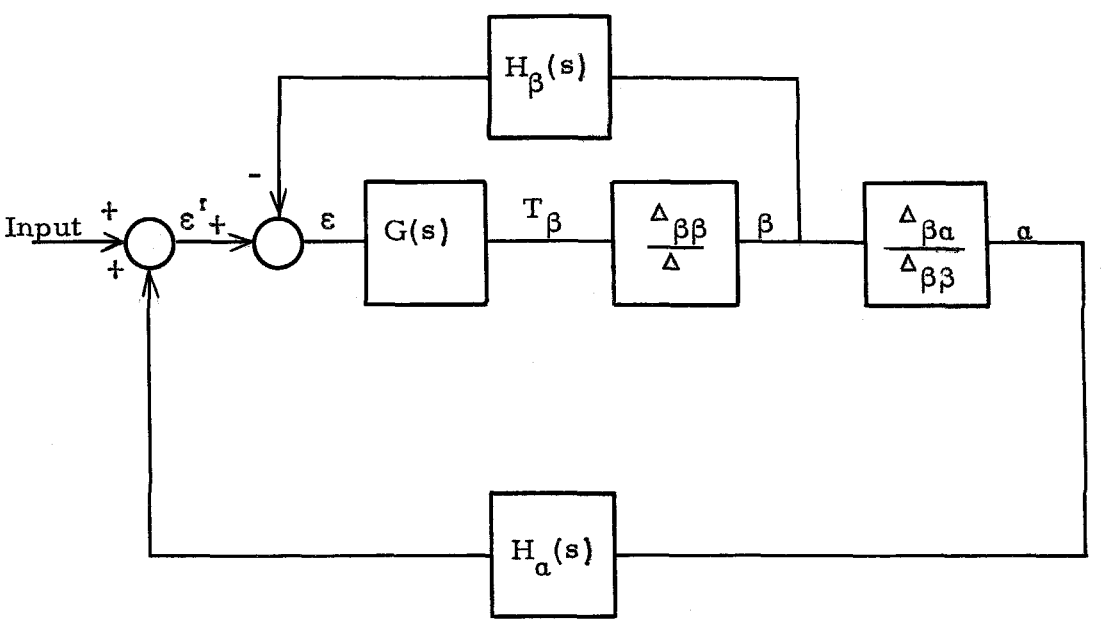

b) With α and β Feedback

Redrawing of Figure 3.2 with No Feedback,

and With α and β Feedback

Figure 3.5

The equivalence of the block diagram of figure 3.5a to that of figure 3.2 is seen from the fact that β and α in both figures are described by the same transfer function, given in equation 3.2.

The form of figure 3.5b places emphasis on the flap servo as an internal loop, whose main purpose is to control β motion to follow the command signal ε'. Thus if the flap servo were ideal, β would equal $\frac{\varepsilon'}{H_\beta(s)}$ and figure 3.5b would reduce to figure 3.6.

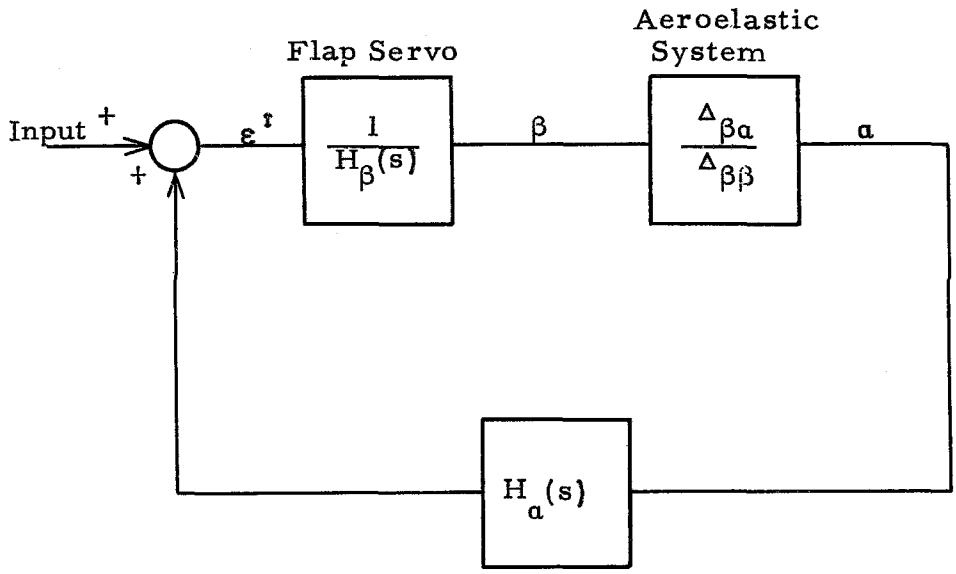

Equivalent Block Diagram of Figure 3.5b,
Assuming Perfect Flap Servo

Figure 3.6

The ideal representation of figure 3.6 shows that the lags and non-linearities of the actuator are removed by the flap servo. The lags in an actual system are shown to be quite small and hence close to this ideal in appendix E. These do not appreciably influence

the theory of this or the following parts.

The characteristic equation of the system of figure 3.6 is given in equation 3.18. This is used in the root locus diagrams of the quantitative study of part V.

$$1 - \frac{H_\alpha(s)}{H_\beta(s)} \frac{\Delta_{\beta\alpha}}{\Delta_{\beta\beta}} = 0 \qquad (3.18)$$

The major difference in form between equation 3.18 and the original equation, equation 3.4, is that the poles of the loop gain* are the zeros of $\Delta_{\beta\beta}$ instead of Δ. This is to be expected, since the poles of equation 3.18 represent the roots of the system with no α feedback ($H_\alpha(s)$ equal to zero in equation 3.18). Instead of these roots being the zeros of Δ, as they were with no β internal feedback, the presence of the very strong β feedback, assumed in figure 3.6, makes these characteristic roots essentially the zeros of $\Delta_{\beta\beta}$, the characteristic determinant with β constrained to zero.

The design of this internal β feedback loop or flap servo is treated in detail in reference 5**. In that study no additional α feedback was considered. It is noted from equation 3.18 that the system of figure 3.6, where a β motion is made to follow some prescribed command, has the same significant zeros in the loop gain as the system of figure 3.2***, where a β torque is made to

---

*The loop is considered closed through α, since β is an internal loop in figure 3.5b, and does not appear in figure 3.6.
**This reference should be referred to for detailed explanation of flap servo design from flutter considerations.
***Consider only α feedback used in figure 3.2.

follow some given order. These significant zeros are those of $\Delta_{\beta a} = 0$ in both cases. Thus the condition for increase in flutter speed is the same in both cases. This illustrates that the major effect of the flap servo is to remove the non-linearities and lags of G(s), but not to change the possibility of the stabilization.

PART IV

QUANTITATIVE INVESTIGATION OF THE POSSIBILITY OF STABILIZATION USING FEEDBACK THROUGH THE CONTROL SURFACE ACTUATOR (11 TEST CASES)

The theory of the last part showed that stability was possible at any speed using feedback control if, and only if, at least one of the quantities $\Delta_{\beta h}$, $\Delta_{\beta \alpha}$ and $\Delta_{\beta\beta}$ had all L.H.P. zeros at that speed (for the distributed system, these refer to the coordinate at an outboard cell). The appropriate feedback coordinate for such a case would be the coordinate associated with the cofactor having only L.H.P. zeros. The present part is a quantitative investigation of a large number of test cases to ascertain the improvement in flutter speed that can be obtained.

Up to the present time, no feasible technique has been developed of finding directly the zeros of the determinant of an aeroelastic matrix representing say four or more finite difference cells or at least ten degrees of freedom (two aileron β coordinates). This is true even when employing large scale digital computers*. On the other hand, it is certainly feasible to find the zeros of the determinant for a three degree of freedom system. It is felt that the examination of ten different, but typical, three degree of freedom systems, and the determination of the improvement obtained in flutter speed by feedback control of each coordinate h, α and β, gives a fairly good picture of what can be accomplished in actual systems with distributed properties.

---

*A program is under way at the California Institute of Technology Computing Center to develop such techniques using digital computers.

To support this statement, consider the normal coordinate representation of a system. The actual distributed system need be represented by only its first two or three modes to obtain flutter results of sufficient accuracy. The three degree of freedom system likewise has three modes. Hence for a given distributed system, there exists a three degree of freedom system with similar flutter properties. While this argument is heuristic it does indicate that examination of many typical three degree of freedom systems in order to establish trends is analogous to examining many distributed systems for the same purpose*. The cases to be studied, therefore, are eleven three degree of freedom systems. One of these is a three degree of freedom model of an actual wing whose flutter properties are well known from previous studies.

4.1 Stability Cofactors of Three Degree of Freedom System

Reference 4 is an extensive quantitative study of two and three degree of freedom systems. It gives the variation in flutter speed as the nine basic non-dimensional parameters of the system are varied. The results tabulated in that reference were used as a guide to indicate those parameters that should be varied in the ten study cases. The values of the nine basic parameters selected for these ten study cases are listed in table 1, where the notation of reference 4 is used with the exception of x_β and r_β (see list of symbols).

---

*The study of three degree of freedom systems to establish trends for distributed systems is an established practice. See reference 4.

TABLE 1

System Parameters for Three Degree of Freedom Study Cases

Case	$\frac{\omega_\alpha}{\omega_h}$	x_r	$\frac{r_\alpha^2}{b^2}$	$\frac{x_\alpha}{b}$	K	$\frac{m}{M}$	c	$\frac{r_\beta^2}{b^2}$	$\frac{x_\beta}{b}$
1	3	.3	.25	.3	.05	.10	.4	.030	.15
2	1.3	.3	.25	.3	.05	.10	.4	.030	.15
3	2.0	.3	.25	.3	.10	.10	.4	.030	.15
4	3.0	.4	.25	.3	.05	.10	.4	.030	.15
5	3.0	.3	.25	.15	.05	.10	.4	.030	.15
6	3.0	.4	.25	.15	.05	.10	.4	.030	.15
7	3.0	.3	.25	0	.05	.10	.4	.030	.15
8	3.0	.3	.25	.30	.05	.10	.4	.006	0
9	3.0	.3	.25	.30	.05	.10	.4	.030	0
10	3.0	.4	.25	.15	.05	.10	.4	.030	0

Case 1 is basic system. Variations from basic system in other cases are underlined. (See list of symbols for definitions)

A base case, case 1, was chosen. Its parameter values* are essentially those of the system studied in reference 5. The major numerical changes from the base case in the other nine test cases studied were in the quantities x_r, x_a, x_β and ω_h/ω_a. These represent geometric variations in elastic axis location, c.g. of the wing relative to the elastic axis, and c.g. of control surface relative to the hinge. Also a variation in bending to torsion frequency is represented by changes in ω_h/ω_a. Thus it is felt these ten cases constitute a fairly representative variation of the parameters which influence flutter. The only additional point concerning the constants of table 1 that may need clarification concerns the change of x_β to a value of zero in cases 8, 9 and 10 (a shift of the c.g. of the control surface to the hinge line). This can be accomplished by mass balancing the control surface, thereby producing very little change in r_β (cases 9 and 10). Again, it might be accomplished by an actual change in hinge line location, thereby substantially reducing r_β (case 8).

Modified expressions are derived in appendix C for the $\Delta_{\beta h}$, $\Delta_{\beta a}$ and $\Delta_{\beta\beta}$ cofactors. These are given in equation C.13, as fifth degree polynomials in the non-dimensional Laplace transform variable, $\bar{s}$. The coefficients of these polynomials are dependent on a non-dimensional speed variable, $\bar{v}$, expressed in per unit of the divergence speed of the wing. The zeros of these polynomials are the required zeros of $\Delta_{\beta h}$, $\Delta_{\beta a}$ and $\Delta_{\beta\beta}$.

---

*Except for the value of ω_h/ω_a.

The representation used for the aerodynamic forces in the aeroelastic matrix, equation C.10, from which $\Delta_{\beta h}$, $\Delta_{\beta \alpha}$ and $\Delta_{\beta \beta}$ are derived, is a slightly simplified form of the subsonic, incompressible flow equations given in reference 6. The aerodynamic inertia terms are neglected in equation C.10 since these usually have small effect. Also the Theodorsen function has been approximated by a ratio of first degree polynomials in s*.

The C constants(C'', C' and C) of equation C.13 are defined in terms of another set, the B constants (B'', B', and B) in equation C.14. These B constants are in turn defined in terms of the nine basic system parameters in equations C.15 a, b, c. Thus for each test case studied, the B constants are computed directly from the physical constants of table 1. In turn the C constants are computed from the B constants, specifying the coefficients of equation C.13 as functions of speed. The zeros of the fifth degree polynomials in $\bar{s}$ are then found** at each speed, usually consisting of two sets of complex conjugate roots and a real root.

The zeros of $\Delta_{\beta h}$, $\Delta_{\beta \alpha}$ and $\Delta_{\beta \beta}$ were obtained over a speed range 0 to divergence. These are plotted in figures 4.1 through 4.3 for each test case, with speed as a parameter. The detailed characteristics of these curves are discussed at length later in this part. For the present only the primary purpose will be considered - the determination of whether right half plane zeros exist.

---

*Even with these approximations, the calculated flutter speed differed by only 10% in typical cases from that calculated by the more exact equations of reference 4.

**Using a Datatron digital computer.

The zeros of $\Delta_{\beta h}$ exist in all ten cases in the right half plane over practically the entire speed range, in particular on the positive real axis. Therefore $\Delta_{\beta h}$ can in no way be a possible stabilizing cofactor in any of these cases. Because of the R. H. P. characteristics of the zeros of $\Delta_{\beta h}$, only one test case is shown explicitly in figure 4. 1, while all ten cases are shown for $\Delta_{\beta\alpha}$ and $\Delta_{\beta\beta}$ in figures 4. 2 and 4. 3. Only the upper half $\bar{s}$ plane zeros are plotted in figures 4. 1, 4. 2 and 4. 3, the complex conjugates existing in the lower half plane.

Table 2 is a listing of the speed range for which each cofactor $\Delta_{\beta h}$, $\Delta_{\beta\alpha}$ and $\Delta_{\beta\beta}$ has L. H. P. zeros, obtained from inspection of figures 4. 1, 4. 2 and 4. 3. It was noted in part III that $\Delta_{\beta\beta}$ represents the characteristic determinant of the aeroelastic system with locked aileron, or that of the basic wing. Therefore, in order to increase the flutter speed of the aeroelastic servo system above that of the basic wing by feedback control, the zeros of $\Delta_{\beta\alpha}$ or $\Delta_{\beta h}$ must be L. H. P. up to a higher speed than those of $\Delta_{\beta\beta}$. Of the ten cases studied, four have this property in $\Delta_{\beta\alpha}$. As mentioned above, none have this property in $\Delta_{\beta h}$.

The result of this ten study case investigation leads to the quite definite conclusion that h feedback offers very little hope of stabilization in any aeroelastic system, and that if any stabilization is to be achieved, it must come from α feedback. This seems plausible from physical reasoning, also, since the destabilizing aerodynamic forces depend primarily on angle of rotation, α, and only secondarily on h. Thus a likely stabilizing feedback would be an α source, not an h source.

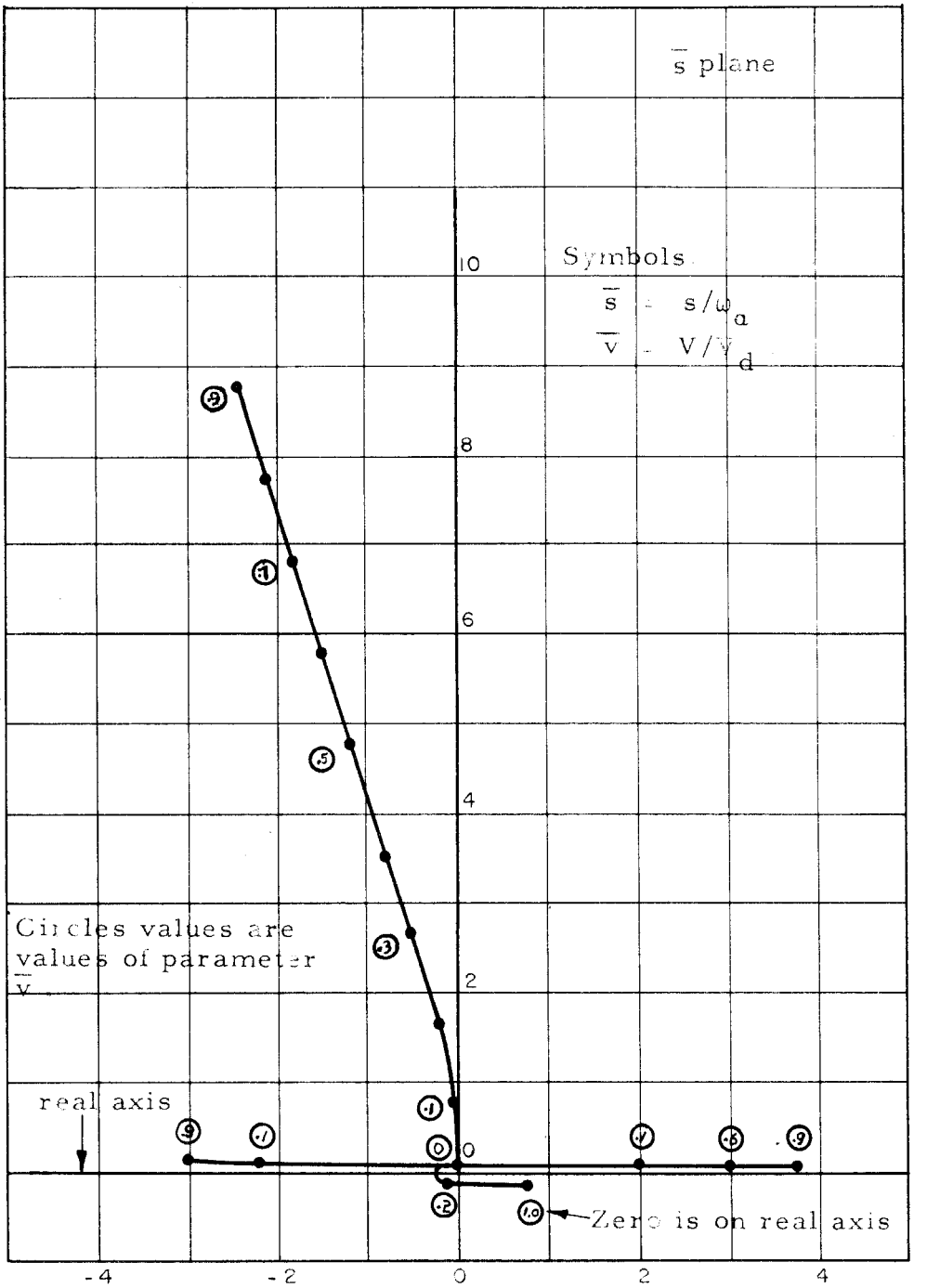

Zeros of $\Delta_{\beta h}$ vs. Speed.
Case 1.

Figure 4.1

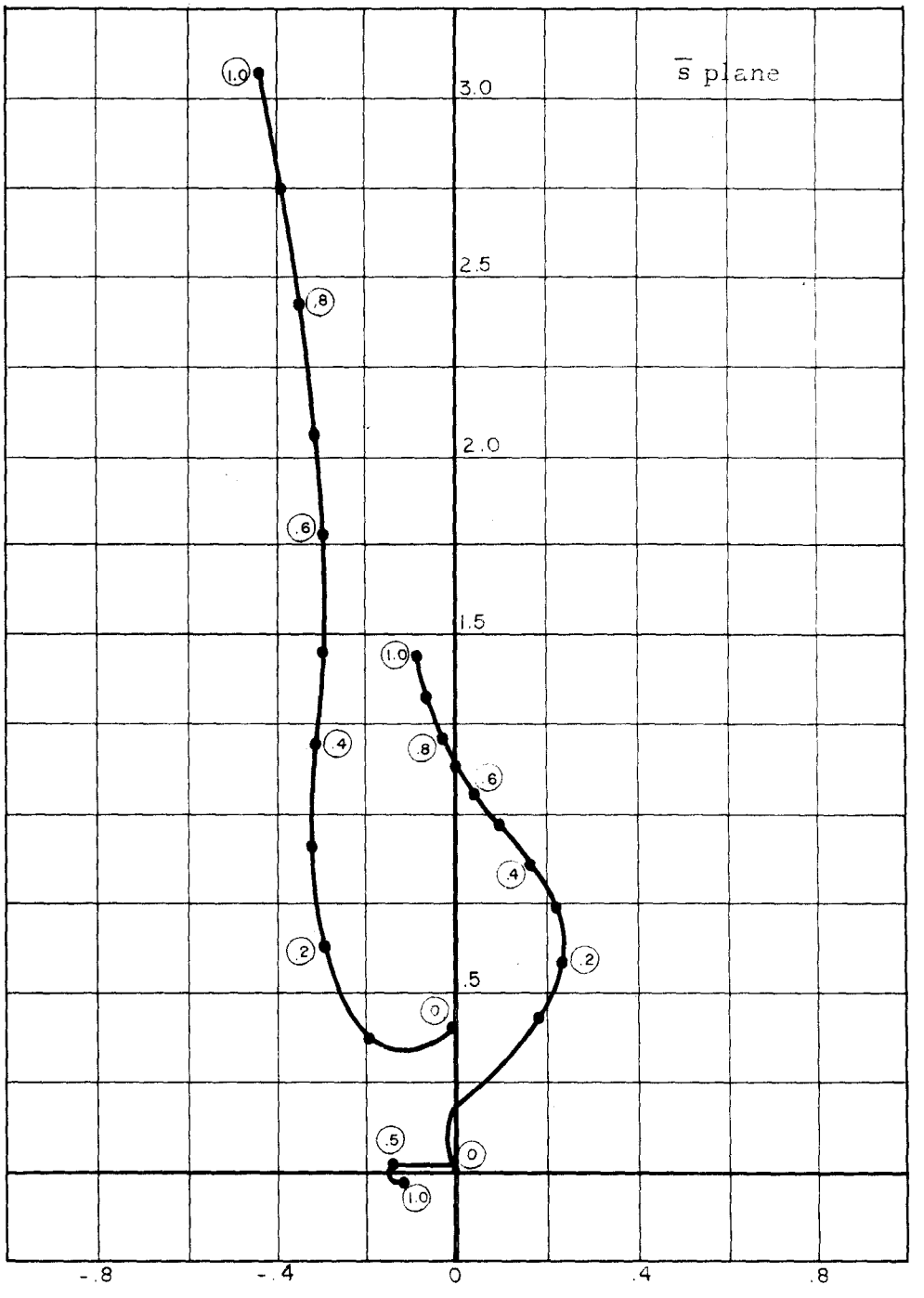

Zeros of $\Delta_{\beta a}$, Case 1.

Figure 4.2a.

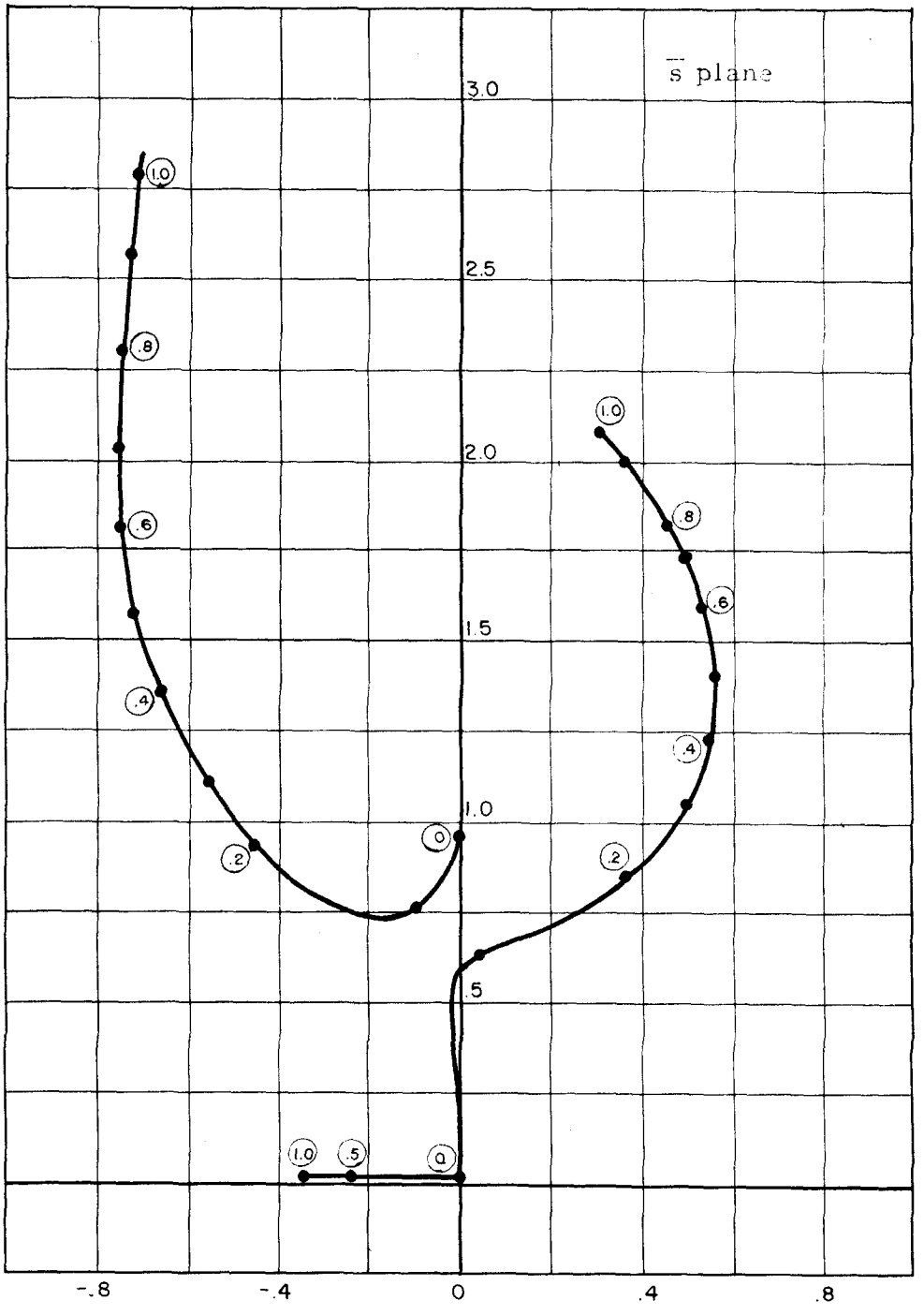

Zeros of $\Delta_{\beta\alpha}$, Case 2

Figure 4.2b

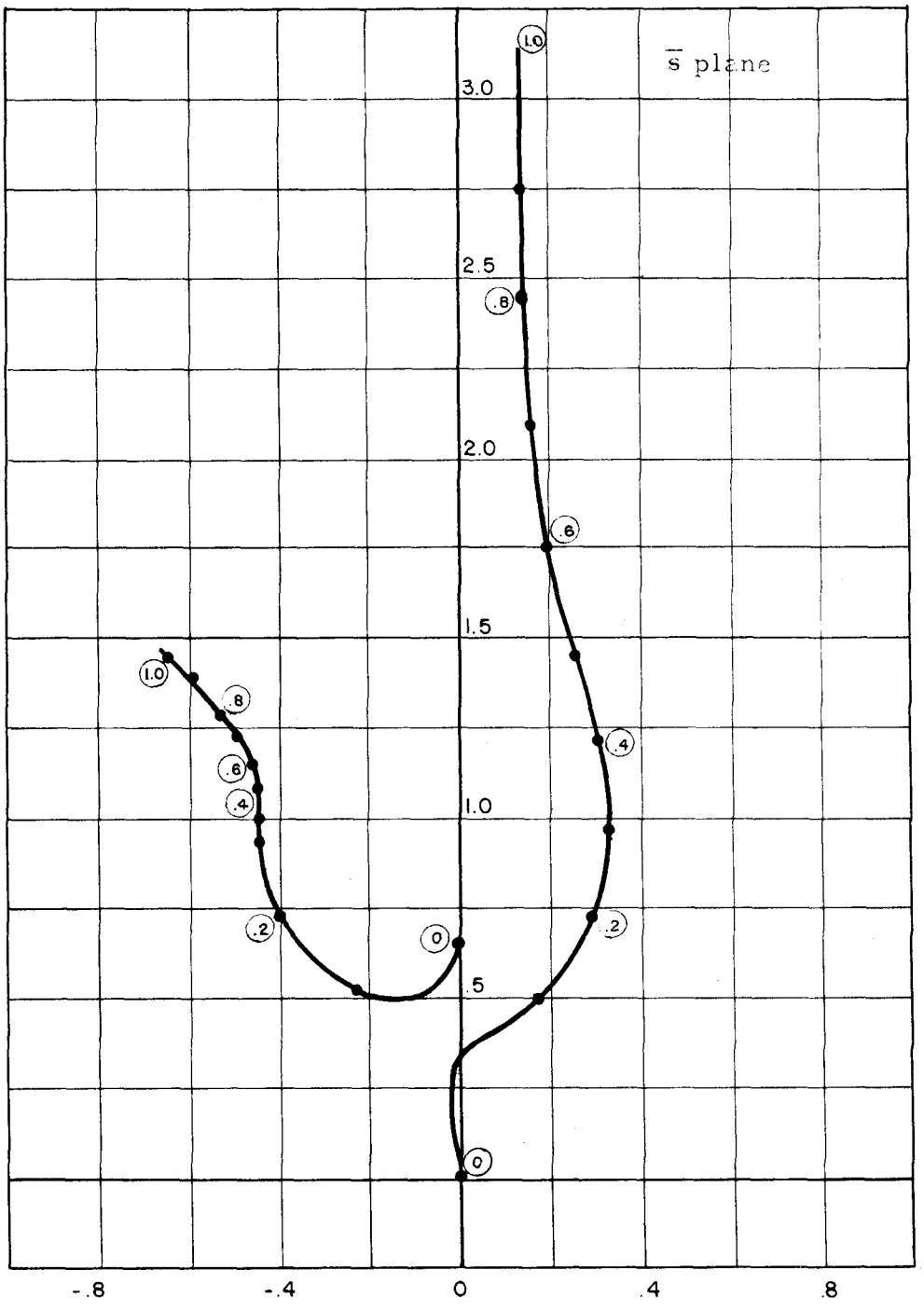

Zeros of $\Delta_{\beta a}$, Case 3

Figure 4.2c.

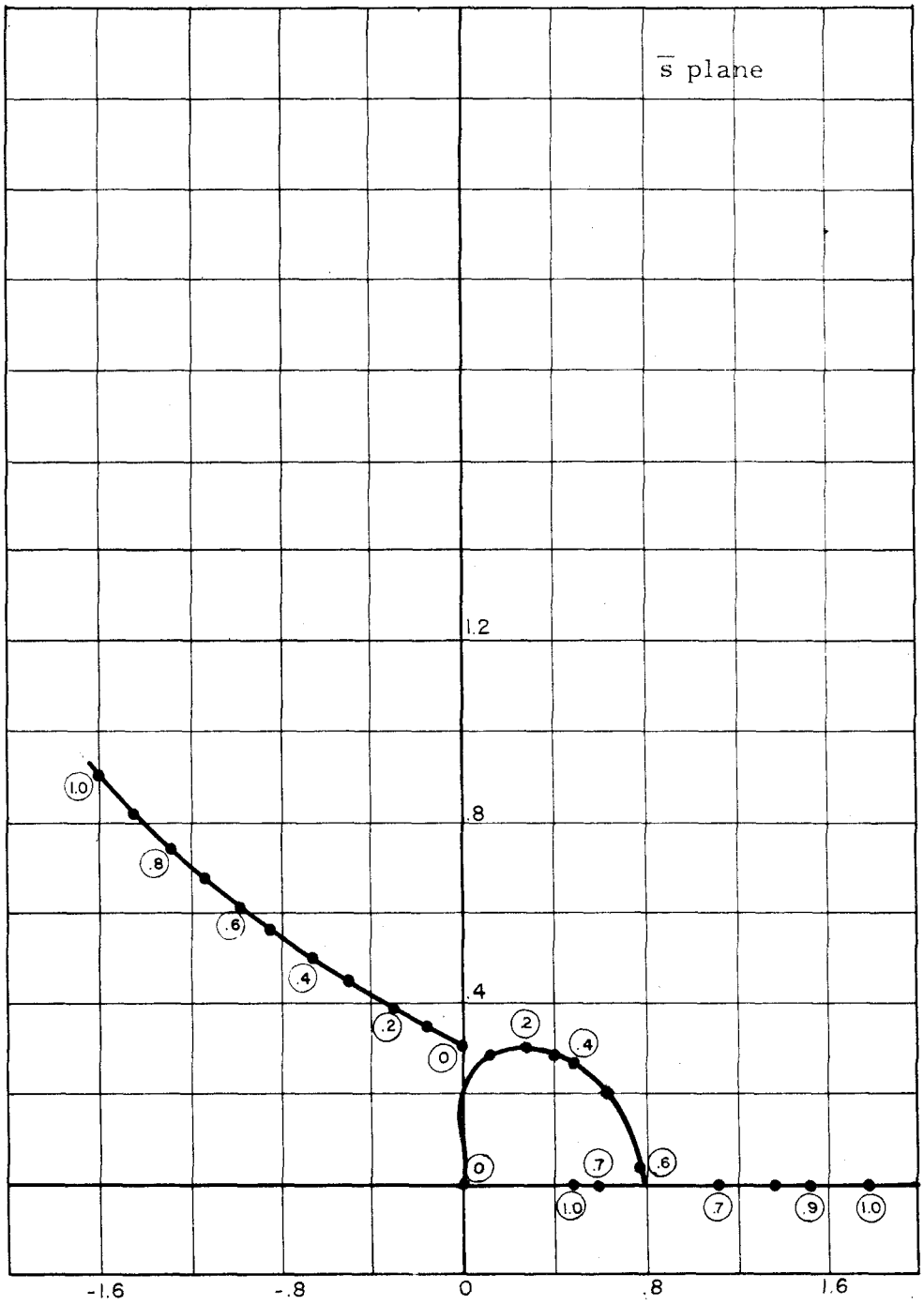

Zeros of $\Delta_{\beta a}$, Case 4.

Figure 4.2d

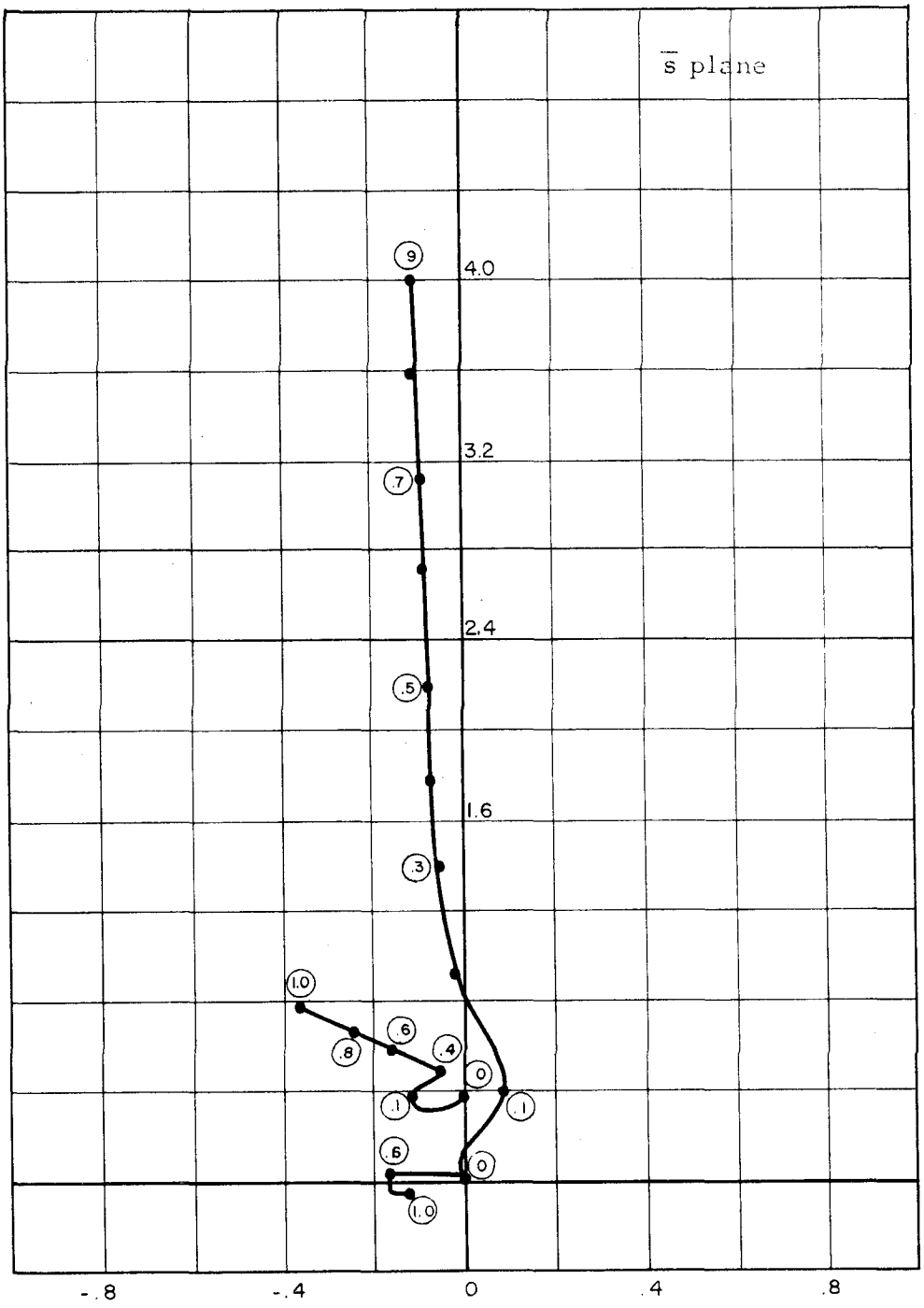

Zeros of $\Delta_{\beta\alpha}$, Case 5.

Figure 4.2e.

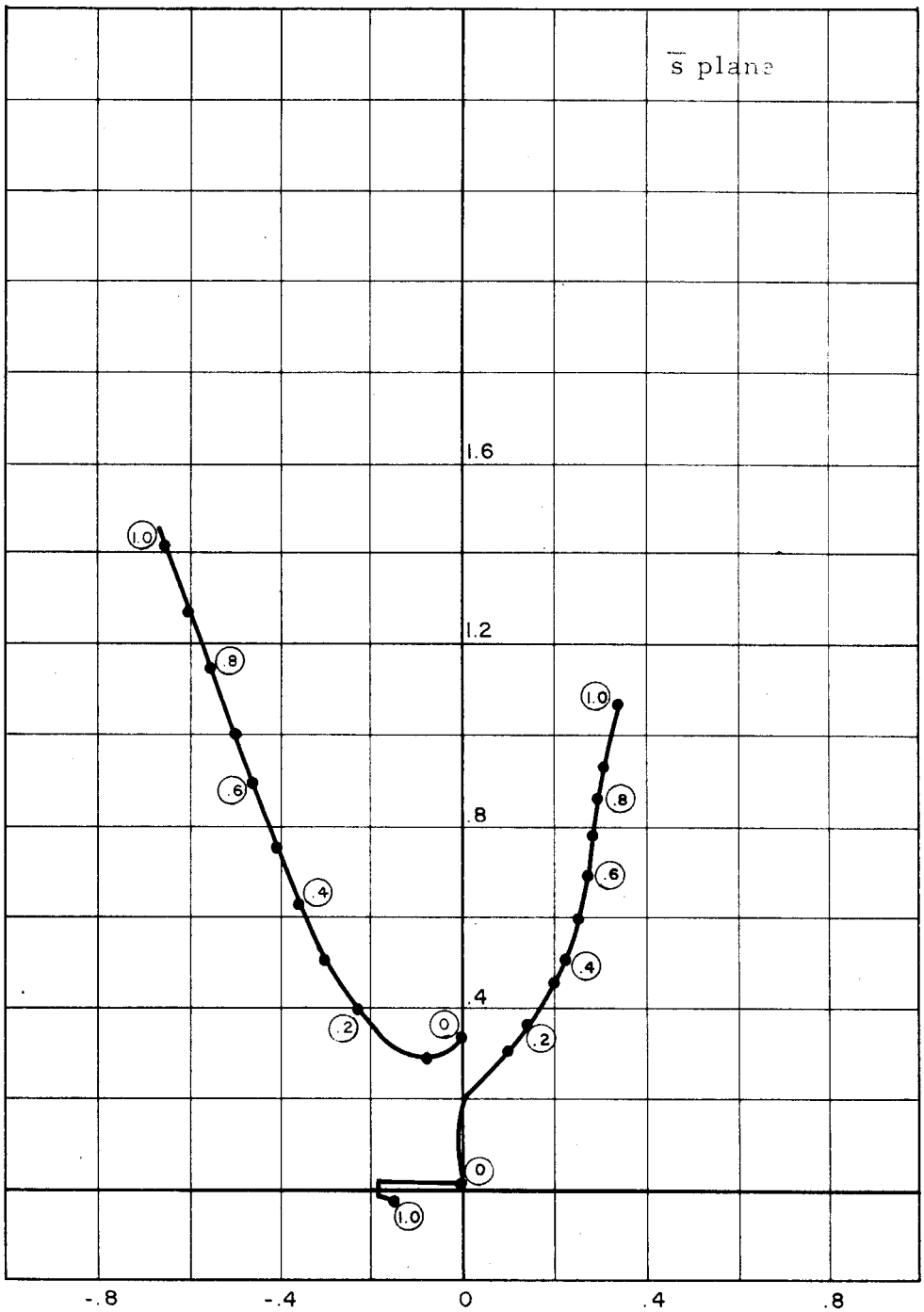

Zeros of $\Delta_{\beta\alpha}$, Case 3.

Figure 4.4f.

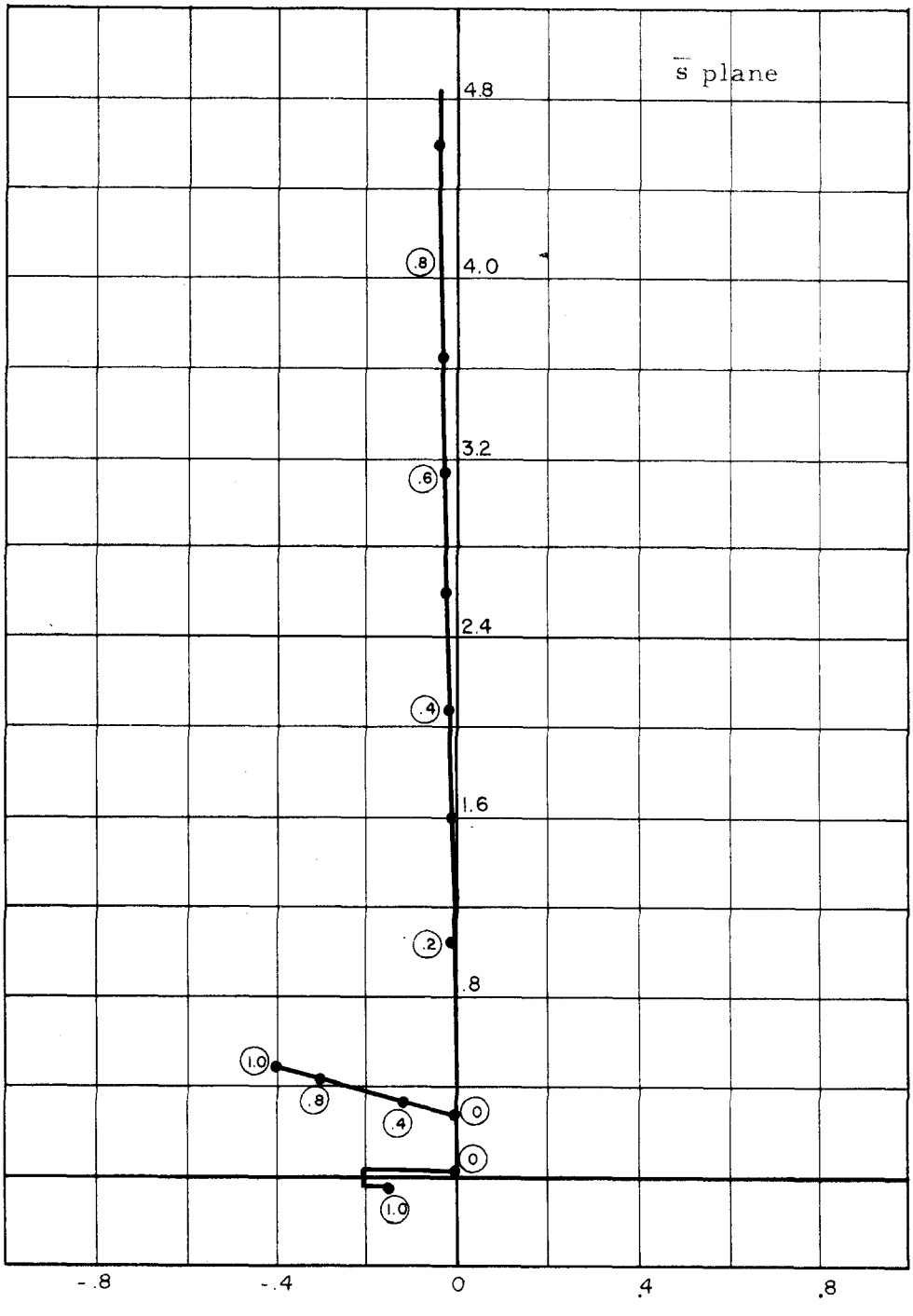

Zeros of $\Delta_{\beta a}$, Case 7.

Figure 4.2g.

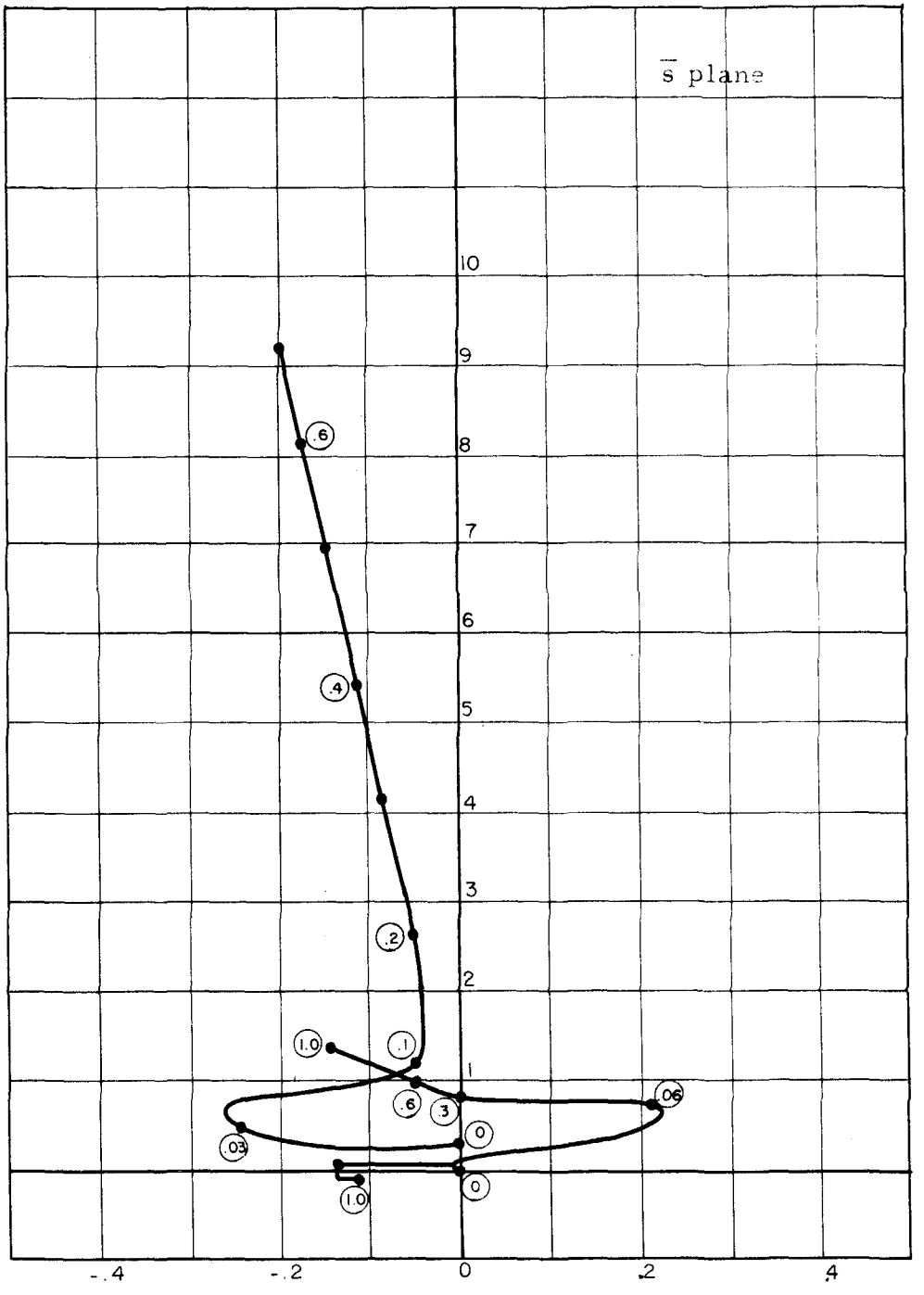

Zeros of $\Delta_{\beta a}$, Case 8.

Figure 4.2h.

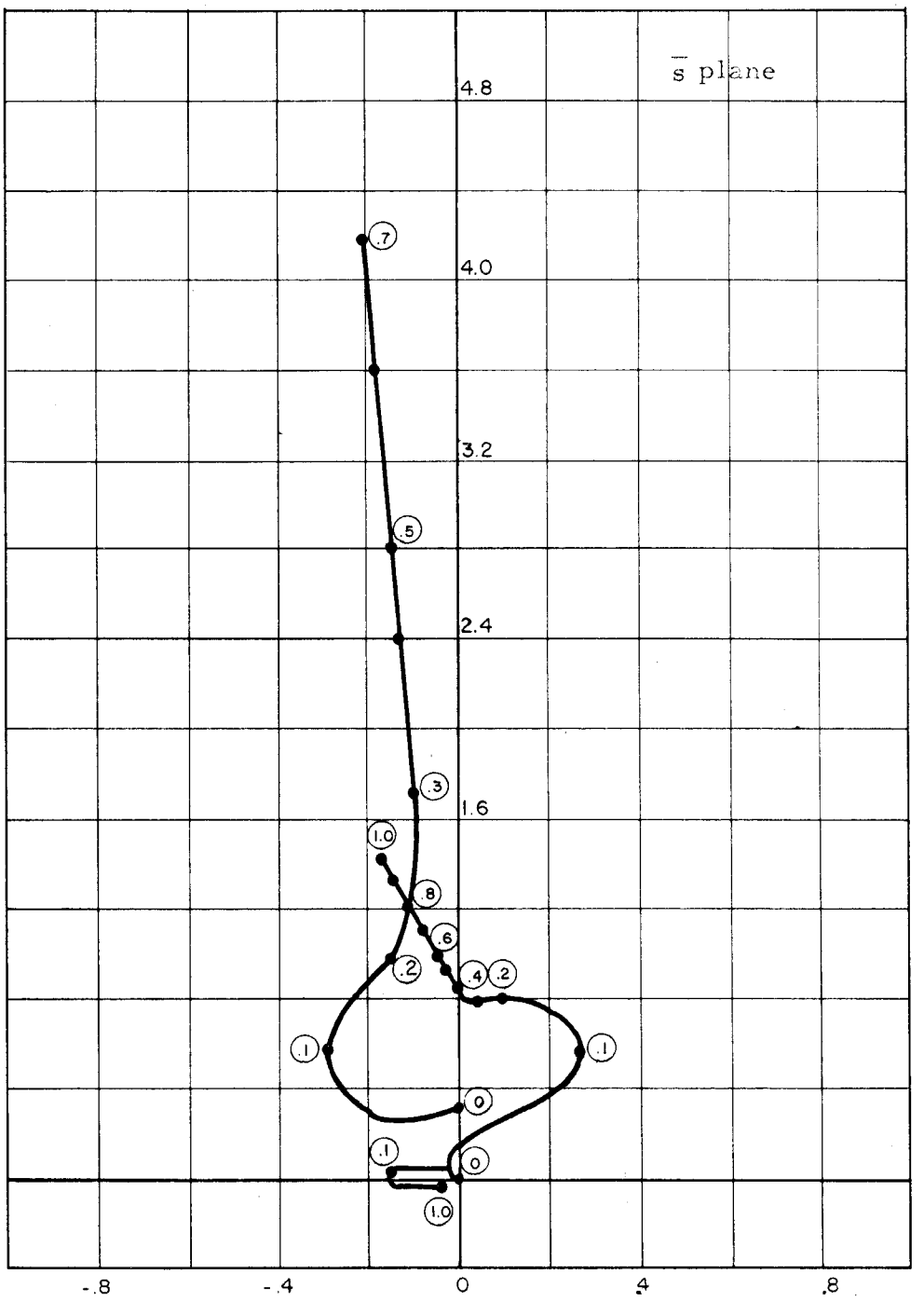

Zeros of $\Delta_{\beta a}$, Case 9

Figure 4.21

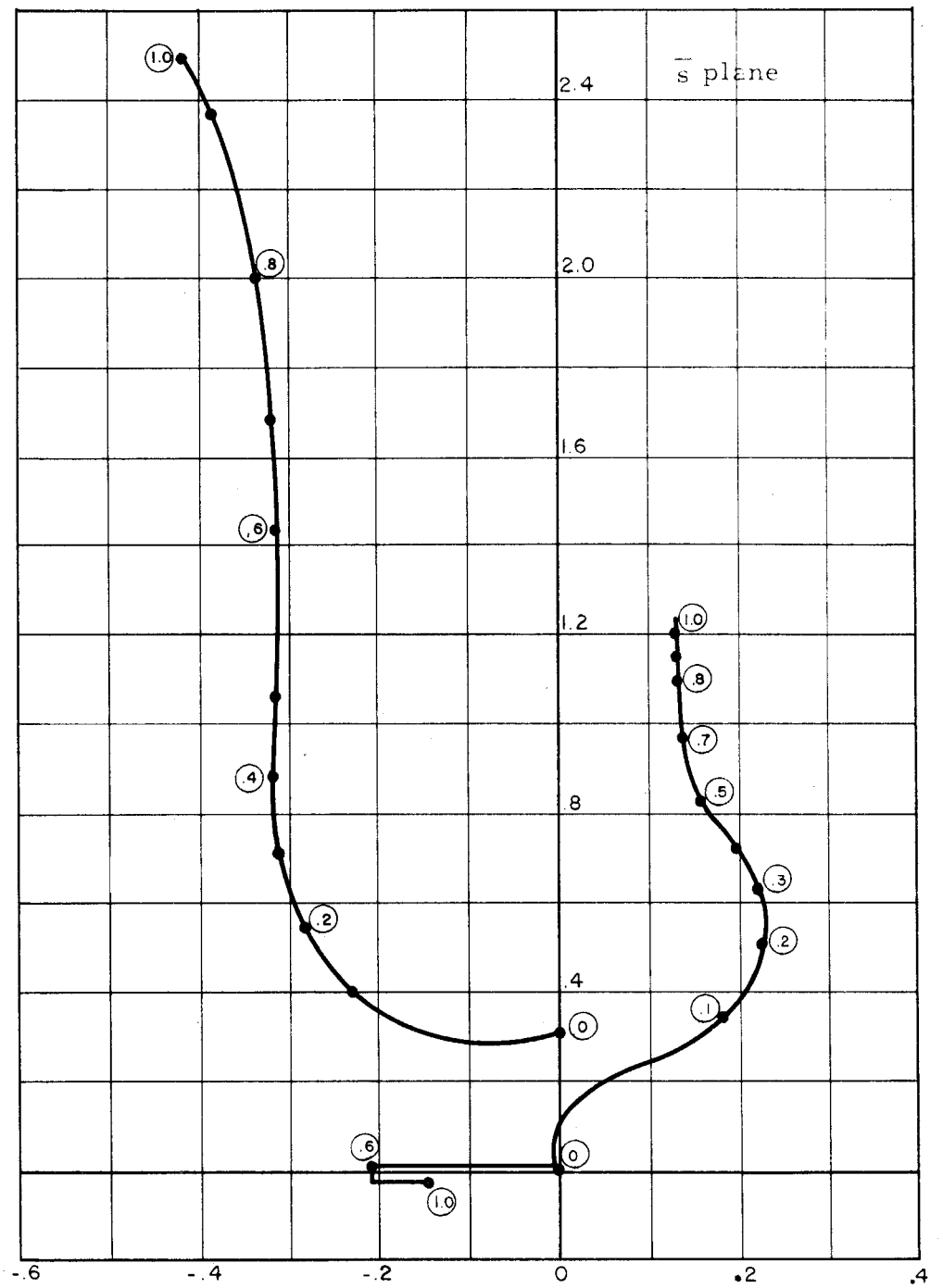

Zeros of $\Delta_{\beta\alpha}$. Case 10.

Figure 1.2j

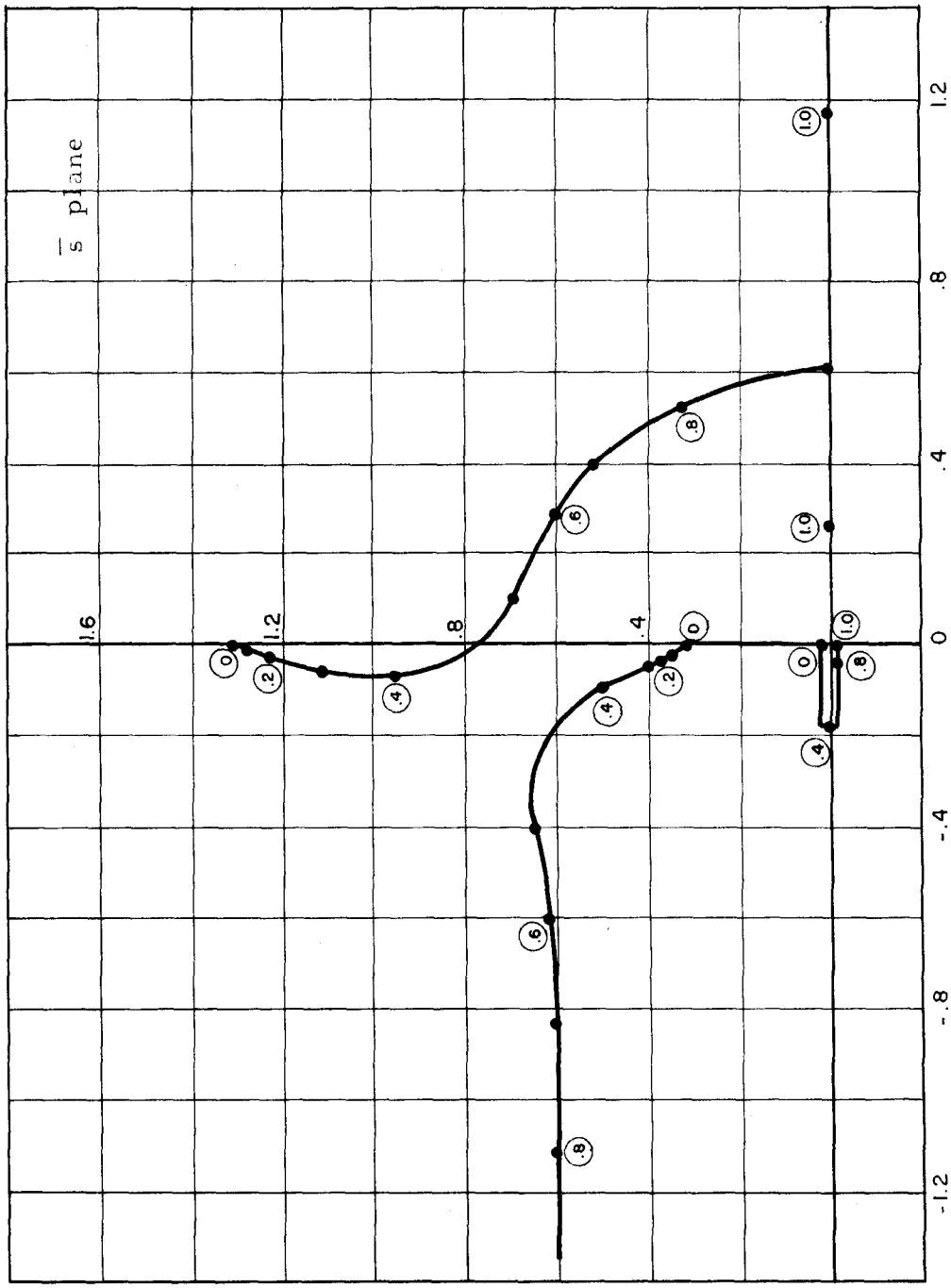

Zeros of $\Delta_{\beta\beta}$, Cases 1, 8, 9

Figure 4.3a

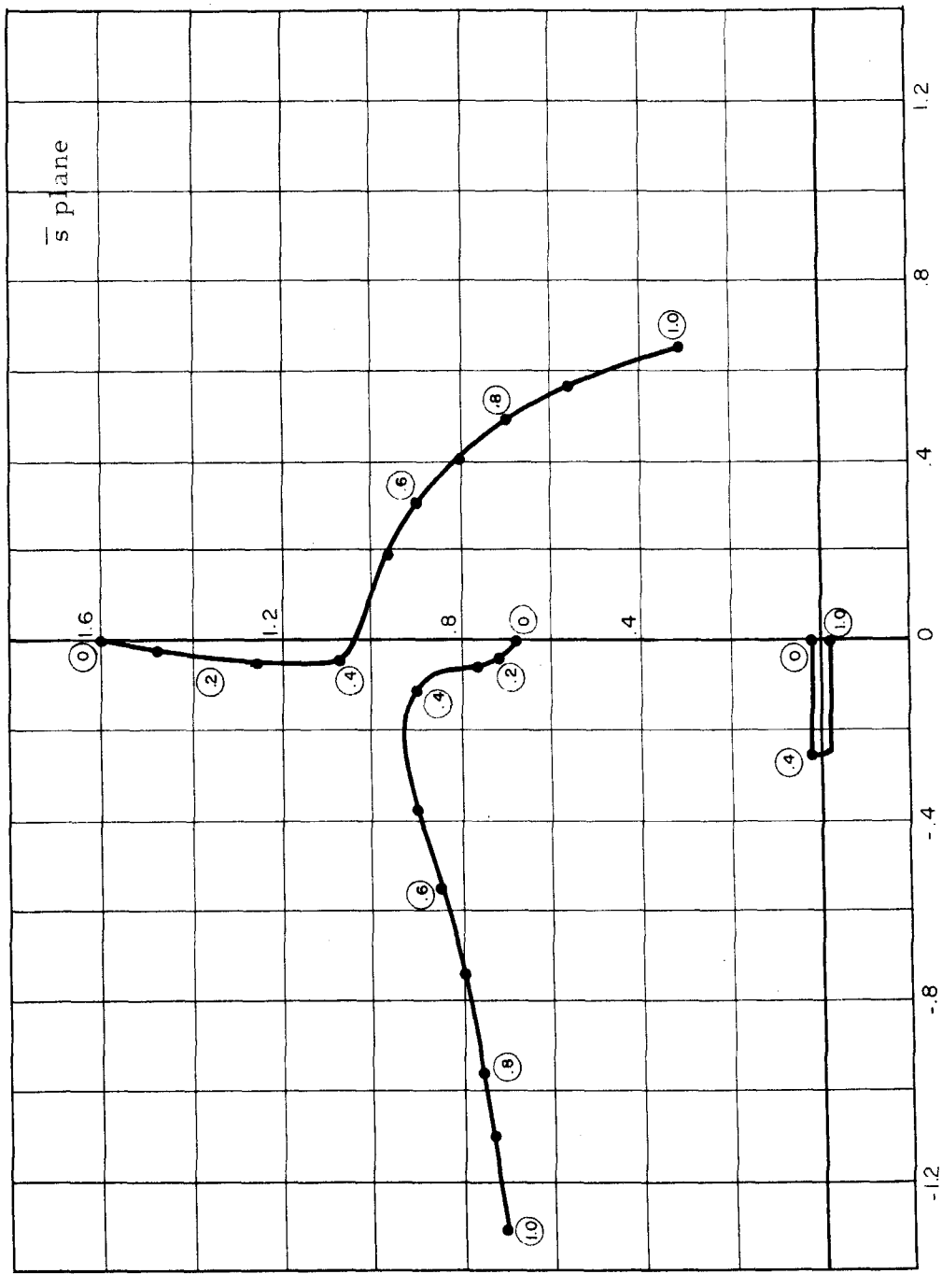

Zeros of $\Delta_{\beta\beta}$, Case 2

Figure 1.3

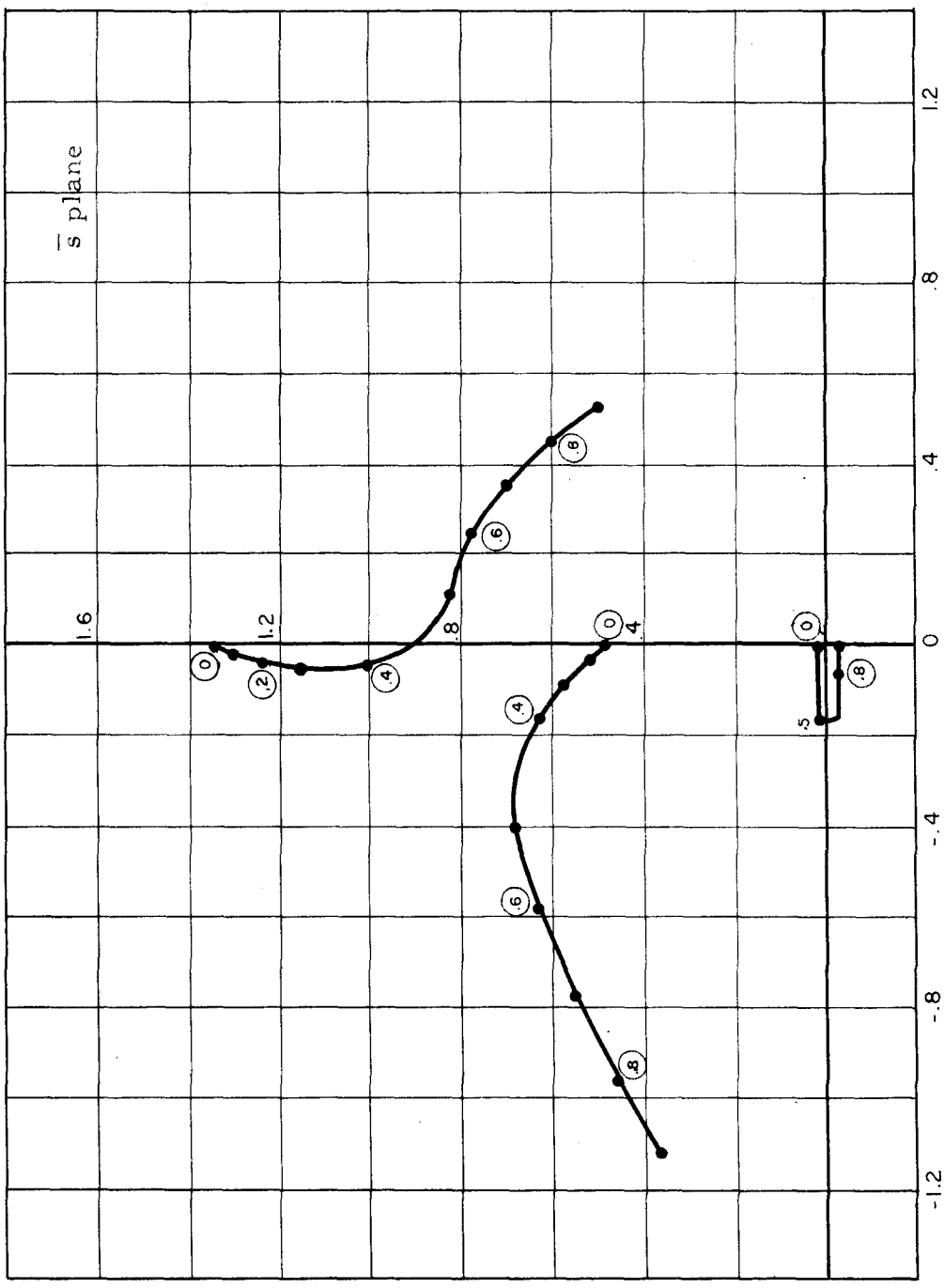

Zeros of $\Delta_{\beta\beta}$, Case 3.

Figure 4.3c.

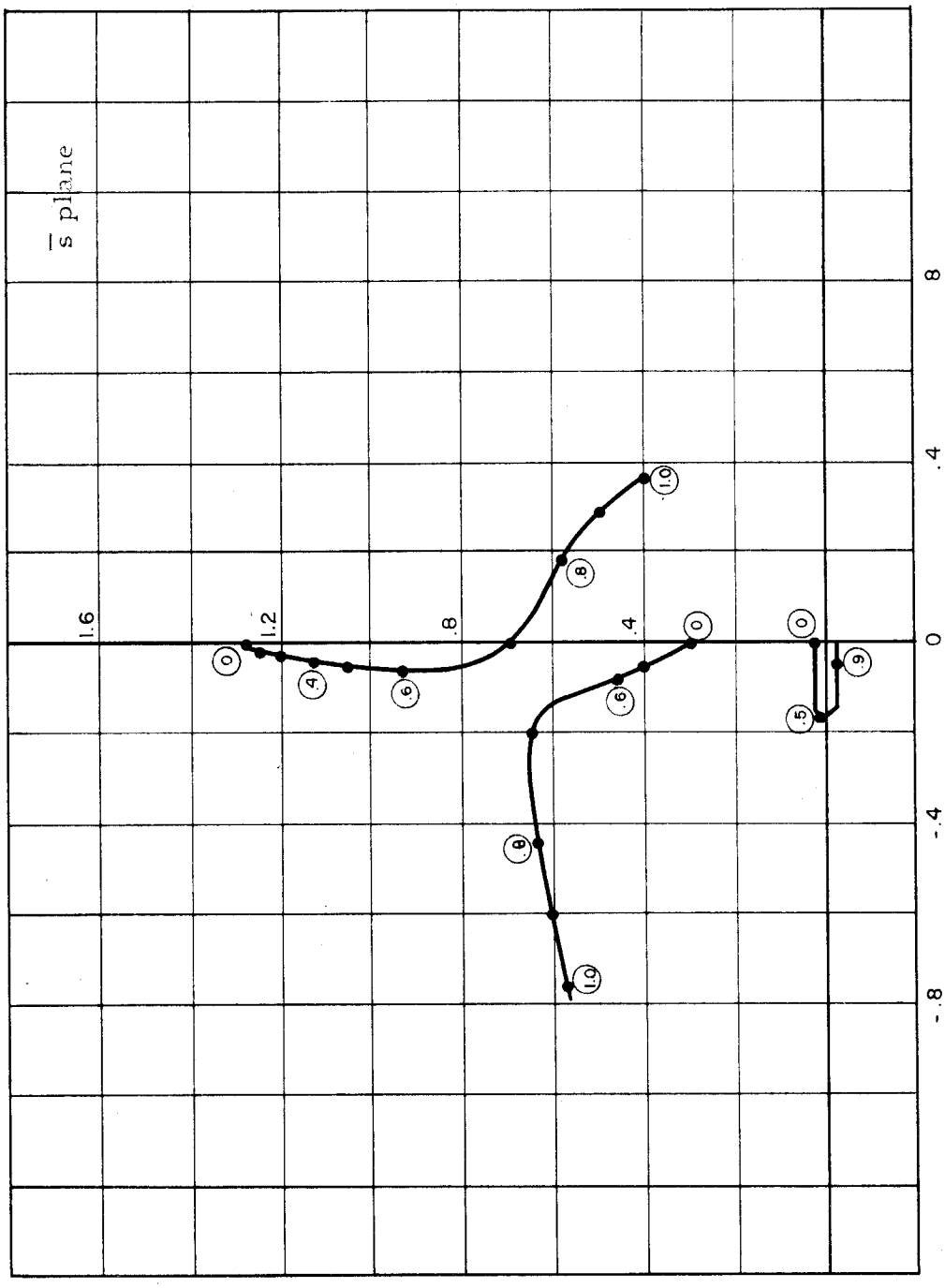

Zeros of $\Delta_{\beta\beta}$, Case 4.

Figure 4.3d

Zeros of $\Delta_{\beta\beta}$, Case 2

Figure 3.2ℓ

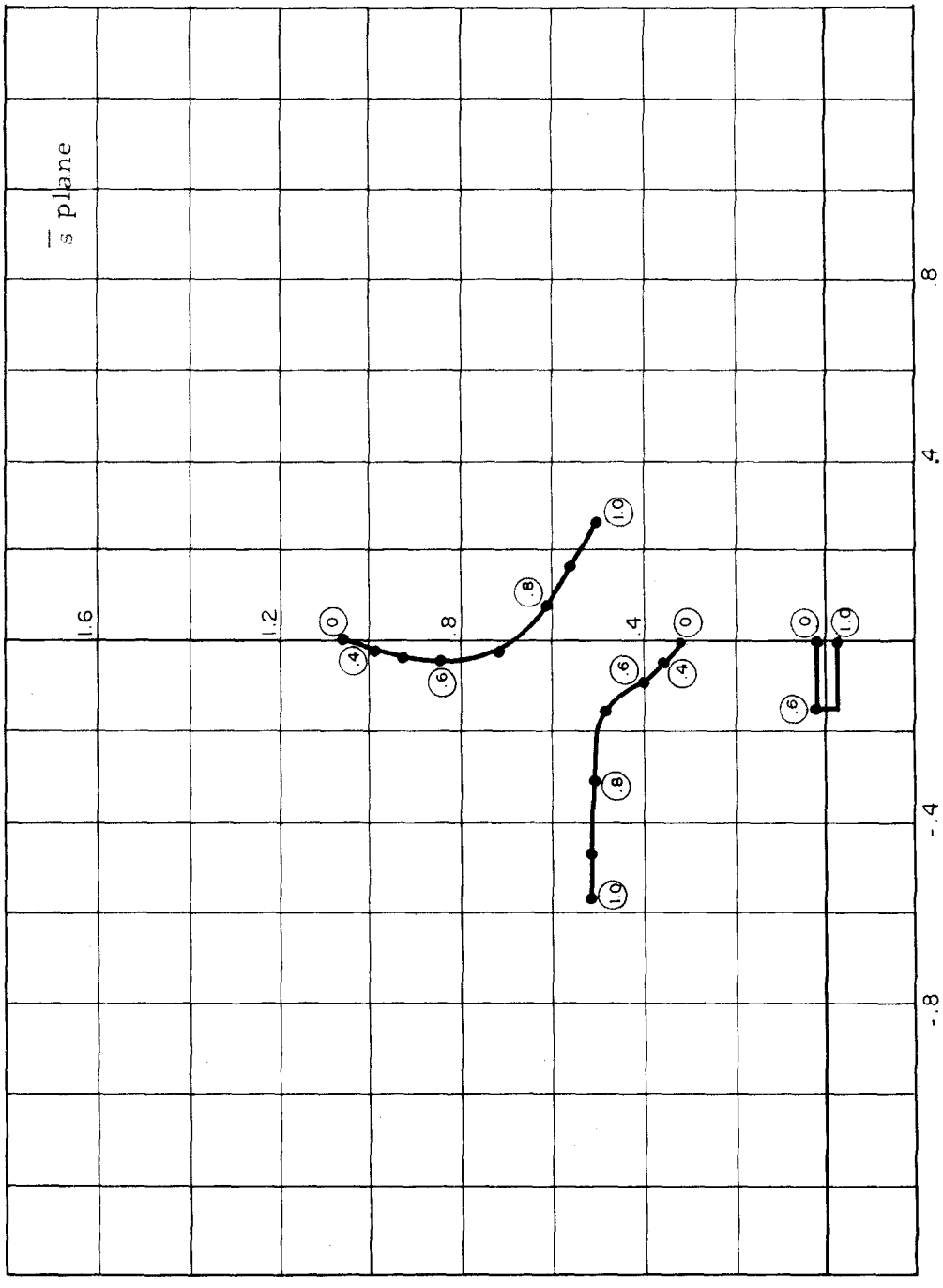

Zeros of $\Delta_{\beta\beta}$, Cases 6 and 10.

Figure 4.3f

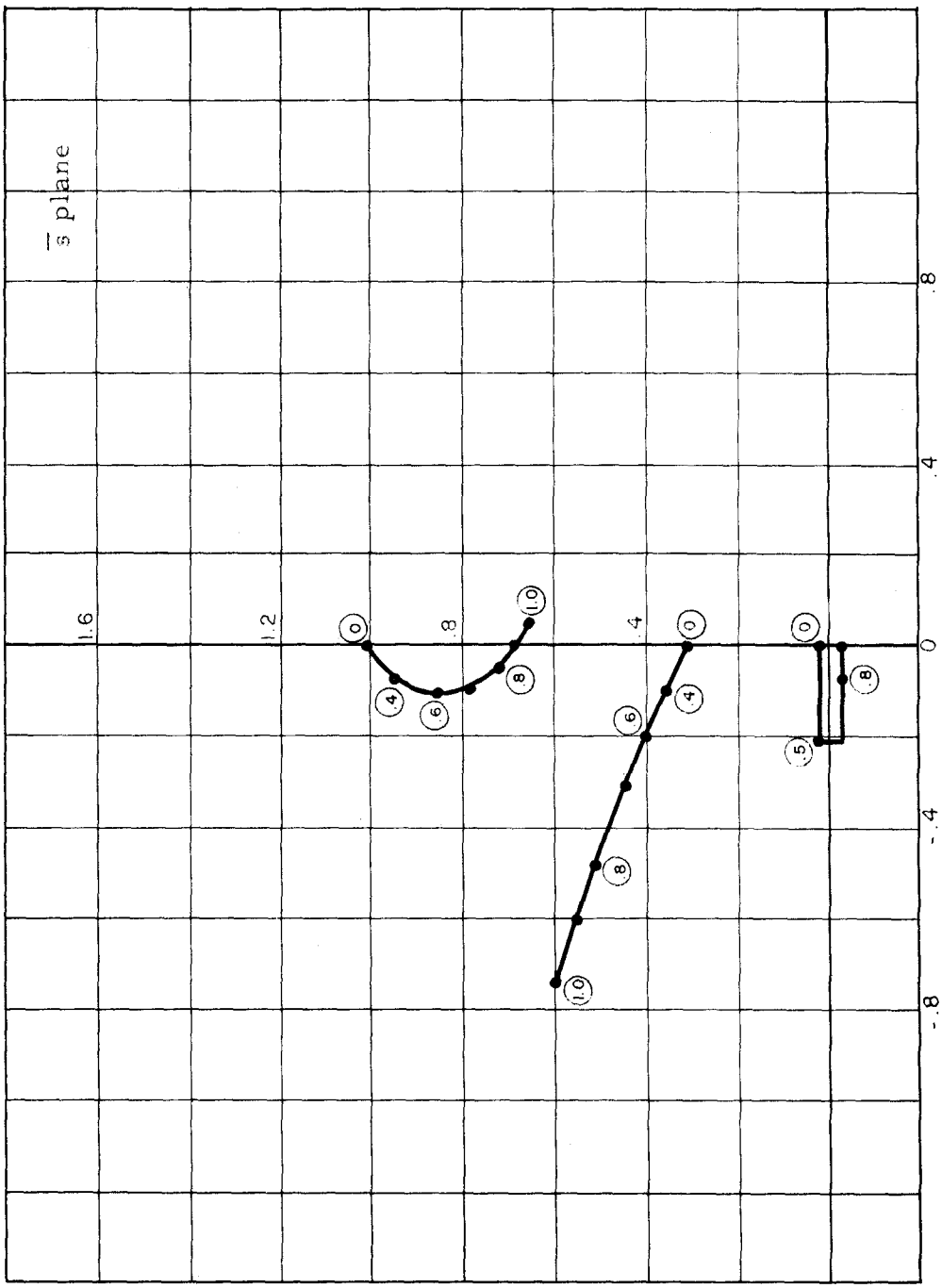

Zeros of $\Delta_{\beta\beta}$, Case 7

Figure 4.3g.

TABLE 2

SPEED RANGE FOR WHICH SYSTEM COFACTORS HAVE ONLY L. H. P. ZEROS (EXPRESSED IN PER UNIT OF WING DIVERGENCE SPEED)

Case	$\Delta_{\beta h}$	$\Delta_{\beta \alpha}$	$\Delta_{\beta \beta}$
1	0	0 to .03 and .7 to 1.0	0 to .46
2	0	0 to .08	0 to .42
3	0	0 to .06	0 to .44
4	0		0 to .70
5	0	0 to .03 .19 to 1.0	0 to .56
6	0	0 to .06	0 to .72
7		0 to 1.0	0 to .90
8	0	0 to .002 and .3 to 1.0	0 to .46
9	0	0 to .01 and .4 to 1.0	0 to .46
10	0	0 to .02	0 to .72

Cases 5, 7, 8 and 9 can be stabilized by α feedback above the flutter speed of the locked aileron.

For the cases studied, speeds only up to 1.0 of divergence were investigated. In all four cases where stabilization is possible by α feedback - cases 5, 7, 8 and 9 - stabilization can be achieved up to and above this divergence speed, the exact excess not determinable since the data only went up to divergence speed. In case 5 the locked aileron flutter speed of .56 can be raised above 1.0 by α feedback, certainly a substantial improvement.

It should be noted in case 5, that the zeros of $\Delta_{\beta\alpha}$ are R.H.P. from a speed range .03 to .19. This means if α feedback is used over this speed range, instability would result, even though the aeroelastic system by itself is stable. However there is no need of using α feedback over this range, since the aeroelastic system is stable from 0 to .56. Thus the α feedback need not be made effective until speeds of .56 and above. While this suffices in principle, it is safer to cause α feedback to be effective at and above a speed which is approximately half way between the highest speed at which it causes destabilization (.19), and the minimum speed at which it is needed (.56). If α feedback is used only at this speed of .37 and above, stabilization should be safely accomplished from 0 speed to above divergence. At speeds above .37, the α feedback is safely above the speed at which it causes instability (.19); yet it has been introduced at a sufficiently low speed to ensure stabilization at speeds for which the aeroelastic system needs it (above .56). The margins are probably adequate even if the actual aeroelastic parameters are somewhat different than the calculated values.

Similar capability of stabilization exists for case 7, where the flutter speed can be raised from 0.9 of divergence to above divergence. For this case, no range of speeds exist for which $\Delta_{\beta\alpha}$ has R.P.H. zeros, as occurred in case 5.

In principle, cases 8 and 9 are also examples for which the flutter speed of the locked aileron (.46) can be raised by α feedback to above divergence. The existence of a large band of speeds over which $\Delta_{\beta\alpha}$ has R.H.P. zeros - from .002 to .3 in case 8, and from .01 to .4 in case 9 - makes the feasibility of such stabilization questionable in an actual system. For example, in case 9 the α feedback can not be introduced at speeds below .4 to avoid instability, and yet it must be effective at speeds below .46 to stabilize the aeroelastic system. Thus the best one could do would be to make the α feedback effective at the mean of these values or 0.43. This seems too close to the nominally unstable values of 0.40 and 0.46, so that a slight variation of system parameters from the nominal ones might cause instability.

The conclusions drawn from table 2 are that four of the ten cases can be stabilized, in principle, to appreciably higher speeds (sometimes doubled) by α feedback control. In practice probably only two cases, cases 5 and 7, could be instrumented with adequate safety margins.

4.2 Trends in Physical Quantities that Influence the Possibility of Stabilization by Feedback Control

These numerical results show that only certain aeroelastic systems can be stabilized by feedback control above the basic flutter speed of the wing. It is desirable to determine what physical parameters in an aeroelastic system influence the possibility of

such stabilization, in addition to the mathematical properties of $\Delta_{\beta\alpha}$ previously noted. Such studies have been previously carried out to determine the significant parameters influencing the flutter speed of the aeroelastic system by itself, such as reference 4, which also examines only three degree of freedom systems*. Page 15 of that reference draws an important conclusion concerning flutter of the basic wing (locked aileron), after examination of many systems numerically. This conclusion is that only one parameter is of great significance in determining the flutter speed for the case of most practical importance (ω_α/ω_h equal to 3 or greater). This parameter is the location of the c.g. of the wing relative to the center of pressure (quarter chord). For maximum flutter speed the c.g. should be as far forward as possible. The location of the e.a. has very small influence on flutter speed.

For our present problem, a careful scrutiny of the constants of the ten study cases in table 1, and also of the location of the c.g. relative to the quarter chord given in table 3, shows that this same parameter seems the important one in determining whether the flutter speed can be raised by feedback control. Of the seven cases studied for which the aileron is severly unbalanced, cases 5 and 7 are the only two cases for which feedback control can stabilize the system. Also these are the only two cases in which the c.g. is pushed forward relative to the base case, case 1, denoting the above mentioned correlation.

---

*Actually mostly 2 degrees of freedom systems.

TABLE 3

LOCATION OF C. G. VS. POSSIBILITY OF

STABILIZATION BY FEEDBACK CONTROL

Case	Distance of C. G. From Quarter Chord (Per Unit of b)	Does Feedback Control Raise the Flutter Speed?
1	.4	no
2	.4	no
3	.4	no
4	.6	no
5	.25	yes
6	.45	no
7	.10	yes
8	.4	yes
9	.4	yes
10	.45	no

Cases 8, 9, 10 $x_\beta = 0$ (balanced aileron)

For the balanced aileron systems, 8, 9, 10, stabilization by feedback control is possible in cases 8 and 9 even though the remaining geometrical quantities have not been changed from the base case. Thus balancing the aileron, a technique long used to prevent aileron-torsion-bending flutter, also seems valuable in permitting stabilization by feedback control. In case 10 even though the aileron is balanced, the slightly rearward change of the c.g. from .40 to .45 prevents stabilization by feedback control.

The conclusion reached therefore from our ten study case investigation is that the two parameters that seem to enhance stabilization by feedback control are a c.g. location as forward as possible and a balanced aileron. Either by itself permitted stabilization above the flutter speed of the basic wing, even above the divergence speed.

A fairly complete understanding of those factors which influence the possibility of stabilization by feedback control is desirable before serious effort is made to incorporate such stabilization techniques in actual systems. Further study of many systems numerically - especially actual wings with distributed properties, having additional masses such as nacelles* - is needed to truly ascertain whether a large percentage of actual systems can achieve a flutter speed increase using this type of feedback control. Also supersonic and transonic speed studies should be

---

*Nacelles, if forward, would shift the c.g. forward thereby probably enhancing the possibility of stabilization by feedback control.

a part of these future efforts.

4.3 General Properties of the Zeros of $\Delta_{\beta a}$ and $\Delta_{\beta\beta}$

The slightly simplified aerodynamics of appendix C for three degree of freedom systems, resulted in expressions for $\Delta_{\beta a}$ and $\Delta_{\beta\beta}$ which were fifth degree polynomials in s. The theory of this study has placed emphasis on the location of these zeros. Hence it is worthwhile to investigate these polynomials, in order to ascertain general properties of the zeros of $\Delta_{\beta a}$ and $\Delta_{\beta\beta}$. Certain of the properties concerning the zeros of $\Delta_{\beta\beta}$ are already well known, since these are the roots of the basic wing with the aileron locked. It will be shown that a corresponding set of properties exists for the zeros of $\Delta_{\beta a}$. While the fifth degree polynomials of equation C.13 describe only three degree of freedom systems, the same basic characteristics of these polynomials hold also for actual wings.

For $\Delta_{\beta\beta}$, the bending and torsion structural modes each contribute a complex conjugate pair of zeros in the s plane. These zeros are purely imaginary at zero speed, but take on positive or negative real parts as speed increases. In addition, a real zero exists, which is associated with the single lag representation of the Theodorsen function. It can be shown from equation C.13 that this real zero starts at the origin at zero speed. This zero invariably moves into the left half plane at low speeds, and then reverses and crosses back through the origin into the right half plane at higher speeds. The speed at which this real zero crosses into the right half plane is called the divergence speed.

This behavior of the real zero with speed can be seen by

examination of the expression for $\Delta_{\beta\beta}$ in equation C.13 of appendix C. At the divergence speed, there occurs a change in sign of the constant term in the polynomial, namely the term

$$C_o \bar{v} (1 - \bar{v}^2)$$

At all speeds above divergence, this term is negative, since C_o is invariably positive. It can be shown by straightforward application of the algebra of complex numbers that a negative value of this constant term is a necessary and sufficient condition for one real zero to exist in the right half plane. Hence this real zero remains in the right half plane for all speeds above divergence.

Three zeros of $\Delta_{\beta\alpha}$ exist at the origin at zero speed, in addition to a complex conjugate imaginary pair. One zero at the origin is associated with the Theodorsen function, as was the case for $\Delta_{\beta\beta}$. The physical explanation of the other pair at the origin now follows.

$\Delta_{\beta\alpha}$ is proportional to the displacement of α resulting from a torque on β, as can be seen from equation 3.2. Because of the absence of a spring restraint on β, the zero speed steady state response of α due to T_β is zero*. Therefore $\Delta_{\beta\alpha}(s)$ must be zero for zero value of s. This locates a pair of zeros of $\Delta_{\beta\alpha}$ at the origin at zero speed. As speed increases an aerodynamic spring or steady state coupling exists between α and β. This effect causes

---

*This conclusion can be arrived at formally by noting the absence of structural spring coupling terms between β and α, and β and h in equation C.10.

this pair of zeros to move from the origin into the complex plane, since the steady state α displacement due to T_β is no longer zero.

The real zero associated with the Theodorsen function remains real for all speeds. Unlike the case with $\Delta_{\beta\beta}$, this zero can move either into the right or left half plane at very low speeds. Furthermore, once committed, it is confined to that particular half plane for all speeds, and can never cross back through the origin. The criterion of which direction it moves at low speeds is determined solely by the constant term, $C_o' \bar{v}^3$, of the polynomial for $\Delta_{\beta\alpha}$ in equation C.13. This constant does not reverse sign with speed as did the corresponding term for $\Delta_{\beta\beta}$. Instead, it is either always positive or always negative for all speeds, depending on the sign of C_o'. An inspection of equations C.14 and C.15b produces the following expression for C_o', in terms of basic constants of the system:

$$C_o' = \left(\frac{\omega_h}{\omega_\alpha}\right)^2 \frac{I_\alpha}{I_c} U_1 \left[\frac{U_4}{U_1 4\pi} \frac{1}{x_r - \frac{1}{4}} - 1 \right] \qquad (4.1)$$

U_1 and U_4 are positive aerodynamic constants dependent only on the aileron value of c. Since all the parameters in equation 4.1 are positive, the sign of C_o' depends only on the value of $(x_r - \frac{1}{4})$, for a specific aileron. A plot of C_o' vs $(x_r - \frac{1}{4})$ is shown in figure 4.4. For C_o' to be positive, the elastic axis must be aft of the center of pressure (quarter chord for this subsonic study), but not excessively so. Hence for C_o' to be positive, and thereby locate the real root of $\Delta_{\beta\alpha}$ in the left half plane for all speeds,

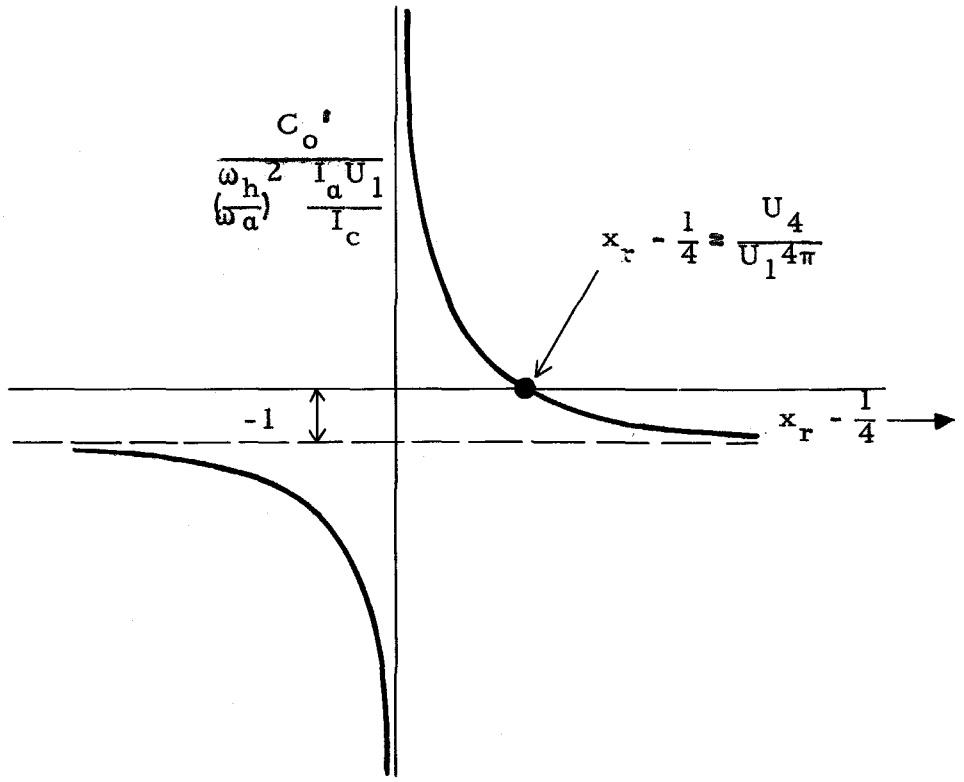

Plot of C_o' vs. $x_r - \frac{1}{4}$

Figure 4.4

the following condition must be satisfied

$$0 < x_r - \frac{1}{4} < \frac{U_4}{U_1 4\pi} \tag{4.2}$$

Equation 4.2 shows that the question of the half s plane in which the real zero of $\Delta_{\beta a}$ exists, is answered entirely by the location of the elastic axis for a specified value of c . One may think of this real zero as being a divergence zero, analogous to the corresponding real zero for $\Delta_{\beta\beta}$. Adopting this viewpoint, one notes that the divergence speed for the zeros of $\Delta_{\beta a}$ must be either zero or infinity. This divergence speed for the zeros of $\Delta_{\beta a}$ can only be changed by a change in elastic axis location (for a given aileron),

and not by the structural stiffness value as is the case for the zeros of $\Delta_{\beta\beta}$.

In summary, therefore, one may state that zeros of $\Delta_{\beta\alpha}$ and $\Delta_{\beta\beta}$ may exist on the real axis due to the Theodorsen function, or as complex conjugate pairs due to the structural modes of the system. Each additional degree of freedom above the three treated here, adds another mode, and hence another complex conjugate pair. The divergence speed of a cofactor may be defined as the speed at which a real zero goes into the right half plane. For $\Delta_{\beta\beta}$, this divergence speed varies in a continuous manner, dependent on elastic axis location, structural stiffness and other quantities, as shown by the expression for V_d at the bottom of equation C.13. For $\Delta_{\beta\alpha}$, this so-called divergence speed can only take on the values zero or infinity, and depends only on the elastic axis location for a given aileron value of c. One may extend the notation associated with the zeros of $\Delta_{\beta\beta}$ to those of $\Delta_{\beta\alpha}$. A R.H.P. real zero can occur (above the divergence speed), or a R.H.P. complex zero can occur (above the flutter speed). Usually the divergence speed occurs above the flutter speed for $\Delta_{\beta\beta}$. In the ten study cases for $\Delta_{\beta\alpha}$ in figure 4.2, the divergence speed likewise occurred above the flutter speed*. On the other hand the uniform wing to be studied next has a divergence speed of zero.

4.4 Investigation of the Stability Cofactors of a Uniform Wing, Approximated by a Three Degree of Freedom System

An actual wing is considered next, a uniform rectangular

---

*It was infinite in all cases.

wing. One reason for studying this particular wing is that its flutter properties are well known, having been studied previously, both theoretically and in a wind tunnel. Reference 8 is a detailed report describing these results. Exact and finite difference solutions of flutter speeds and frequencies are given in this reference.

The constants of this wing are listed in table 4, with the geometry shown in figure 4.5. The $1\frac{1}{2}$ cell finite difference mechanical model of the wing with the aileron locked is shown in figure 4.6a. The original and simplified electric analogies of this mechanical model are given in figures 4.6b and 4.6c. The only purpose in drawing these analogies is to obtain the constants of the two degree of freedom system, as given in figure 4.6c. The equivalent bending and torsion springs, the mass, and the inertia terms are listed in this figure. With these determined, the quantities ω_a, ω_h and V_d are computed from the standard formulas. This is carried out in equations 4.3 to 4.5.

$$\omega_a = \sqrt{\frac{C_a}{I_a}} = \frac{1}{\Delta x}\sqrt{\frac{GJ}{I_a'}} = 290\ \frac{\text{rad}}{\text{sec}} \text{ or } 46.2 \text{ cps} \qquad (4.3)$$

$$\omega_h = \sqrt{\frac{C_h}{M}} = \left(\frac{1}{\Delta x}\right)^2\sqrt{\frac{4EI}{M'}} = 53.5\ \frac{\text{rad}}{\text{sec}} \text{ or } 8.50 \text{ cps} \qquad (4.4)$$

$$V_d = \frac{\omega_a r_a}{2}\left[\frac{1}{K\left(x_r - \frac{1}{4}\right)}\right]^{\frac{1}{2}} = 331 \text{ ft/sec} \qquad (4.5)$$

The values of the nine non-dimensional parameters of the equivalent three degree of freedom system are obtained from table 4 and equations 4.3 to 4.5. These are listed in table 5.

TABLE 4

b	=	1/3 ft.
ℓ	=	4 ft.
M^s	=	.02703 slugs/ft. = mass per unit length of wing plus aileron
I_a^s	=	.000800 slug ft.^{2} = moment of inertia per unit length about e.a.
EI	=	977.1 lbs. ft.^{2}
GJ	=	480.6 lbs. ft.^{2}
K	=	.0309
m	=	.05 M = effective mass of control surface
b_c	=	.2b = half chord of aileron
x_b	=	$.50b_c$ = .0333 ft = c.g. of aileron aft of hinge
r_b	=	b_c = .0666 ft. = radius of gyration of aileron

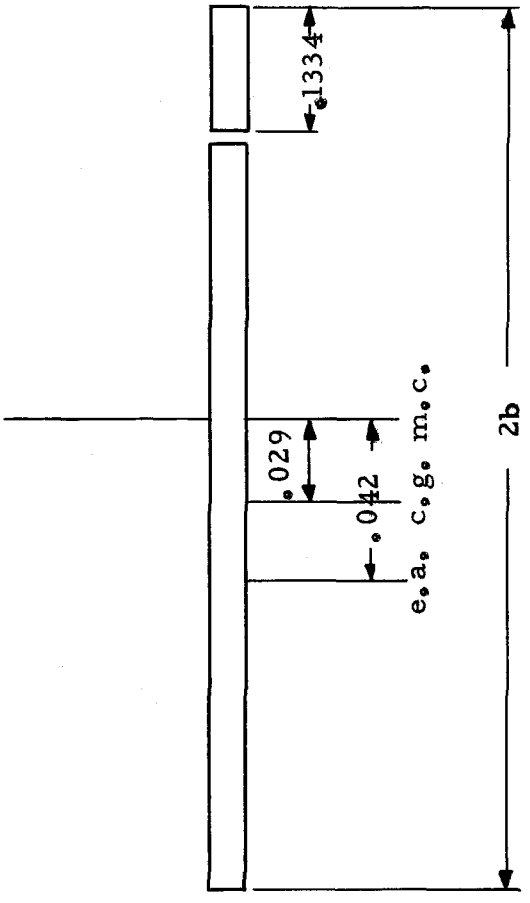

2b = .6667

Geometry of Uniform Rectangular Test Case Wing
(elevation view)

Figure 4.5

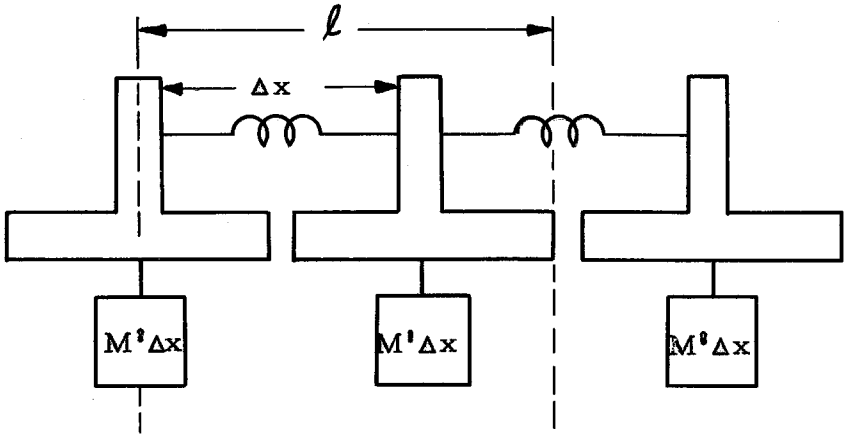

a) Mechanical Model

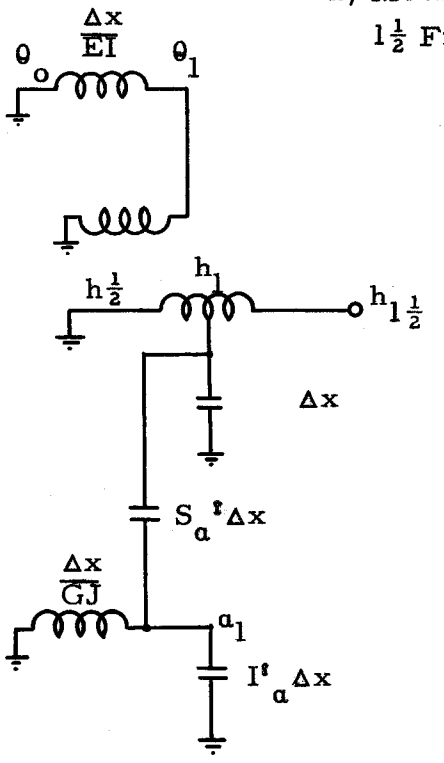

b) Electric Nodal Analogy

$1\frac{1}{2}$ Finite Difference Cells

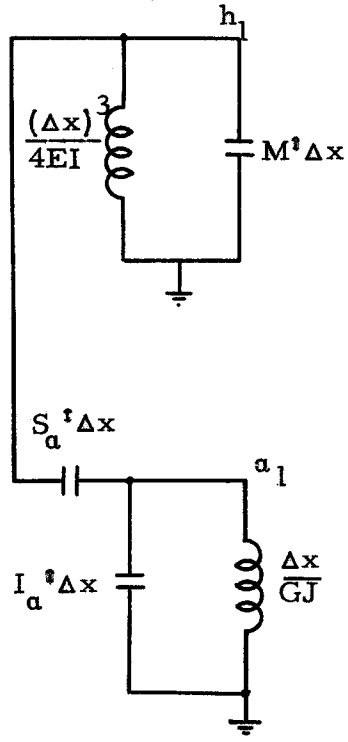

$C_a = \frac{GJ}{\Delta x}$

$C_h = \frac{4EI}{(\Delta x)^3}$

$M = M'\Delta x$

$I_a = I_a'\Delta x$

c) Equivalent Circuit of Electric Analog, with Two Degrees of Freedom

Finite Difference and Electric Analogs of Basic Wing

Figure 4.6

TABLE 5

CONSTANTS OF THREE DEGREE OF FREEDOM

APPROXIMATION TO UNIFORM WING

Non Dimensional Parameters	
$\frac{\omega_a}{\omega_h} = 5.45$	$\omega_a = 290$ rad/sec
$x_r = .437$	$V_d = 331$ ft/sec
$\frac{r_a^2}{b^2} = .268$	
$\frac{x_a}{b} = .039$	
$K = .0309$	
$\frac{x_\beta}{b} = .1$	
$\frac{m}{M} = .05$	
$c = .6$	
$\frac{r_\beta^2}{b^2} = .04$	

Equations C. 13, C. 14 and C. 15 are used, as before, to determine the zeros of $\Delta_{\beta\alpha}$ and $\Delta_{\beta\beta}$ for this three degree of freedom representation of the wing. These zeros are shown in figures 4. 7 and 4. 8.

It is instructive to compare the flutter results of the basic wing, obtained from the exact solution of reference 8, and obtained by the three degree of freedom approximation with simplified aerodynamics used in the present study. Table 6 gives this comparison.

TABLE 6

COMPARISON OF EXACT SOLUTION WITH

APPROXIMATE SOLUTION OF OUR STUDY

	Exact Solution of Reference 8	Approximate Solution of Present Study	Percentage Deviation from Exact Solution
Divergence Speed	409 ft/sec	331 ft/sec	-16%
Flutter Speed	333	293	-12%
Flutter Frequency	25. 3	25. 8	+ 2%

The errors of the present study are due to the coarse finite difference approximation and due to the simplified aerodynamics mentioned in appendix C. The accuracy involved is considered adequate for our main purpose of establishing trends in flutter capability.

In figure 4. 7 it is noted that the real zero of $\Delta_{\beta\alpha}$ exists in the R. H. P. for all speeds other than zero, though its magnitude is small. The complex zeros move with speed monotonically further into the left half plane. According to the theory of part II, no practical stabilization is possible for this wing.

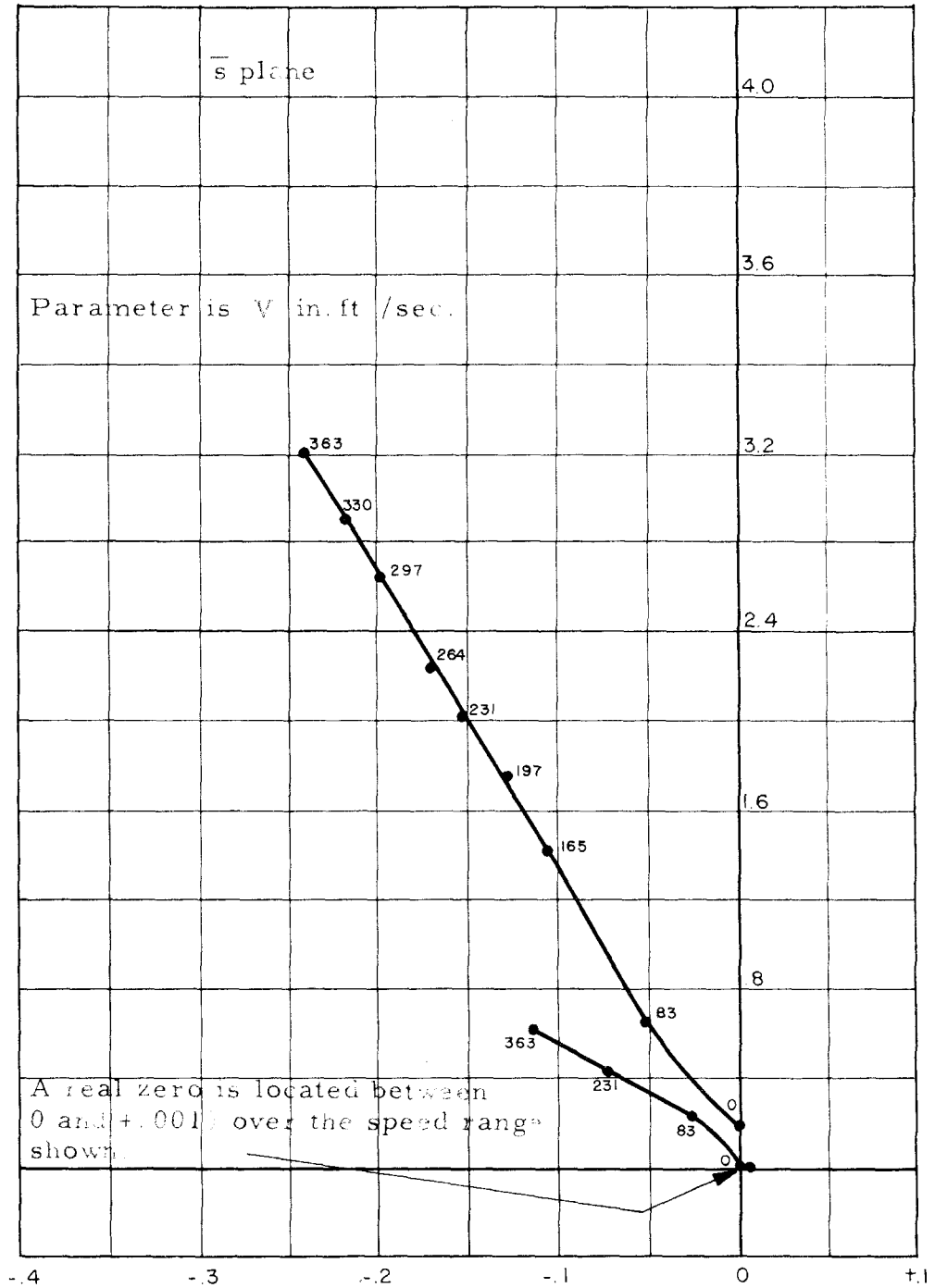

Zeros of $\Delta_{\beta a}$ for Uniform Wing. (3 Degree of Freedom Model)

Figure 4.7.

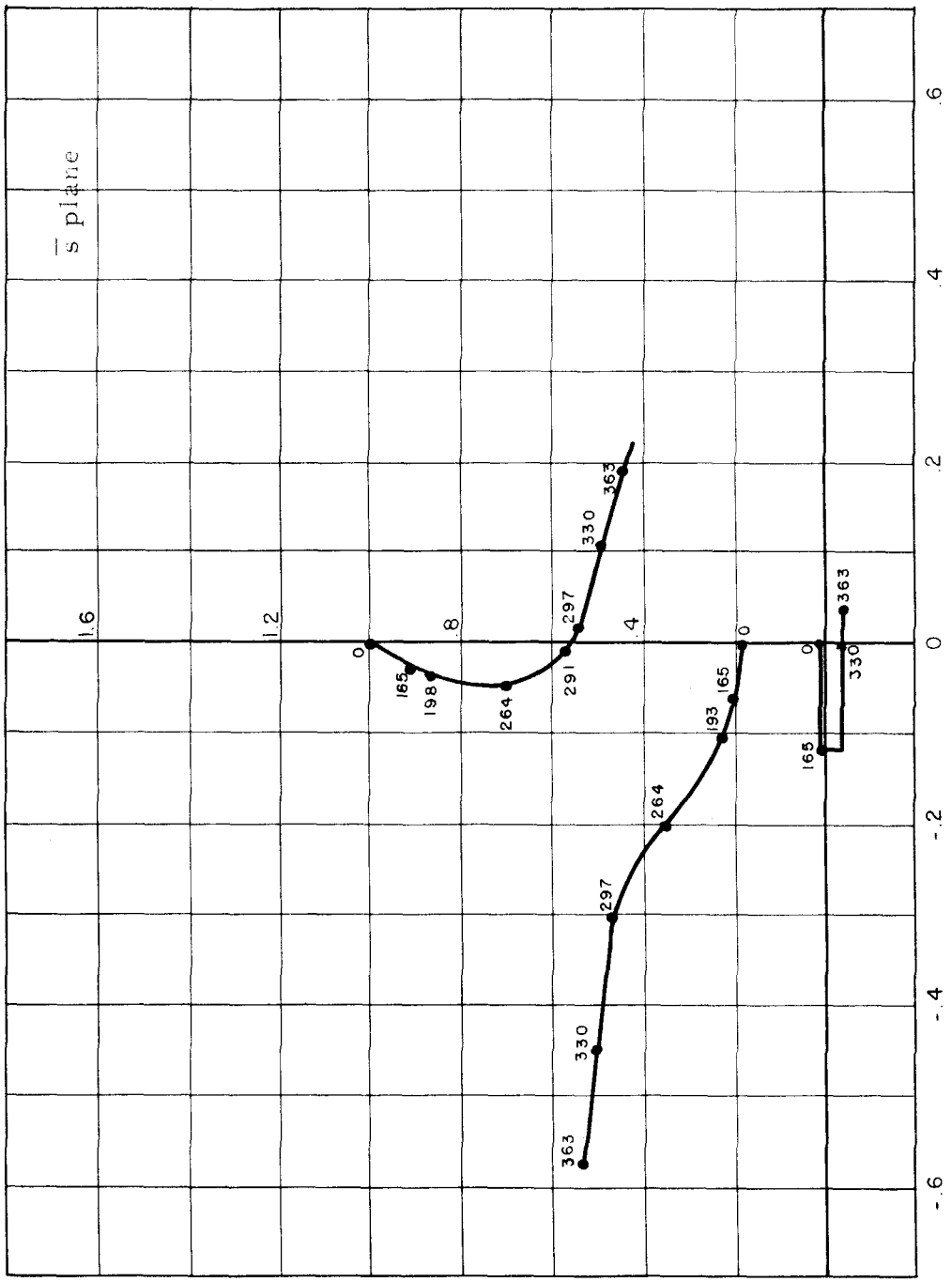

Zeros of $\Delta_{\beta\beta}$ for Uniform Wing. (3 Degree of Freedom Model)

Figure 4

The reason the real zero of $\Delta_{\beta\alpha}$ is a R. H. P. zero for all speeds is that the critical quantity $x_r - \frac{1}{4}$ is larger than the limit $\frac{U_4}{U_1 4\pi}$ of equation 4.2. It is noted in table 5 that the x_r value of 0.437 is somewhat large, representing an elastic axis location close to the mid chord. If the elastic axis were shifted forward by .05 of the full chord, then x_r would reduce by .05. The value of $x_r - \frac{1}{4}$ would fall between the limits of equation 4.2, and the R. H. P. location of the real zero would be removed. For this case of $x_r - \frac{1}{4}$ shifted forward by .05*, the zeros of $\Delta_{\beta\alpha}$ are as shown in figure 4.9. Stabilization by feedback control becomes possible for speeds in excess of 825 ft/sec., as compared to an original flutter speed of 293 ft/sec.

The uniform wing just studied demonstrated two important related facts. The first is that a R. H. P. real zero of $\Delta_{\beta\alpha}$ may occur, unlike the cases studied in figure 4.2, if the elastic axis is far aft. The second is that slightly forward relocation of the elastic axis may convert this real zero of $\Delta_{\beta\alpha}$ into the left half plane, and thus make stabilization by feedback control possible up to very high speeds. This second fact may be important in stabilizing actual systems**, since it may be accomplished by shifting more of the wing material slightly forward, a relatively simple change in many cases.

---

*The other eight parameters of table 5 remain the same.
**Of course, still using feedback control.

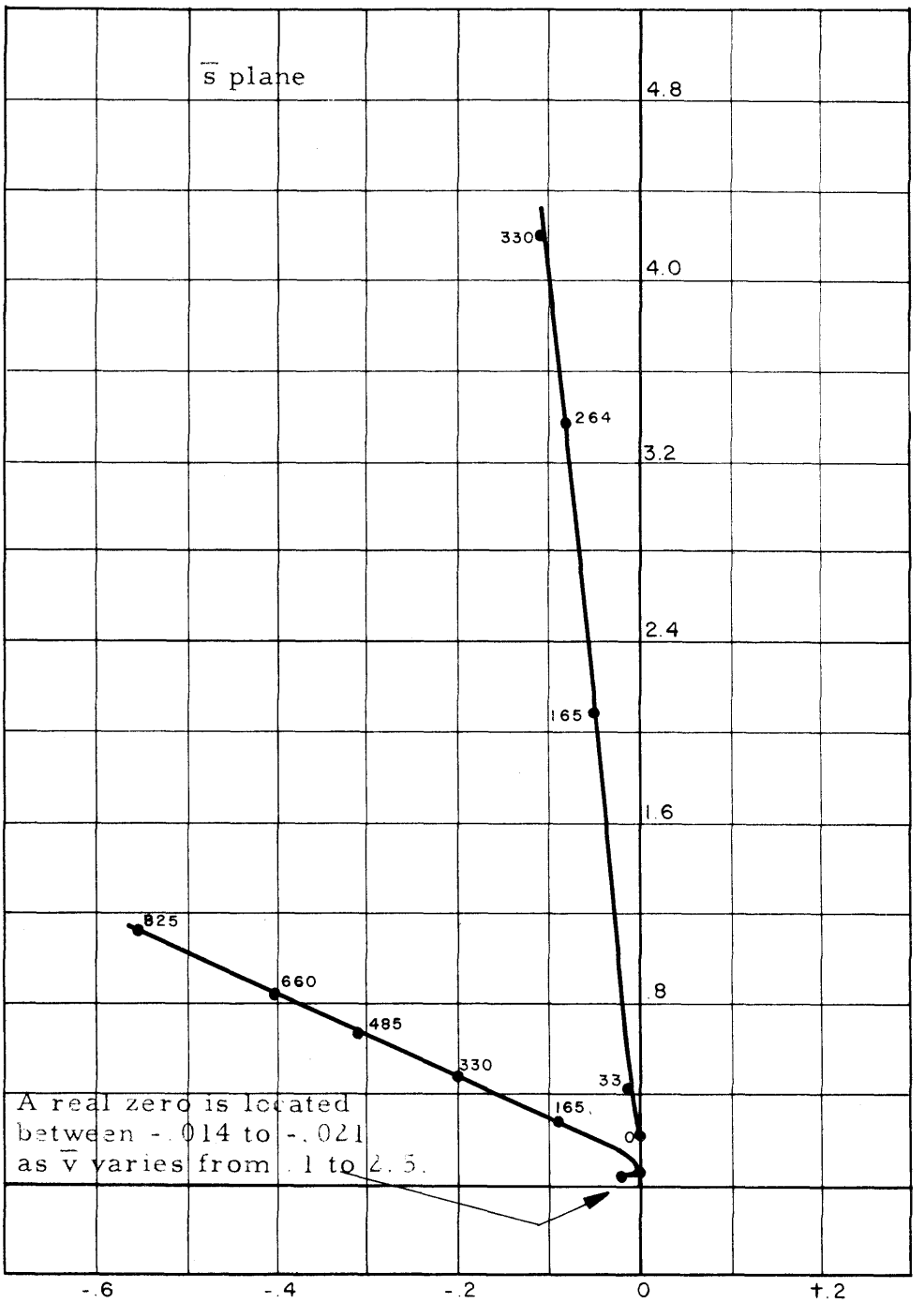

Zeros of $\Delta_{\beta a}$ for Modified Uniform Wing.
(3 Degree of Freedom Model).

Figure 4.9.

PART V

DETERMINATION OF THE WIDTH OF THE CONDITIONALLY STABLE BAND BY ROOT LOCUS DIAGRAMS AND BY THE ANALOG COMPUTER

Parts II and III developed a general feedback theory applicable to aeroelastic systems. A resume of this theory was given in figure 2.11 and the associated discussion of part II. Below a speed of V_1 in figure 2.11, the first speed at which both zeros and poles move into the right half plane, the stable range of k_1k_2 values has an infinite K_2/K_1 ratio. In this region unconditional stability occurs and stabilization by feedback control is feasible in actual systems. Above this speed the stable range becomes finite, progressively reducing to zero.

There is need of investigating this region above the speed V_1 in typical aeroelastic systems to determine how much can be used for practical stabilization by feedback control. The conclusion to be reached after the numerical study carried out in this part has already been used in the development of rule 3 in part II. This states the usable speed range above V_1 is negligible. Thereby follows the criterion of rule 3 used in the numerical examples of part IV - an increase in flutter speed is possible only when the zeros of $\Delta_{\beta\alpha}$ are L.H.P. zeros above the flutter speed of the basic wing.

In this part the demonstration that the usable portion of the conditionally stable region is negligible is carried out by two methods of analyzing the aeroelastic servo system.

1) Root locus diagrams of the systems studied in part IV

2) Determination of the conditionally stable region on an analog computer

5.1 Use of Root Locus Diagrams to Determine the Band of Conditional Stability

Three of the ten three degree of freedom systems investigated in part 4.1 are now treated in more detailed manner by root locus diagrams. These represent two cases for which practical stabilization is impossible ($\Delta_{\beta\alpha}$ has R.H.P. zeros above the flutter speed), namely cases 1 and 6. In addition, case 5 is treated for which stabilization is possible (the zeros of $\Delta_{\beta\alpha}$ are L.H.P. above the flutter speed).

It was shown in part 3.4 that the characteristic equation of the aeroelastic system using the α coordinate as the principal feedback, and β as an internal feedback was

$$1 - \frac{\Delta_{\beta\alpha}}{\Delta_{\beta\beta}} H'(s) = 0 \quad * \tag{5.1}$$

where

$$H'(s) \equiv \frac{H_\alpha(s)}{H_\beta(s)} \tag{5.2}$$

$H'(s)$ can be adjusted to achieve best stability.

Equation 5.1 shows that the aeroelastic system with feedback has the zeros of $\Delta_{\beta\alpha}$ as the fixed zeros of the loop gain, and the zeros of $\Delta_{\beta\beta}$ as the fixed poles of the loop gain. Hence these

---

*It can be deduced from equation C.13 that $\Delta_{\beta\alpha}$ has a negative value for $s = 0$, while $\Delta_{\beta\beta}$ has a positive value. Hence a negative feedback loop requires that the k_2 constant in $H'(s)$ be positive.

represent the fixed zeros and poles in the root locus diagrams of the aeroelastic system with feedback.

The stabilizer, $H'(s)$, of equation 5.2 is chosen to be of the following forms:

$$H'(s) = k_2 \qquad \text{(a constant)} \qquad (5.3)$$

$$H'(s) = k_2 s \qquad \text{(a pure derivative)} \qquad (5.4)$$

$$H'(s) = k_2 s^2 \qquad \text{(a pure second derivative)} \qquad (5.5)$$

The stabilizers represented by equations 5.4 and 5.5 represent limiting cases of single and double lead networks, respectively.

The speeds chosen for investigation are slightly above flutter speed ($5^{o}/o$) in case 1, and a moderate amount above flutter speed ($25^{o}/o$) in case 6. For the system that is capable of stabilization (case 5), the speed chosen is a large amount above flutter speed ($60^{o}/o$). It will be shown that no practical stabilization is possible for cases 1 and 6, and a semi-infinite stability band exists for case 5, substantiating the theory of parts II and III.

Figures 5.1, 5.2 and 5.3 are root locus diagrams for these cases and speeds. The aeroelastic system employing the feedback stabilizers represented by equations 5.3, 5.4 and 5.5, are depicted in figures 5.1, 5.2 and 5.3, respectively. Figure 5.1a is for case 1, figure 5.1b for case 6, and figure 5.1c for case 5, with similar designation in the other figures.

Figure 5.1 shows that cases 1 and 6, even at these small speeds above flutter, cannot be stabilized for any value of k_2, the

loop gain constant*, since an entire root trajectory lies in the right half plane. On the other hand, for case 5 the system can be stabilized for all values of k_2 above K_1.

It is seen in figure 5.2a and b that the perfect damper stabilizer, $k_2 s$, cannot stabilize cases 1 and 6 for any value of k_2. Note that the unstable locus has not been shifted appreciably (insofar as stabilization is concerned) by the presence of the derivative operator, as can be seen by comparison with figure 5.1a and b. The presence of the lead operator makes the root locus of figure 5.2c for case 5 even more stable than that of figure 5.1c without the lead device. Its principal oscillatory root can be made to have a damping factor, ζ, of 0.4 for a large value of k_2. The very high frequency root is stable though not heavily damped, which is satisfactory, since its excitation will be small. In practice, instead of a pure derivative stabilizer in case 5, a term of the form of equation 2.11 would be used, to increase the damping of the real root, while not modifying the oscillatory roots appreciably.

In figure 5.3a, the second derivative feedback is seen to produce a stable system for a K_2/K_1 ratio of 5. This is not adequately broad according to rule 2. Also, the damping factor, ζ, of the troublesome root is very poor, never exceeding .02. Hence even at this slight increase in speed above flutter (5%), no practical stabilization is possible using second derivative feedback.

---

*$k_1 k_2$ as described in part II is the actual loop gain constant. However only ratios of maximum and minimum stable values are of importance here. Hence k_1 is assumed unity.

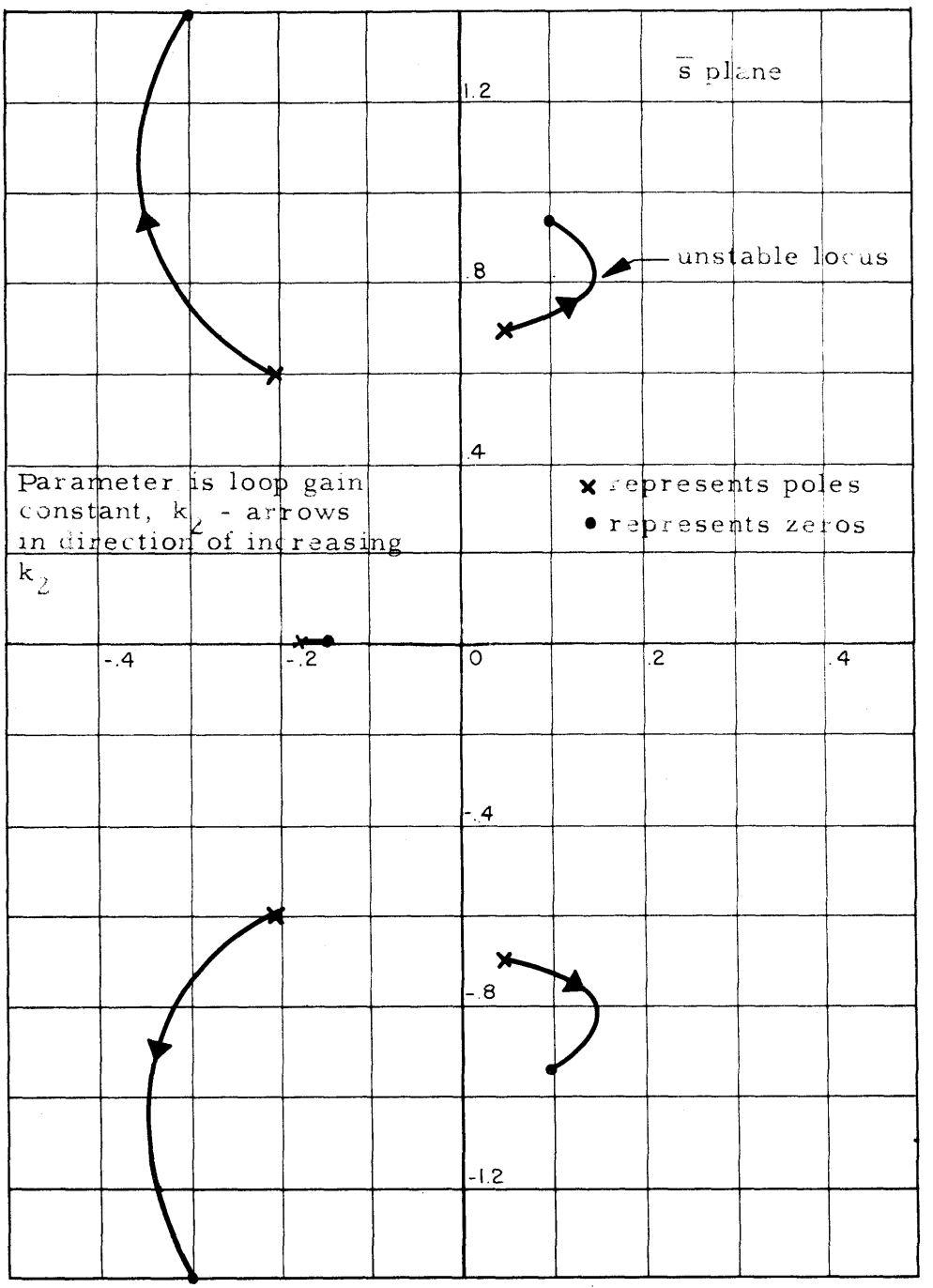

Root Loci of Case 1, Three Degree of Freedom System. Speed is 5% Above Basic Wing Flutter Speed. Feedback Stabilizer Represents a Positive Constant, k_2, or Negative Feedback.

Figure 5.1a.

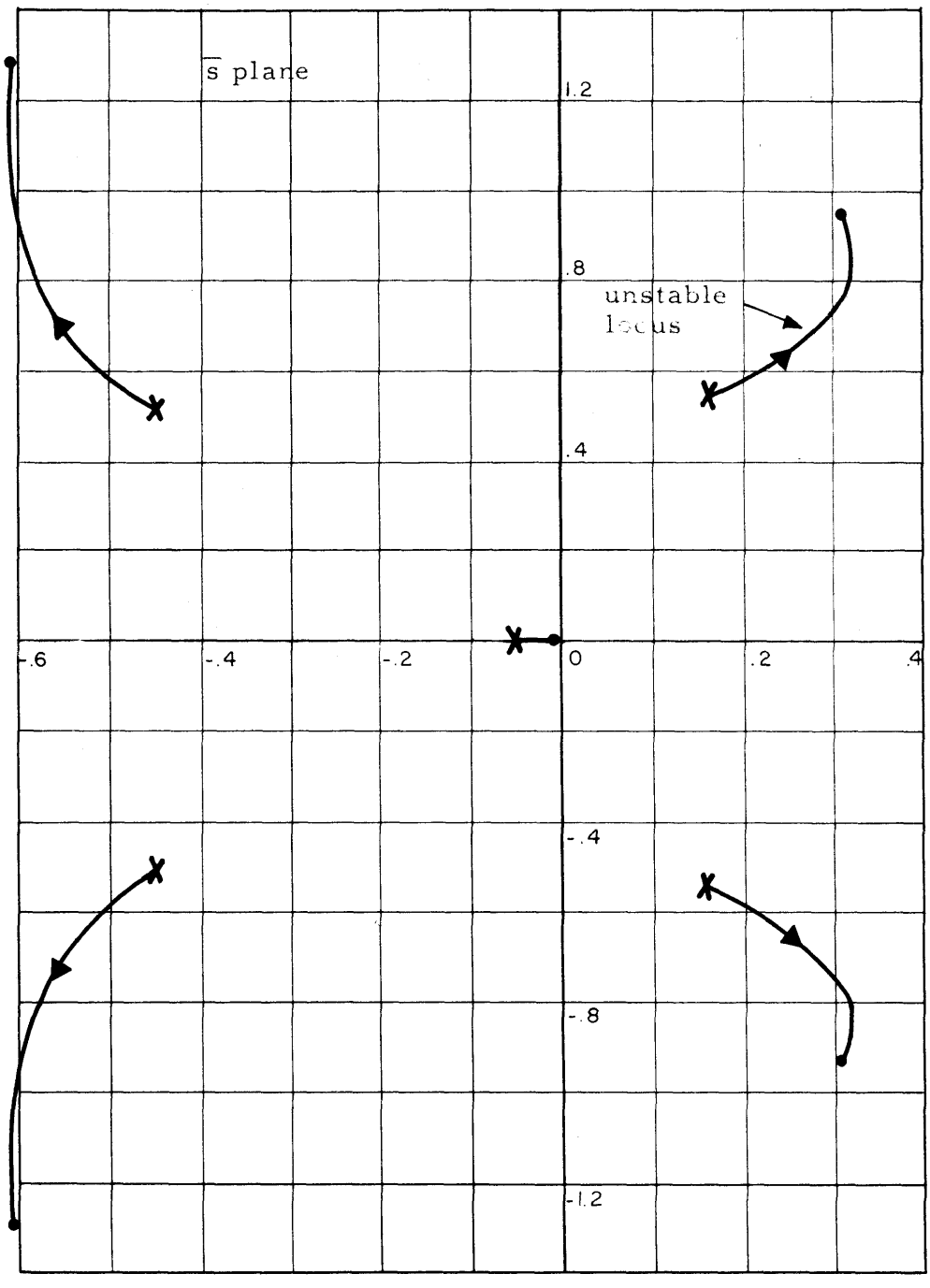

Root Loci of Case 6, Speed 25% Above Flutter.
Constant Feedback, k_2

Figure 5.1b.

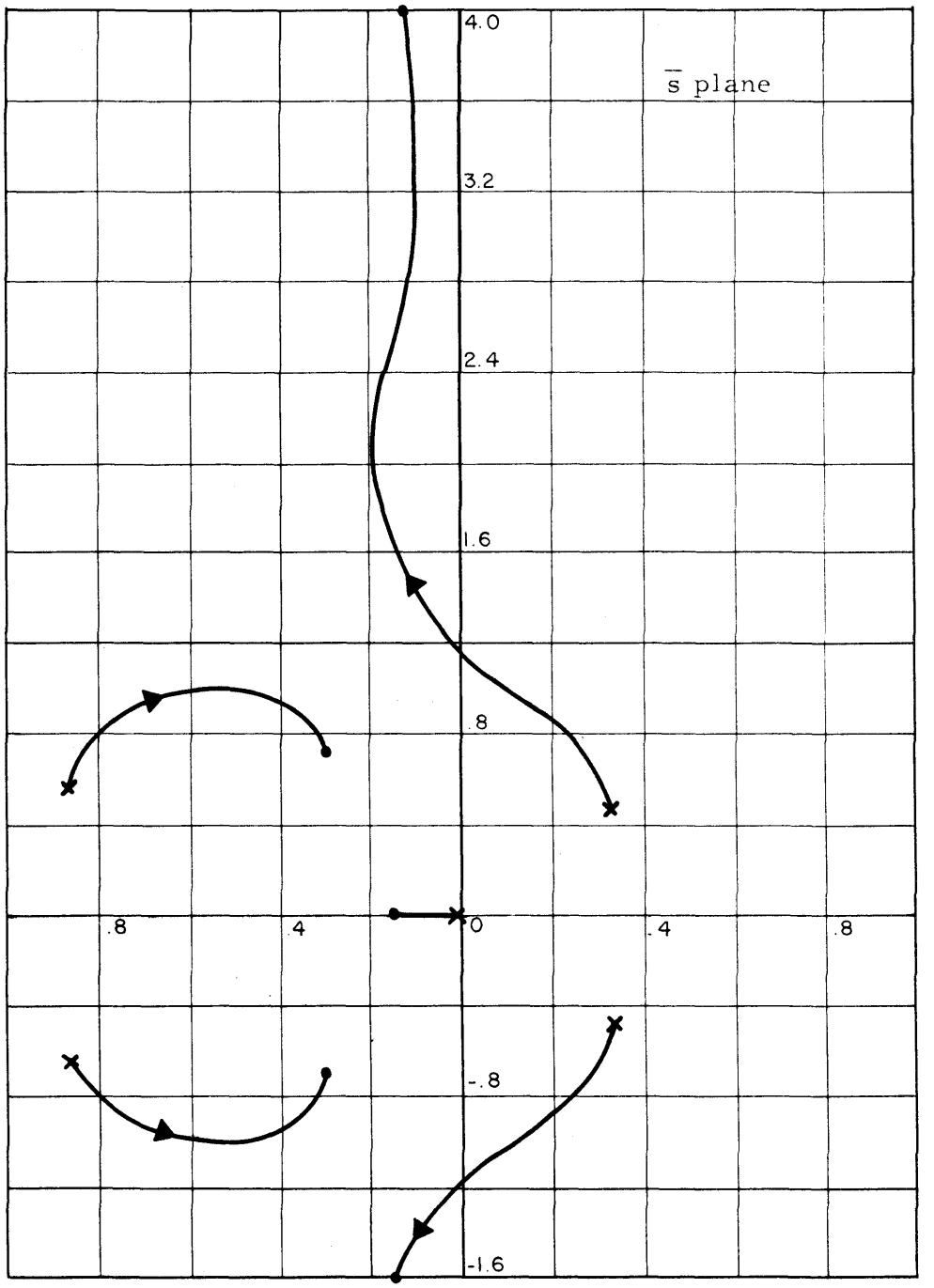

Root Loci of Case 3, Speed 10% Above Flutter
Constant Feedback, k_2

Figure 5.1c

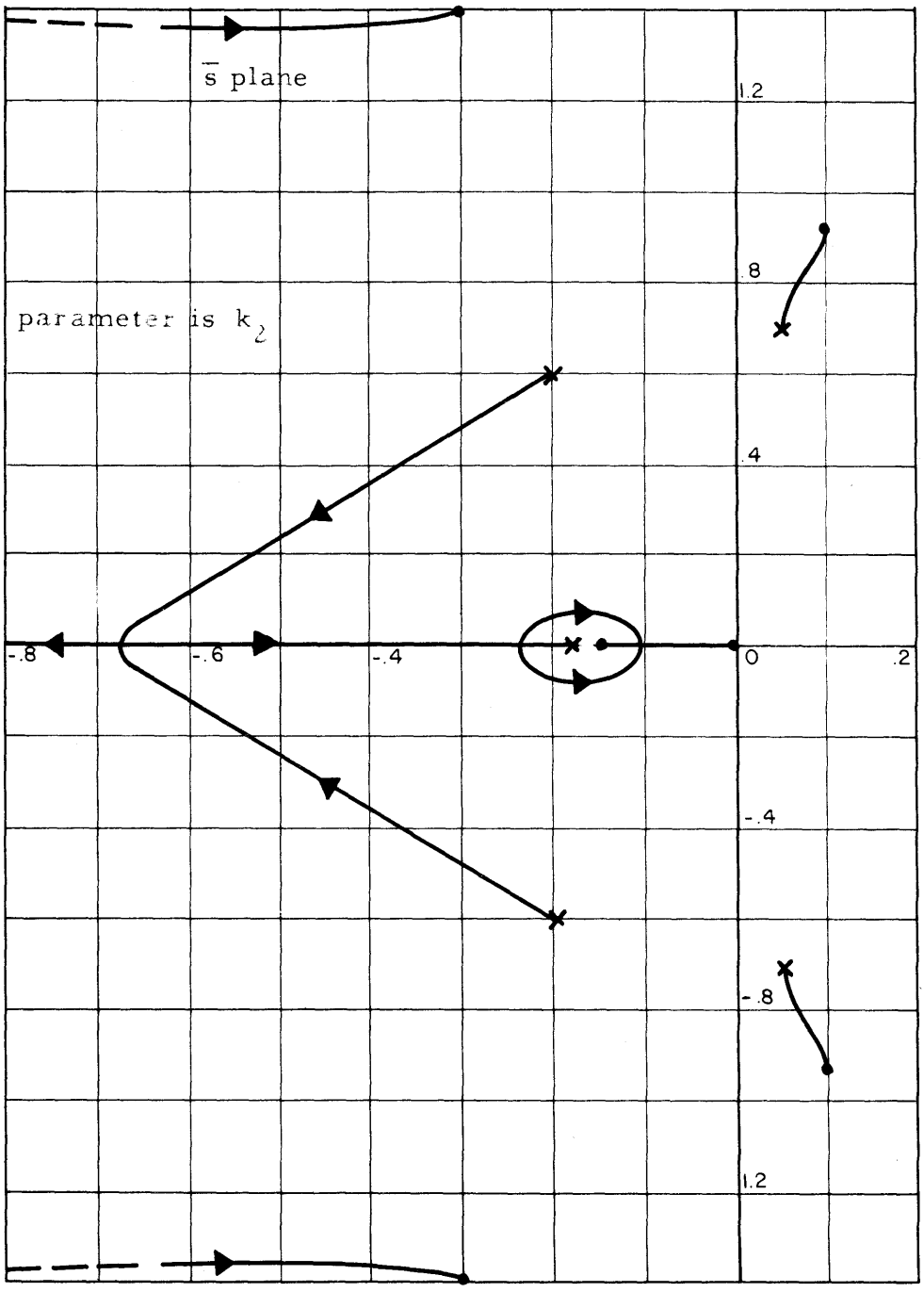

Root Loci of Case 1, 5% Above Flutter Speed.
k_2s Feedback Operator.

Figure 5.2[illegible]

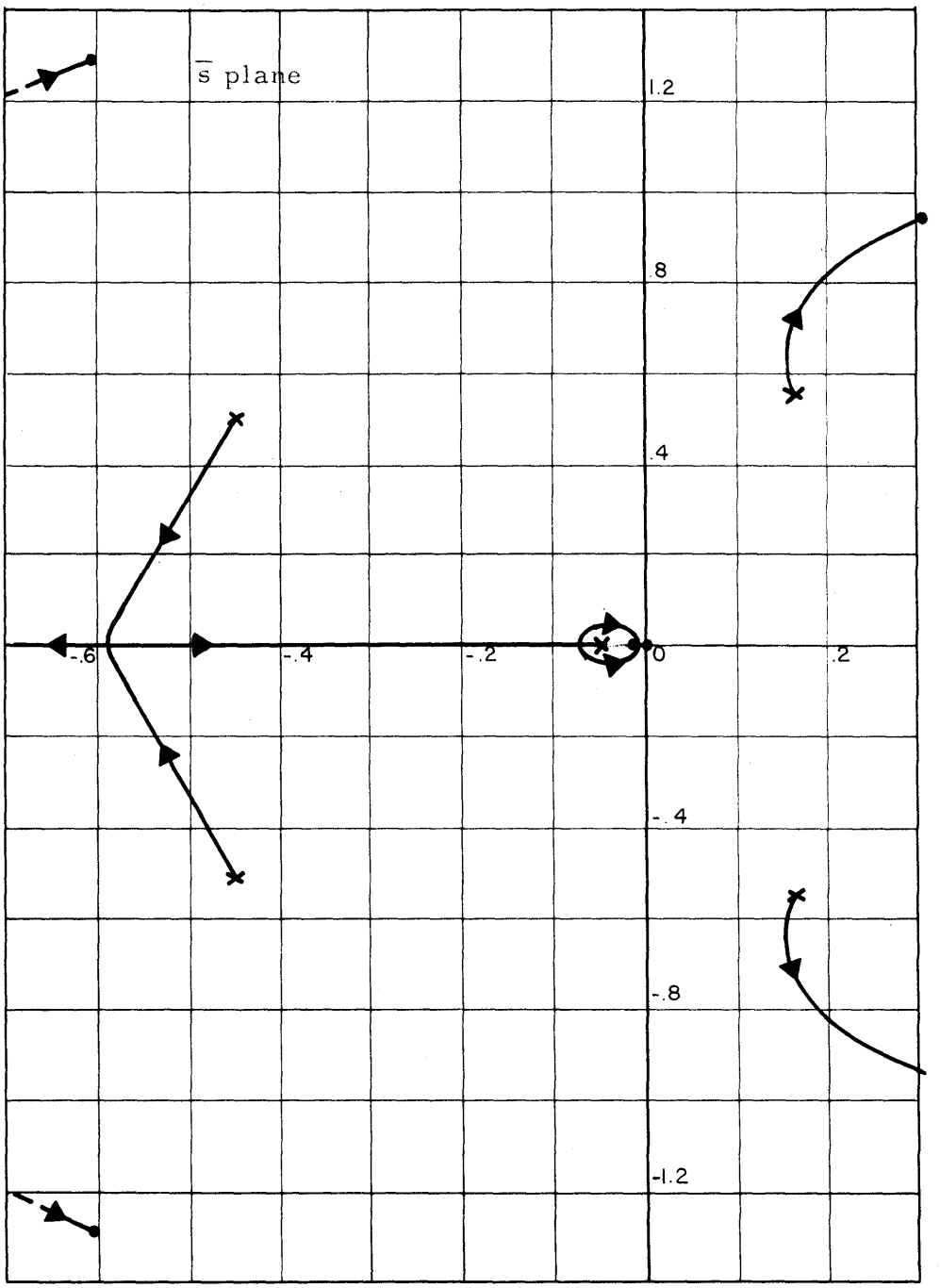

Root Locus of Case 6, 25% Above Flutter Speed.
$k_2 s$ Feedback Operator.

Figure 5.28.

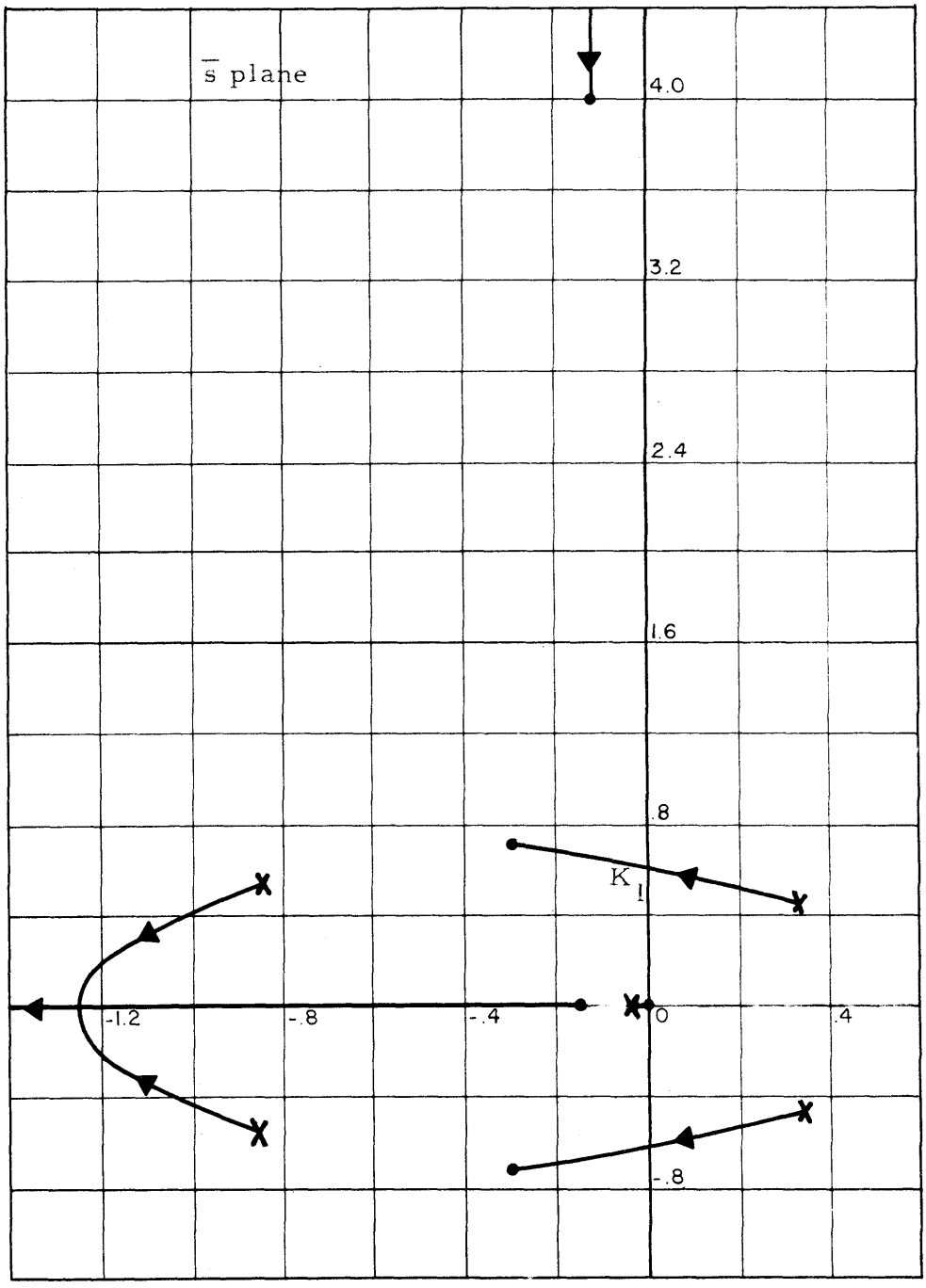

Root Loci of Case 5, 60% Above Flutter Speed.
k_2 s Feedback Operator.

Figure 5.2c.

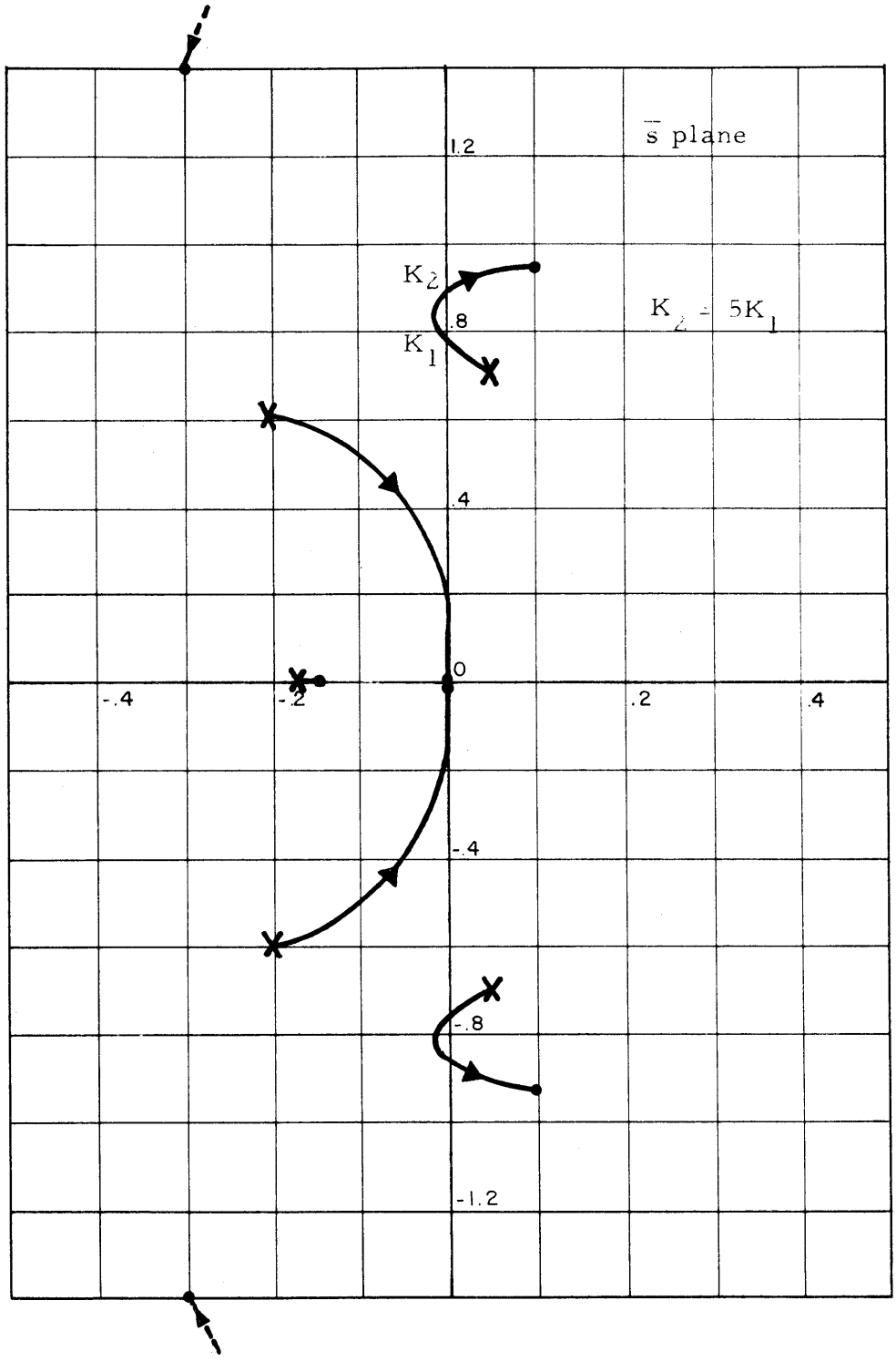

Root Loci of Case 1, 5% Above Flutter Speed.
$k_2 s^2$ Feedback Operator.

Figure 5.3a.

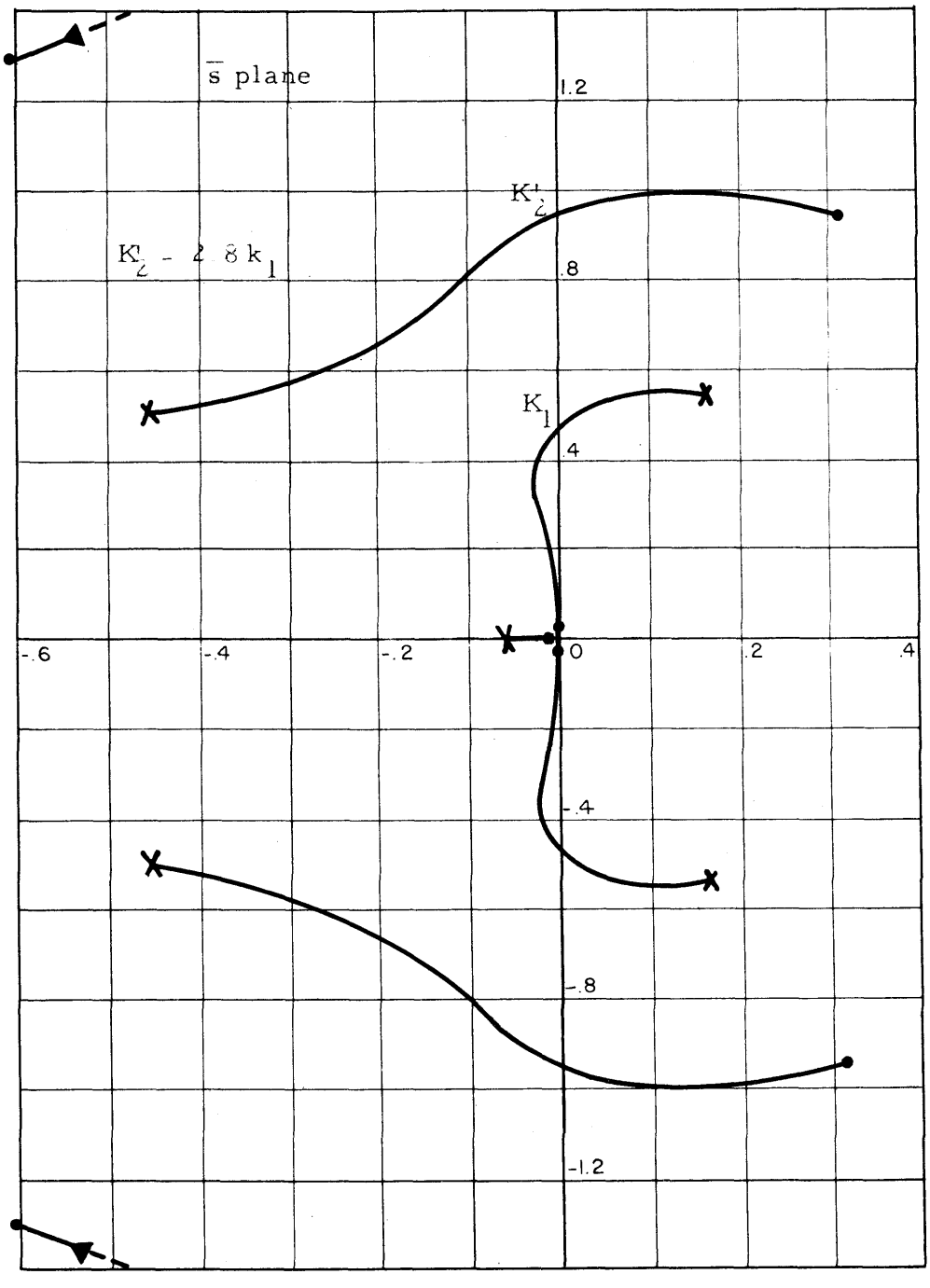

Root Loci of Case 1, 45% Above Flutter Speed
$k_2 s^2$ Feedback Operator.

Figure 5.3b

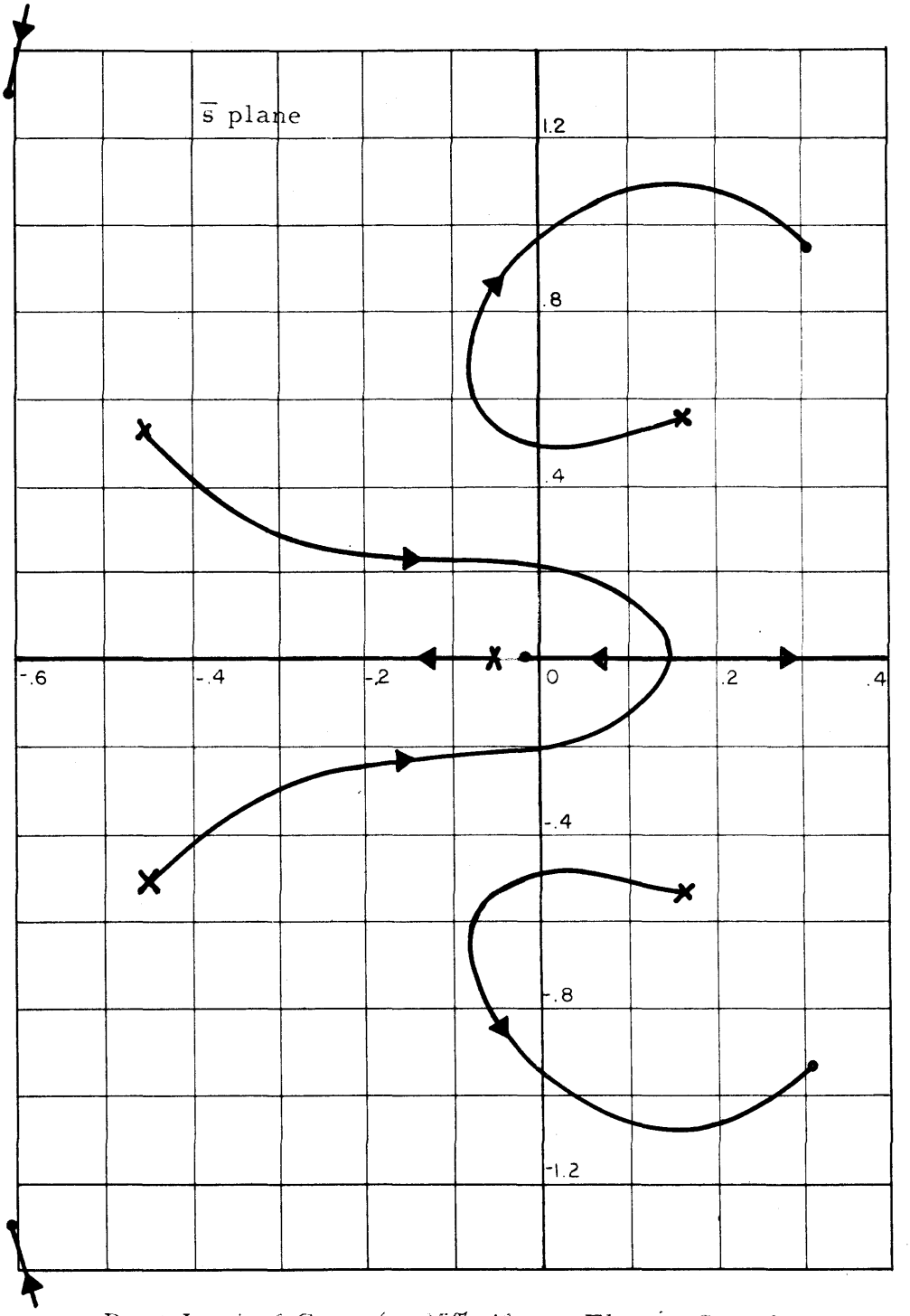

Root Loci of Case 6, 25% Above Flutter Speed. Negative Value of k_2 Constant, or Positive Feedback.

Figure 5.4.

In figure 5.3b for case 6, the stable range of K_2/K_1 is 2.8, certainly an insufficient range.

Reversing the sign of the feedback produces an exponentially divergent real root, as can be seen by figure 5.4. Hence this positive feedback does not offer a stabilization possibility.

The conclusions deduced from figures 5.1, 5.2 and 5.3 are that no stable range of values of k_2 exist for cases 1 and 6 for either a constant or a derivative feedback, while a semi-infinite stable range exists for case 5, well damped when derivative feedback is used. If the extreme of second derivative feedback* is used for cases 1 and 6, a stable range of k_1k_2 values exist. However this range of stable values is too narrow to achieve practical stabilization. Thus the basic rule, rule 5, is substantiated in these test cases.

5.2 Analog Computer Determination of the Width of the Conditionally Stable Band

One system was studied on the large scale direct electric analog computer at the C.I.T. Computing Center. This was a three degree of freedom system, the same system that was studied in the test example of reference 5. This was, in turn, approximately the same system as case 3 in part IV of the present study.

In the setup the complete subsonic, incompressible, two dimensional strip theory aerodynamics of reference 6 was used, including the aero inertia terms. The ratio of second degree

---

*A double differentiation of the feedback signal, obtained from noisy sources such as accelerometers and gyros, is probably not feasible in practice.

polynomials in s was used for the Theodorsen function, a familiar and quite accurate representation.

The block diagram of the physical system represented on the analog is shown in figure 5.5. The stabilizer output is made to control β, rather than T_β, according to the theory of part 3.4.

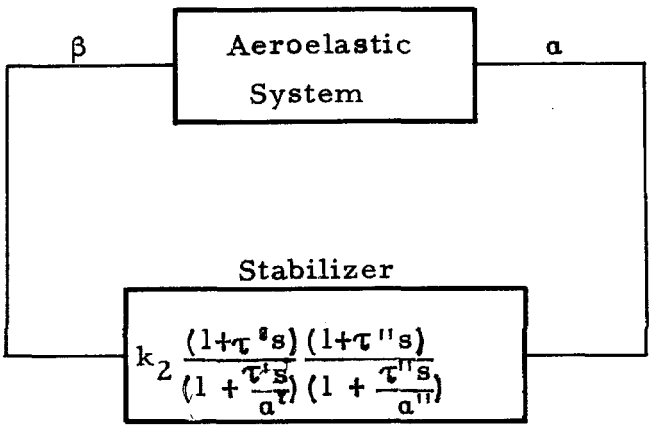

Unstable Aeroelastic System Plus Lead Stabilizer

Figure 5.5

The feedback operator is an adjustable double lead operator, where both zeros and poles can be varied as τ', τ'', a', and a'' are varied. Also the gain of the feedback stabilizer can be adjusted by varying k_2, both in magnitude and sign.

The variation of the parameters, τ', τ'', a', a'' and k_2 over essentially all values showed the following conclusions.

1) Stabilization produced without the lead devices was essentially as good as that using the optimum set of values of τ', τ'', a' and a''. Hence the technique of stabilization invariably used in servos does not apply here.

2) The conditionally stable zone was narrow. The total width was only 7°/o above the aeroelastic flutter speed. The criterion of rule 2 was satisfied only for speeds about 1°/o above the flutter speed.

Thus the same conclusion, deduced for cases 1 and 6 from root locus diagrams, is deduced for case 3 from an analog computer study. The width of the conditionally-stable zone, above the speed at which both a zero and a pole of the aeroelastic transfer function first move into the right half plane, is negligibly small.

PART VI

ADDITIONAL TECHNIQUES OF STABILIZATION BY FEEDBACK CONTROL

The entire discussion of the first five parts considered the possibility of raising the flutter speed by feedback control driving through the control surface. The desirability of using such a feedback scheme is obvious - no additional power source is required besides the normal autopilot actuator. It was shown in parts IV and V that only in certain cases was such stabilization possible.

A stabilization technique is now considered that can raise the flutter speed in essentially all aeroelastic systems. The drawback of this technique is an instrumentation one, in that it requires an additional power source. This technique - the use of jet reaction forces on the wing itself - may be practical to instrument in many cases. This point will be discussed later in this part after the mathematical considerations are completed. The distinction on physical grounds between this type of control and that through a control surface, is treated later in this part.

6.1 Stabilization By Jet Reaction Torquer

The technique of driving through the control surface places an immediate restriction on the cofactors that may be utilized for stability - only $\Delta_{\beta h}$, $\Delta_{\beta\alpha}$, $\Delta_{\beta\beta}$. This is true because the force is on the β coordinate as seen in figure 3.2. Now, if the stabilizing force is on the α coordinate, instead of the β coordinate, then figure 3.2 is changed to figure 6.1*. The possible cofactors to be

---

*As can be seen by examining equation 3.1 for the case a T_α exists instead of a T_β.

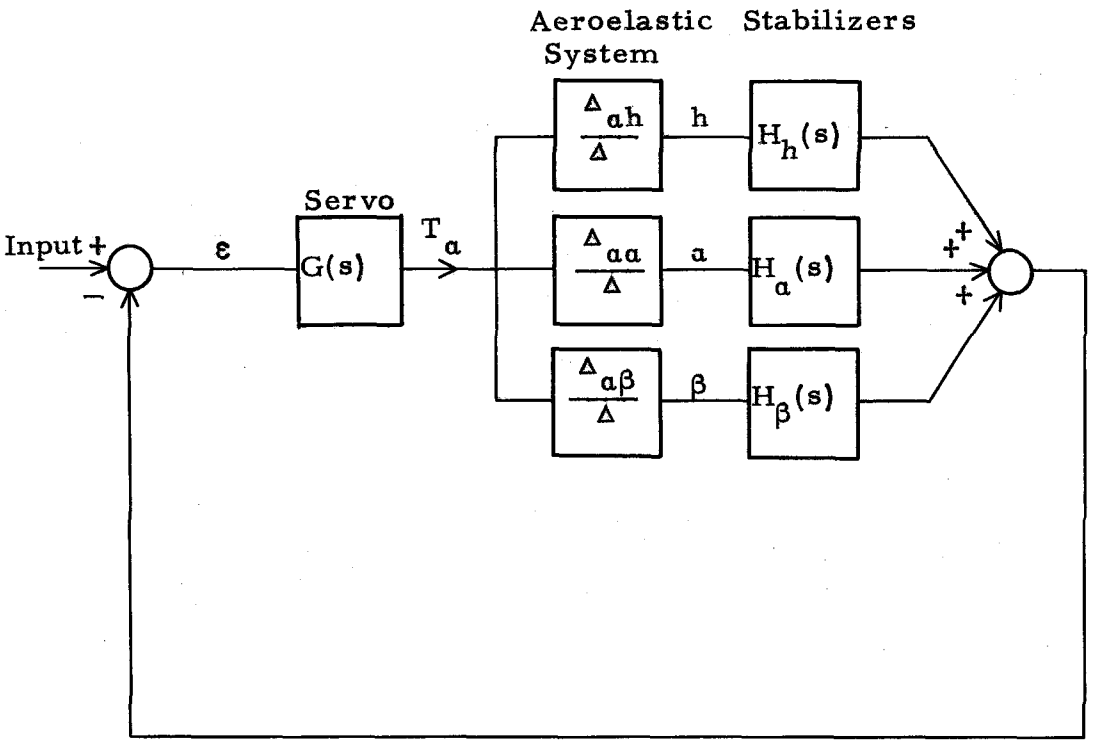

Block Diagram of Aeroelastic System and Stabilizers when Servo is a Jet Reaction Force on the α Coordinate

Figure 6.1

used for stabilization now become Δ_{ah}, $\Delta_{a\alpha}$, $\Delta_{a\beta}$. It turns out the $\Delta_{a\alpha}$ cofactor will almost always contain only L.H.P. zeros at speeds above the flutter speed of the aeroelastic system. This is true since $\Delta_{a\alpha}$ represents the characteristic determinant of the system with the α coordinate locked. Physical reasoning indicates that locking the α coordinate at say the outboard cell of a distributed wing will usually stabilize*. Thus the important distinction between an actuator force on β and an actuator force

---

*It is well known that in a three degree of freedom system, locking α prevents wing flutter.

on α is given in theorem 3.

Theorem 3

An actuator force on β properly chosen as discussed previously, ensures stability up to the flutter speed with β locked, the flutter speed of the basic wing. Only in certain cases can further improvement be made by α feedback. A properly chosen jet reaction torque on α ensures stability up to the flutter speed with α locked, which invariably is above the flutter speed of the wing. Hence an α force is more promising than a β force feedback control, in attempting to increase the flutter speed above that of the basic wing.

6.2 Numerical Investigation of Stabilization by a Jet Reaction Torque on α

For such a scheme, figure 6.1 reduces to one with only $H_\alpha(s)$ feedback as shown in figure 6.2.

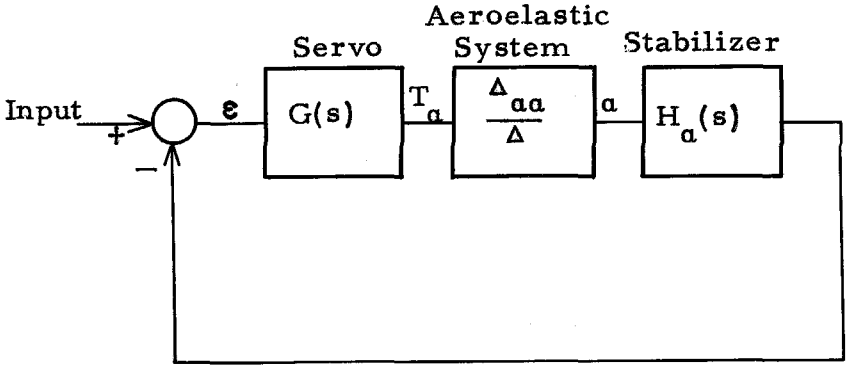

Figure 6.2

Such a configuration will essentially always produce stability in a three degree of freedom system, because only aileron-bending flutter would then be possible. This type flutter does not exist for speeds above the flutter speed of the locked aileron

(or can be removed by a flap servo as previously described). Hence in investigating numerical cases of a scheme as figure 6.2, the distributed system alone need be investigated, wherein the jet reaction force is applied to an outboard cell. The uniform rectangular wing, previously examined in part IV by a three degree of freedom approximation, was investigated on the analog computer for this purpose. A $4\frac{1}{2}$ cell finite difference approximation was used. Also the complete subsonic, incompressible flow aerodynamics were represented, with the more accurate ratio of second degree polynomials used for C(k).

A speed of $\sqrt{2}$ times the aeroelastic flutter speed was examined. The determination of whether Δ_{aa} had left half plane zeros at this speed, which would permit a semi-infinite band of stable k_1k_2 values in figure 2.11, was easily determined on the analog. G(s) was made unity and $H_a(s)$ was made infinite. For this condition, the feedback loop in figure 6.2 is made equivalent to an infinite spring. This is done on the analog by merely locking the α coordinate. For this condition, the system was stable, thereby ensuring that Δ_{aa} has only left half plane zeros at that speed.

Since K_2 of figure 2.11 is infinite at that speed of $\sqrt{2}$ times the aeroelastic flutter speed, K_1 alone is needed to determine the stable range of k_1k_2 at this speed. To accomplish this $H_a(s)$ is reduced in magnitude until marginal stability occurs. From figure 6.2 it is noted that $H_a(s)$ is equivalent to a pure spring on α, when $G(s) = 1$. The value of this spring needed for marginal stability at this speed was 66.7 ft. lb/radian, or about 1/2 the basic torsional stiffness of the structure ($\frac{GJ}{\ell} = 120$ ft. lb./radian).

The conclusion is that a jet reaction drive on the outboard cell in place of a control surface actuator, is approximately* equivalent to a torsional spring on that α coordinate. Invariably this produces a semi-infinite stable band of k_1k_2 values well above the flutter speed of the aeroelastic system. For the uniform wing studied, any value of this spring greater than 1/2 the basic structural torsional stiffness produces stability at $\sqrt{2}$ times the aeroelastic flutter speed. In contrast no semi-infinite stable band existed for the same wing above the aeroelastic flutter speed when a control surface actuator was used, as previously stated in part 4.4.

6.3 Instrumentation Feasibility of a Jet Reaction Torquer

The mathematical improvement in flutter speed when using a jet reaction torque on α has been shown by heuristic argument to be quite good in part 6.1, and demonstrated by numerical example in part 6.2. The only real question about this type of control is the instrumentation feasibility of adding such a power source.

This question is really a practical one rather than a theoretical one, and can hardly be answered in this study. One must investigate specific cases to determine the additional weight, size, etc. of such a power source. For each case, overall system considerations will determine whether the gain in flutter speed is achieved in more practical fashion by this technique or by competing techniques of doing the same (for example, stiffening the wing).

---

*Exactly if the servo were perfect, or G(s) equal to a constant.

It may be mentioned that a storage system might be used to reduce the peak power requirements of the air supply to the jet reaction torquer. The stabilizing torque required from the actuator as a function of time depends on the size of the gust disturbance acting on the wing. This latter is a statistical quantity with severe peaks occurring only infrequently. Thus, maximum air flow is required to the jet reaction torquer only occasionally, and a compressed air storage tank, supplied by a small compressor, may satisy this requirement. This is an argument that may permit incorporation of a jet reaction torquer at a small cost in weight.

Another argument for the instrumentation feasibility of a jet reaction torquer is that it may be supplied with air from a source already existent on the airplane or missile. Since the flutter stabilizer does not require a large continual air supply, the additional load it produces on the air system may well represent a small average value.

6.4 Difference in the Two Types of Feedback Stabilization from a Physical Standpoint

Part 6.1 showed the mathematical distinction between driving through a control surface, or driving on the wing itself by a jet reaction torquer. It is instructive to compare the difference in these two types of control on a more physical basis, as will now be done.

A typical jet reaction torquer is shown in figure 6.3.

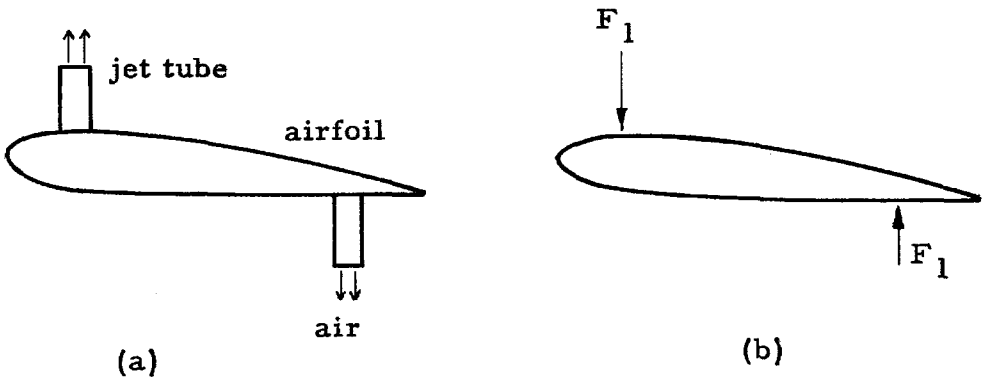

Jet Reaction Torque Applied to an Airfoil

Figure 6.3

The electrical signal to the controller (ε in figure 6.1) controls the flow of air from each tube in figure 6.3a, so that equal and opposite reaction forces (F_1 in figure 6.3b) act on the wing. Thus a pure couple (T_a in figure 6.2) is produced on the wing approximately proportional to the control signal. An additional set of torquers is used for the opposite sign of the controller signal, ε . It is to be noted that the stabilizer forces acting on the wing are directly supplied from the controller and not by the aerodynamics.

In contrast, for the control surface actuator the major stabilizing forces are produced by the aerodynamics. A simplified, but adequate, description of the significant forces acting on the wing is shown in figure 6.4. Only an aerodynamic force L' is shown which acts at the center of pressure. The pitching moment is ignored in this discussion since it does not change the validity of the argument.

Significant Forces on Wing

Figure 6.4

The important property of the L' force acting at a specific point, the center of pressure, is that it produces not only a moment on α (say about the elastic axis or c.g.), but it also produces a force on h. Thus it produces a generalized force on two coordinates h and α, rather than on just the one coordinate, α, as did the jet reaction torquer.

Obviously the two types of control produce different stabilizing effects. The question arises: which is the better stabilizing control, a pure couple on α, or a force on h besides a moment on α?

One might suspect a pure couple on α might be a better control because it acts without coupling the bending and torsion modes (usually a destabilizing action). One can go further from physical reasoning and note that the pure couple (T_α in figure 6.2) produced by the jet reaction torquer is proportional to α when the factor $H_\alpha(s)\, G(s)$ equals a constant. Thus the jet reaction torquer is equivalent to a spring on α. This can be made a positive or negative spring depending on the sign used for $H_\alpha(s)$. Thus the important conclusion stated in Theorem 4.

Theorem 4

Since the jet reaction torquer can be made to have the effect of a spring on α, it can have the same effect on flutter as stiffening the structure in torsion (in the limit locking the α coordinate). This usually is a stabilizing effect. The control surface actuator cannot produce this desired effect alone, but also must produce a force on h.

One can therefore see, completely from physical reasoning, that the jet reaction torquer will essentially always produce a stabilizing effect or an increase in flutter speed. For the control surface actuator, one cannot tell by physical reasoning the added effect of the force on h, but must resort to the mathematics of the previous parts. This showed that in many cases the effect of the force on h counteracted the stabilizing effect of the torque on α, thereby permitting no increase in flutter speed.

There exists another interesting interpretation of the physical differences in the two types of control. The jet reaction torquer produces an effect which is the same as changing the aerodynamic center of pressure. To prove this, it is noted that the combined generalized forces on the wing, due to the aerodynamics and the jet reaction torquer, are as follows: a lift L' on h, and a moment due to the jet reaction torquer. Since the latter is adjustable it may be made to increase or decrease the original aerodynamic moment, without changing the lift. This is, of course, the same effect as changing the center of pressure of the aerodynamic forces.

In the limit of an infinitely stiff effective spring produced

by the jet reaction torquer there exists a finite force and an infinite moment. This has the effect of shifting the center of pressure to infinity in either direction (depending on the sign of $H_a(s)$). Thus the center of pressure of the aerodynamics can be equivalently moved any distance fore or aft of the wing by the jet reaction control. It can readily be shown that a positive effective spring shifts the center of pressure aft. This is the desired direction for improved stabilization as shown in part IV.

Since the control surface actuator changes both the force and moment, no such simple interpretation is possible for this type of control.

The physical reasoning of this section, shows that a pure couple produced by the jet reaction torquer, usually has a more stabilizing effect than a moment and force produced by the control surface actuator. This substantiates the mathematical distinction earlier in this part concerning the R. H. P. properties of the zeros of $\Delta_{\alpha\alpha}$ compared to $\Delta_{\beta\beta}$ or $\Delta_{\beta a}$ or $\Delta_{\beta h}$.

PART VII

CONCLUSIONS AND RECOMMENDATIONS FOR FURTHER STUDY

7.1 Conclusions

The investigations of this study can be summarized in the five major points listed below.

(1) It is possible only in certain cases to raise the flutter speed in practice by feedback control. To examine the mathematical possibility of practical stabilization rule 3 of part II suffices. Thus the possibility of raising the flutter speed is answered by simple examination of a cofactor of the aeroelastic system such as $\Delta_{\beta\alpha}$ or $\Delta_{\alpha\alpha}$ for left or right half plane zeros. No explicit consideration of a specific servo or stabilizer transfer function is necessary in this determination. Note the similarity between this and the examination of Δ of the aeroelastic system, which determines stability of the system without feedback control.

The determination of the actual stabilizer transfer function, H(s), necessary to produce this stabilization, is easily found by the techniques of part 2.2.

(2) There exists the important conclusion that feedback of many coordinates is no better than the feedback of a single coordinate (rule 5 of part III). This reduces the stabilization investigation to the investigation of a single loop rather than investigation of many interacting loops, a monumental task.

(3) Two general types of feedback exist; the first, through the control surface or a torque on β; the second, a jet reaction torquer

on α. Theorem 3 describes the distinction in mathematical feasibility of stabilization in the two cases. For the former, stabilization above the basic wing flutter speed is possible only in certain cases, this by the use of α feedback rather than h or β. However β feedback can always remove aileron flutter. For the jet reaction torquer case, stabilization above the wing flutter speed is almost always possible. The jet reaction torquer type of stabilization pays the price of additional instrumentation.

(4) In considering the possibility of raising flutter speed by feedback control, the obvious order of investigation of the two techniques should be as follows. The control surface actuator type should always be investigated first for mathematical feasibility because of simpler instrumentation. If this is not possible mathematically, then the jet reaction torquer should be investigated. Since this technique is usually possible mathematically, the only question would be the practicality of the additional equipment. A scheme was suggested in part VI to simplify this instrumentation (stored air supply).

(5) Eleven three degree of freedom systems were studied in this investigation. Certain trends were presented in part IV. Similar investigations on specific actual systems can be made using either of the two techniques mentioned in this study: a) the examination of the cofactors $\Delta_{\beta\alpha}$, $\Delta_{\alpha\alpha}$, etc. for left half plane zeros by digital computer techniques, b) the examination of the aeroelastic servo system on the direct electric analog.

It is felt that mathematical and instrumentation feasibility of raising flutter speed can be achieved by at least one of the two feedback types of this study in many airplane and missile systems. It is hoped that flutter and autopilot analysts will give serious consideration to these techniques of stabilization.

7.2 Recommendations for Further Study

As mentioned previously, numerical examination of many more test cases is needed, in particular actual systems with distributed properties, to ascertain the percentage of cases in which either, or both, types of control are practically feasible.

A recommended study would be the examination of ten typical actual wings with distributed properties. If digital computers were used in this study, the same techniques would be employed as used in conventional flutter analysis. The only difference would be that the significant determinant now becomes $\Delta_{\beta a}$ and Δ_{aa}, instead of Δ. For analog study, the aeroelastic system is represented in the conventional manner; the servo and stabilizer is represented by an operator as shown in figure 5.5.

It is suggested that the ten systems studied be wings for which flutter studies have previously been carried out. This reduces considerably the amount of work involved in setup of the problem, and also ensures examination of known systems so that checking of results is easily performed. For either type of computation, digital or analog, the basic setup would be available from the previous studies. The new data concerning the feasibility of stabilization would not be difficult to obtain from the existing problem setup.

The present study has laid the mathematical groundwork and investigated a few systems numerically in considering the possibility of increase in flutter speed by feedback control. The numerical data from further studies as recommended above would indicate more definitely the practical feasibility of these techniques.

REFERENCES

1. Truxall, John G.: Automatic Feedback Control System Synthesis. McGraw Hill, New York, 1955.

2. Evans, W. R.: Control System Synthesis by Root Locus Method. Trans. A.I.E.E., Vol. 69, 1950.

3. McRuer, D. T.; Benun, D.; Click, C. E.: Influence of Servo-Mechanisms on the Flutter of Servo Controlled Aircraft. AF Technical Report 6287, March 1954.

4. Theodorsen, T.; Garrick, I. E.: Mechanism of Flutter A Theoretical and Experimental Investigation of the Flutter Problem. NACA Report No. 685, 1940.

5. Braham, H. S.: Wing Flutter in Coupled Aeroelastic Servo Systems. California Institute of Technology Analysis Laboratory Report, April 1957.

6. Scanlan, R. H.; Rosenbaum, R.: Introduction to the Study of Aircraft Vibration and Flutter. MacMillan Company, New York, 1951.

7. Fung, Y. C.: Theory of Aeroelasticity. John Wiley and Sons, New York, 1955.

8. Wilts, C. H.: Finite Difference Errors in the Flutter Speed of a Uniform Wing with an Arbitrarily Placed Mass. C.I.T. Analysis Laboratory Report, June 30, 1954.

APPENDIX A

DEMONSTRATION THAT THE CLOSED LOOP TRANSFER FUNCTION OF A FEEDBACK SYSTEM WITH MINIMUM PHASE BASIC ELEMENTS CONTAINS ONLY LEFT HALF PLANE ZEROS

Consider a complex feedback system such as figure 2.6 of the text.* By assumption the zeros and poles of the basic elements, the G's and H's lie in the left half s plane. The conditions under which the closed loop transfer function c'/r has right half plane zeros is now derived. It is then shown that virtually all servos, feedback amplifiers, autopilots, etc. do not satisfy this condition, and hence have only left half plane zeros in the closed loop transfer function.

Consider the specific system of figure 2.6. To analyze the system, one can eliminate all the inner loops in a series of steps, leaving only the single outer loop. This can be done by replacing each feedback operator by an equivalent operator from output to input of the next larger loop. Thus, figure 2.6 is first reduced by replacing $H_4(s)$ by an equivalent operator, as shown in figure A.1.

---

*The systems under consideration are restricted as follows, with no loss in generality. From any point along the forward transmission from r to c', a feedback H_i exists from that point back to some earlier point in the forward transmission, such that the transmission along the H_i path exists only in the one direction. The H_i themselves may contain internal loops. Also the G operators are connected in simple cascade.

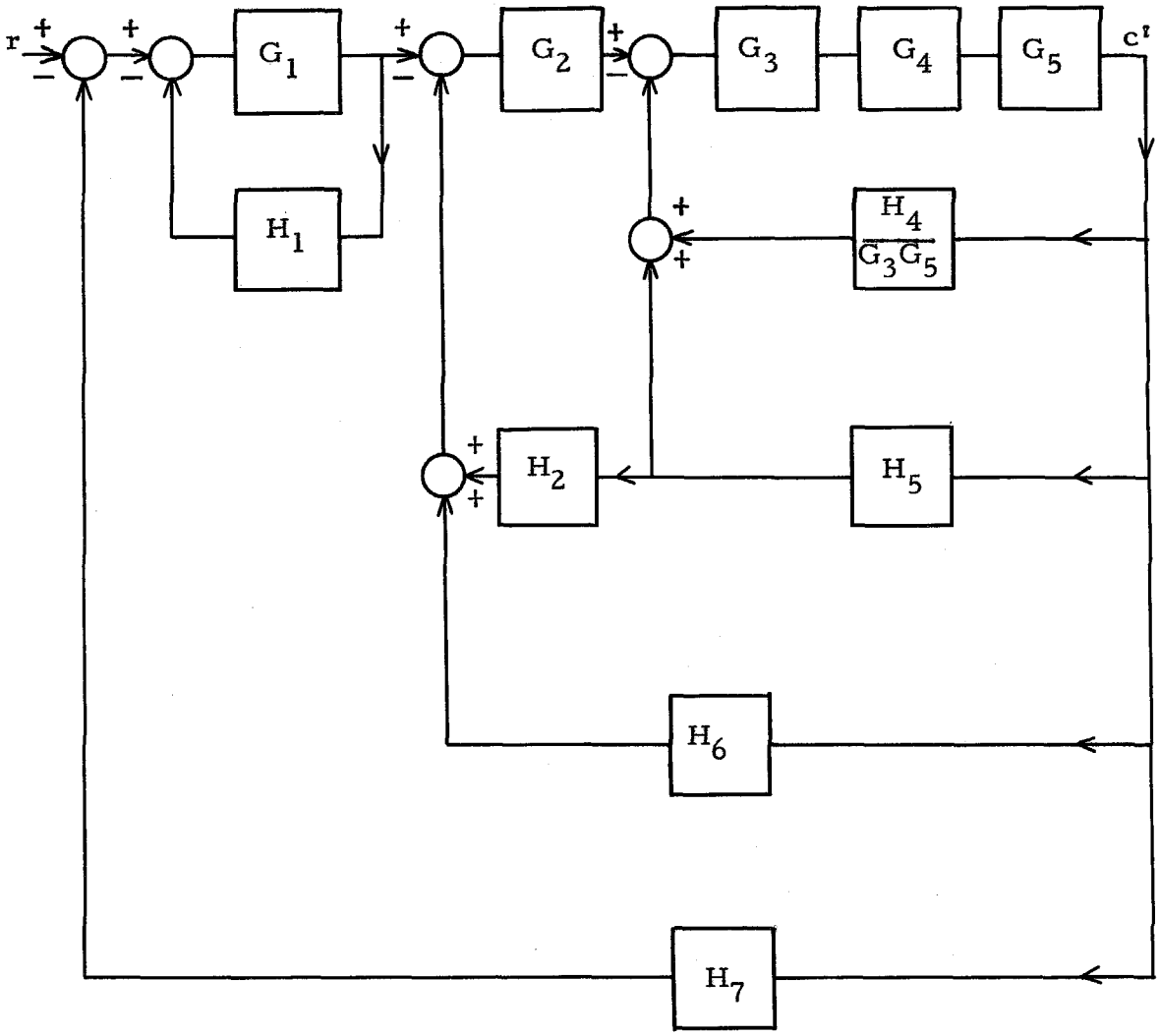

Block Diagram of Figure 2.6 when H_4 Feedback
is Replaced by Equivalent Feedback in Next Larger Loop

Figure A.1

The next loop elimination is produced by adding $\frac{H_4}{G_3G_5}$ to H_5, and replacing this by an equivalent operator at the input to G_2. Thus figure A.1 becomes

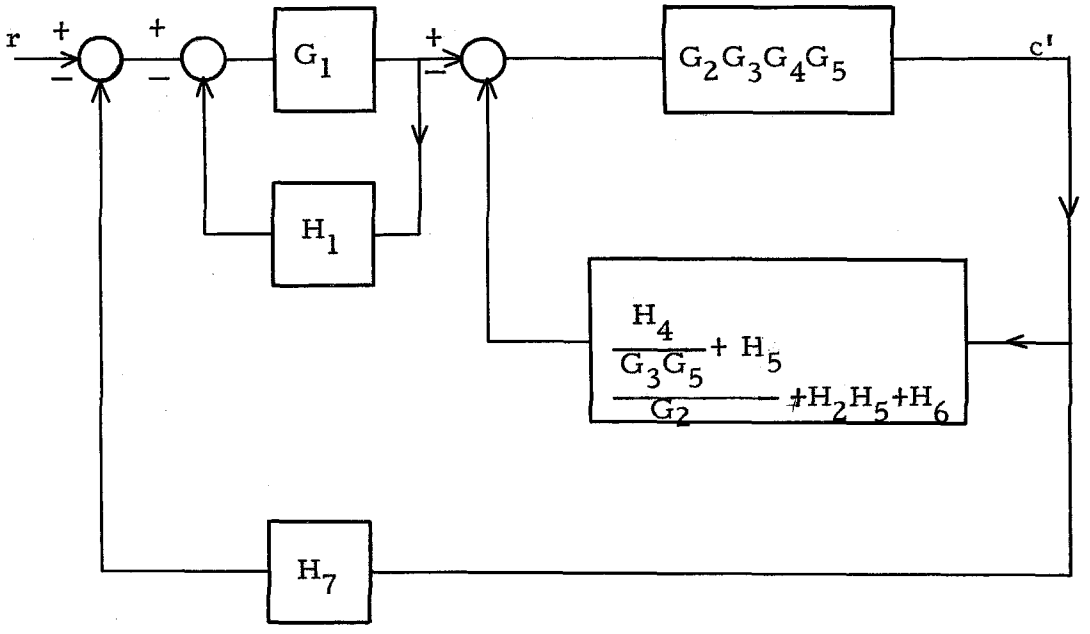

Simplification of A. 1

Figure A. 2

A final reduction leaves only the outer loop shown in figure A. 3.

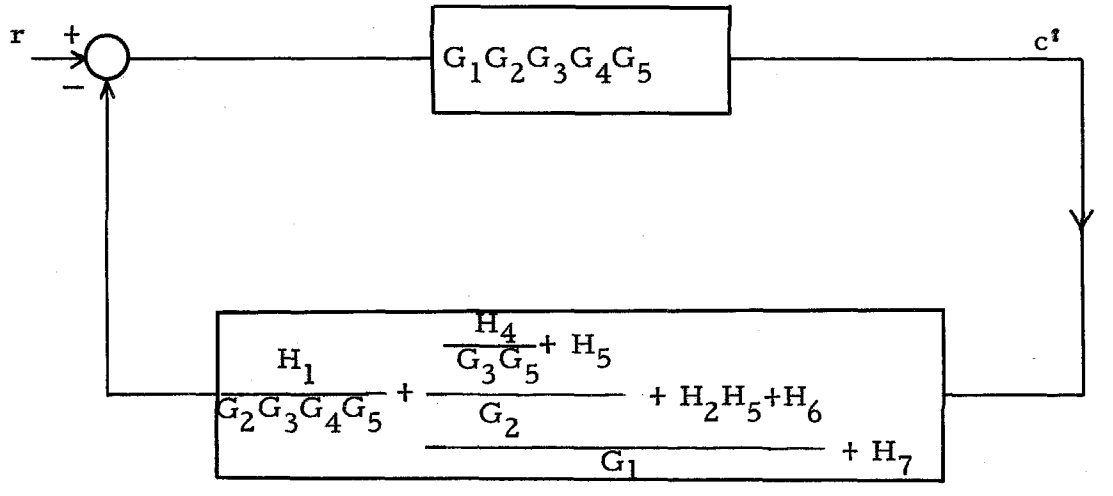

Final Reduction of Figure 2. 6 into a Single Loop

Figure A. 3

Figure A. 3 can be redrawn as in figure A. 4 by rationalizing the fractions in figure A. 3, and defining,

$$G \equiv G_1G_2G_3G_4G_5 \tag{A. 2}$$

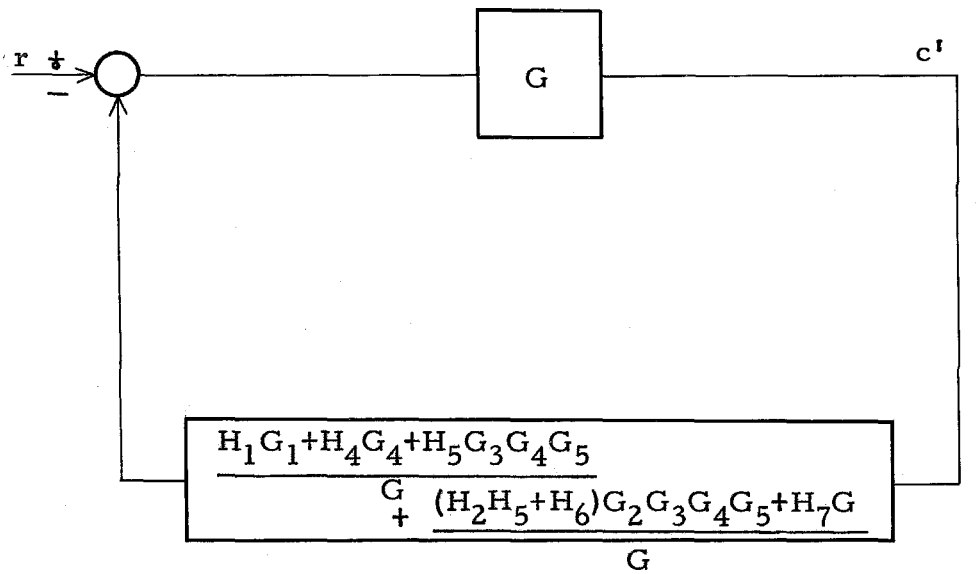

Same as Figure A. 3 Except for Rationalized Expressions

Figure A. 4

The ratio of c'/r can readily be found from figure A. 4.

$$\frac{c'}{r} = \frac{G}{1+H} \tag{A. 3}$$

where

$$H = H_1G_1 + H_4G_4 + H_5G_3G_4G_5 + (H_2H_5 + H_6)\, G_2G_3G_4G_5 + H_7G \tag{A. 4}$$

Clearly the zeros of equation A. 3 are due to:

a) The zeros of G defined in equation A. 2.

b) The poles of H defined in equation A. 4.

Thus the zeros of c'/r will lie in the right half plane if, and only if, some forward gain quantity, G_1, G_2, G_3, G_4 or G_5 has right half plane zeros, or some feedback quantity, H_1, H_2, H_4, H_5, H_6 or H_7 has right half plane poles. But this is prohibited by assumption in the type of systems under consideration. Thus c'/r cannot contain right half plane zeros.

By simple extension, this can be demonstrated for systems with even more loops than figure 2. 6. Thus the original premise is proved by induction.

It should be mentioned that the transfer function of c'/r in a system such as figure 2. 6 would have right half plane zeros, if the feedback basic elements $H_1, H_2, H_4, H_5, H_6, H_7$ were permitted to consist of feedback loops themselves which were unstable. Thus if H_1 were actually made up of a feedback loop as follows,

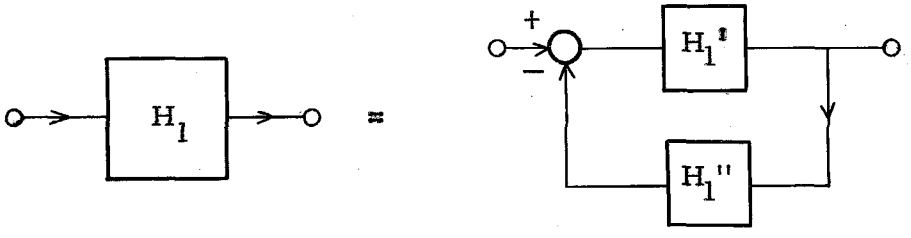

then the transfer function of H_1 might contain right half plane poles (an unstable operator for H_1). This leads to right half plane zeros of c'/r according to the above discussion. However the use of feedback operators such as $H_1, H_2, H_4, H_5, H_6, H_7$ of figure 2. 6

which have feedback loops within themselves, is rare indeed. The case of unstable feedback loops constituting the basic H_1, H_2, etc. operators, the necessary condition for right half plane zeros of c'/r , is practically non-existent. Thereby results the premise stated in the text that virtually all servos, feedback amplifiers, and similar systems, no matter how many loops in the system, have only left half plane zeros in the transfer functions.

APPENDIX B

SERVO TORQUE IN h, α, β COORDINATE SYSTEM

The effect produced by the powered actuator is a torque of magnitude T_β, acting between the control surface and parent surface. Consider that cell along the span where the torque is applied. The following free body diagram shows the equal and opposite torques exerted by the servo on the α and γ absolute coordinates of that cell.

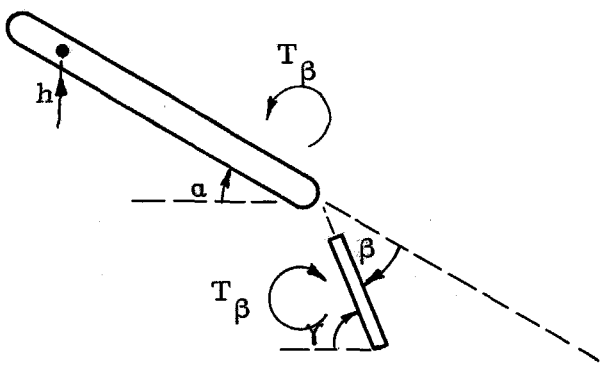

Free Body Diagram of Servo Torque Acting on

Parent and Control Surfaces

Figure B. 1

Thus the forces on the h, α, γ coordinate system are known. One desires to transform the forces to the h, α, β coordinate system.

To do this, the well-known matrix laws of transforming coordinates and displacements are used. The following definitions are made.

$[\bar{y}]$ displacement vector in h, α, γ system

$[y]$ displacement vector in h, α, β system

$[\bar{F}]$ force vector in h, α, γ system

$[F]$ force vector in h, α, β system

$[W]$ matrix relating $[\bar{y}]$ to $[y]$

$[W]^T$ transpose of $[W]$

Therefore,

$$[\bar{y}] = [W][y] \tag{B.1}$$

and

$$[F] = [W]^T [\bar{F}] \tag{B.2}$$

The W matrix which transforms the h, α, β coordinates to h, α, γ is written by simple inspection of figure B.1.

$$[W] = \begin{bmatrix} 1 & 0 & 0 \\ 0 & 1 & 0 \\ 0 & 1 & 1 \end{bmatrix} \tag{B.3}$$

$[\bar{F}]$, the force vector on h, α, γ, is simply

$$[\bar{F}] = \begin{bmatrix} 0 \\ -T_\beta \\ T_\beta \end{bmatrix} \tag{B.4}$$

$[F]$, the force vector on h, α, β is found using equations B.2, B.3, and B.4.

$$[F] = \begin{bmatrix} 1 & 0 & 0 \\ 0 & 1 & 1 \\ 0 & 0 & 1 \end{bmatrix} \begin{bmatrix} 0 \\ -T_\beta \\ T_\beta \end{bmatrix} = \begin{bmatrix} 0 \\ 0 \\ T_\beta \end{bmatrix} \qquad \text{(B.5)}$$

Thus the servo torque in the h, α, β coordinate system is a torque of the original magnitude, T_β, acting on only one coordinate, the β coordinate.

APPENDIX C

REPRESENTATION OF $\Delta_{\beta h}$, $\Delta_{\beta\alpha}$, $\Delta_{\beta\beta}$ OF A THREE DEGREE OF FREEDOM SYSTEM AS A FIFTH DEGREE POLYNOMIAL IN s.

The matrix equation for the three degree of freedom system of figure 3.1 is

$$[F] = [A][X] \tag{C.1}$$

where $[F]$ represents the external force vector, $[A]$ represents the aeroelastic force matrix, and $[X]$ represents the h, α, β coordinate vector. $[A]$ may be written as the sum of the structural matrix $[A]_1$ plus the aerodynamic matrix $[A]_2$.

$$[A] = [A]_1 + [A]_2 \tag{C.2}$$

The structural matrix is given in reference 6, page 196. It is repeated in equation C.3 where the sign convention of our study for h (positive up) differs from the sign convention of reference 6. Using the notation of reference 6, $[A]_1$ becomes, for coordinates h, α, and β in that order,

$$[A]_1 = \begin{bmatrix} M s^2 + C_h & -S_\alpha s^2 & -S_\beta s^2 \\ -S_\alpha s^2 & I_\alpha s^2 + C_\alpha & I_c s^2 \\ -S_\beta s^2 & I_c s^2 & I_\beta s^2 + C_\beta \end{bmatrix} \tag{C.3}$$

where

$$I_c \equiv I_\beta + (c - a) b S_\beta \tag{C.4}$$

The following simplified subsonic, incompressible two dimensional, aerodynamics is used.

$$\bar{\alpha} \equiv \alpha - \frac{\dot{h}_{3/4}}{V} + U_1\beta = \alpha - \frac{\dot{h}_{e.a.}}{V} + \frac{2b}{V}\left(\frac{3}{4} - x_r\right)\dot{\alpha} + U_1\beta \qquad (C.5)$$

and

$$L' = 2\pi(q')\,(2b)\,C(k)\,\bar{\alpha}$$

$$Q_\alpha = 2b\left(x_r - \frac{1}{4}\right)L' - \frac{\pi}{8}(q')\,(2b)^2\,\frac{2b}{V}\,\dot{\alpha} - q'\,(2b)^2\,\frac{U_4}{2}\,\beta \qquad (C.6)$$

$$Q_\beta = -2b\left(\frac{U_6}{2}\right)L' - q'\,(2b)^2\,\frac{U_8}{2}\,\beta$$

This represents the ordinary C_{L_α} term or lift due to angle of attack $\bar{\alpha}$, and the C_{M_q} or α moment due to pitching velocity, as well as the major moment terms due to the aileron. The aero inertia terms, or terms proportional to the second derivative of h, α, and β, have only a small influence on flutter speed. For our purpose of ascertaining trends of relative stability of the $\Delta_{\beta h}$, $\Delta_{\beta\alpha}$ and $\Delta_{\beta\beta}$ operators for many different systems, it is felt safe to ignore these terms as is done in equation C.6.

The U quantities used in equations C.5 and C.6 are a composite of the T functions of Theodorsen. These depend only on the geometrical value c, as defined below.

$$U_1 = \frac{1}{\pi}(1-c^2)^{\frac{1}{2}} + \frac{1}{\pi}\cos^{-1}c$$

$$U_4 = (1+c)\,(1-c^2)^{\frac{1}{2}}$$

$$U_6 = \frac{1}{2\pi}(2+c)\,(1-c^2)^{\frac{1}{2}} - \frac{1}{2\pi}(1+2c)\cos^{-1}c \qquad (C.7)$$

$$U_8 = \frac{1}{\pi}(1+c)\,(1-c^2)^{\frac{1}{2}}\cos^{-1}c - \frac{1}{\pi}(1+c)\,(1-c^2)$$

Equations C.5 and C.6 can be combined to form the aerodynamic matrix, $[A]_2$, the negative of the L', Q_α, and Q_β forces.

$$[A]_2 = \begin{bmatrix} C(k)\frac{Ds}{2bs_o} & -C(k)\,D\left[1 + (\frac{3}{4} - x_r)\frac{s}{s_o}\right] & -C(k)\,DU_1 \\ C(k)\frac{DK_5 s}{2bs_o} & -C(k)\,DK_5\left[1 + (\frac{3}{4} - x_r)\frac{s}{s_o}\right] & -C(k)DK_5U_1 \\ & + \frac{Dbs}{8s_o} & +D\frac{bU_4}{2\pi} \\ -C(k)\frac{DU_6 s}{2s_o} & C(k)\,DbU_6\left[1 + (\frac{3}{4} - x_r)\frac{s}{s_o}\right] & C(k)\,DbU_6U_1 \\ & & + 2qb^2U_8 \end{bmatrix} \quad (C.8)$$

The following definitions pertain to equation C.8.

$$D \equiv 2\pi b\rho V^2 \ell$$

$$s_o \equiv \frac{V}{2b} \quad (C.9)$$

$$K_5 \equiv 2b\,(x_r - \frac{1}{4})$$

The addition of the $[A]_2$ matrix of equation C.8, and the $[A]_1$ matrix of equation C.3 yields the entire aeroelastic matrix, $[A]$, given in equation C.10.

$$
[A] = \begin{bmatrix}
\underline{h} & \underline{\alpha} & \underline{\beta} \\
M s^2 + C_h + C(k) \frac{Ds}{2bs_o} & -S_\alpha s^2 - C(k) \frac{Ds}{s_o} \left(\frac{3}{4} - x_r\right) - C(k)D & -S_\beta s^2 - C(k)\, DU_1 \\
-S_\alpha s^2 + C(k) \frac{DK_5 s}{2bs_o} & I_\alpha s^2 - C(k) \frac{Ds}{s_o} K_5 \left(\frac{3}{4} - x_r\right) + \frac{Dbs}{8s_o} & s^2 I_c - C(k)\, DK_5 U_1 + \frac{DbU_4}{2\pi} \\
 & + C_\alpha - C(k) K_5 D & \\
-S_\beta s^2 - C(k) \frac{DU_6 s}{2s_o} & I_c s^2 + C(k)\, DU_6\, b\left(\frac{3}{4} - x_r\right) \frac{s}{s_o} & I_\beta s^2 + C_\beta + C(k) DbU_6 U_1 \\
 & + C(k)\, DU_6 b & + 2qb^2 U_8
\end{bmatrix}
$$

where

$$D \equiv 2\pi b \rho V^2 \ell \qquad K_5 \equiv 2b\left(x_r - \frac{1}{4}\right)$$

$$s_o \equiv \frac{V}{2b} \qquad I_c = I_\beta + (c - a)\, bS_\beta$$

Equation C.10. Entire Aeroelastic Matrix

Representation of $\Delta_{\beta h}$, $\Delta_{\beta \alpha}$, and $\Delta_{\beta\beta}$ as Fifth Degree Polynomials in s

$\Delta_{\beta h}$, $\Delta_{\beta \alpha}$ and $\Delta_{\beta\beta}$ may each be formed as a cofactor of the [A] matrix of equation C.10, represented by a fourth degree polynomial in s, wherein C(k) is contained in the coefficients of s. C(k) may be suitably approximated for our purposes by a ratio of first degree polynomials in s.

$$C(k) = \frac{1 + T_1 \frac{b}{V} s}{1 + T_3 \frac{b}{V} s} \qquad \text{(C.11)}$$

T_1 and T_3 are dimensionless constants, which, for best flutter prediction, are given the following values.

$$T_1 = 4.311$$

$$T_3 = 7.221 \qquad \text{(C.12)}$$

After insertion of the expression for C(k), given by equation C.11, into the matrix of equation C.10, a straightforward but rather lengthy manipulation yields expressions of modified $\Delta_{\beta h}$, $\Delta_{\beta \alpha}$, $\Delta_{\beta\beta}$ as fifth degree polynomials in s. The zeros of these expressions, given in equation C.13, yield the zeros of $\Delta_{\beta h}$, $\Delta_{\beta \alpha}$ and $\Delta_{\beta\beta}$. The C'', C' and C constants of $\Delta_{\beta h}$, $\Delta_{\beta \alpha}$ and $\Delta_{\beta\beta}$ in equation C.13 are defined in terms of the B'', B', and B constants in equation C.14. These B'', B' and B constants in turn are defined in terms of the nine basic non-dimensional parameters of the aeroelastic system in equations C.15a, C.15b, C.15c. Thus a specification of these nine basic parameters in effect determines the constants C'', C'

and C of equation C. 13. These nine basic parameters are

$$\frac{\omega_h}{\omega_a}\ ,\ K\ ,\ \frac{x_a}{b}\ ,\ \frac{r_a}{b}\ ,\ x_r\ ,\ \frac{x_\beta}{b}\ ,\ \frac{r_b}{b}\ ,\ \frac{m}{M}\ ,\ c$$

$$\frac{(1 + k_3 \frac{b}{V} s)\bar{v}}{I_a S_\beta \omega_a{}^4} \Delta_{\beta h} = C''_5 \bar{s}^5 + C''_4 \bar{v} \bar{s}^4 + (C''_{31} - \bar{v}^2 C''_{32}) \bar{s}^3$$

$$+ \bar{v}\left[1 - C''_{22}\bar{v}^2\right] \bar{s}^2 + \bar{v}^2 \left[C''_{11} - C''_{12} \bar{v}^2\right] \bar{s} + \bar{v}^3 \left[C''_{01} - C''_{02} \bar{v}^2\right]$$

$$- \frac{(1 + k_3 \frac{b}{V} s)\bar{v}}{I_c M \omega_a{}^4} \Delta_{\beta a} = C'_5 \bar{s}^5 + C'_4 \bar{v} \bar{s}^4 + (C'_{31} - \bar{v}^2 C'_{32}) \bar{s}^3$$

$$+ \bar{v}\left[\frac{\omega_h{}^2}{\omega_a{}^2} - \bar{v}^2 C'_{22}\right] \bar{s}^2 + \bar{v}^2 \left[C'_{11} + C'_{12} \bar{v}^2\right] \bar{s} + \bar{v}^3 C'_o$$

$$\frac{(1 + k_3 \frac{b}{V} s)\bar{v}}{I_a M \omega_a{}^4} \Delta_{\beta\beta} = C_5 \bar{s}^5 + C_4 \bar{v} \bar{s}^4 + (C_{31} - \bar{v}^2 C_{32}) \bar{s}^3$$

$$+ \bar{v}\left[C_{21} - \bar{v}^2 C_{22}\right] \bar{s}^2 + \left[C_{11} - C_{12} \bar{v}^2\right] \bar{s} + C_o \bar{v} (1 - \bar{v}^2)$$

where

$$\bar{v} \equiv \frac{V}{V_d} \qquad V_d = \frac{r_a \omega_a}{2} \left[\frac{1}{K(x_r - \frac{1}{4})}\right]^{\frac{1}{2}}$$

$$\bar{s} = \frac{s}{\omega_a}$$

Equation C.13. Expressions for $\Delta_{\beta h}$, $\Delta_{\beta a}$, $\Delta_{\beta\beta}$ at Any Speed.

C''	C'	C
$C''_5 = T_3 k_d B''_4$	$C'_5 = T_3 k_d B'_4$	$C_5 = T_3 k_d B_4$
$C''_4 = B''_4 + B''_{31} T_3 k_d - B''_{32} T_1 k_d$	$C'_4 = B'_4 + T_1 k_d B'_3$	$C_4 = B_4 + T_1 k_d B_{32} + T_3 k_d B_{31}$
$C''_{31} = T_3 k_d$	$C'_{31} = \frac{\omega_h^2}{\omega_a^2} T_3 k_d$	$C_{31} = T_3 k_d B_{21}$
$C''_{32} = B''_{21} T_3 k_d - B''_{22} T_1 k_d - B''_{31} + B''_{32}$	$C'_{32} = T_1 k_d B'_{22} - T_3 k_d B'_{21} - B'_3$	$C_{32} = T_1 k_d B_{22} - (B_{32} + B_{31})$
$C''_{22} = B''_{21} - B''_{22} - B''_{11} T_1 k_d$	$C'_{22} = B'_{22} - B'_{21} - B'_1 \; T_1 k_d$	$C_{21} = B_{21} + T_1 k_d B_{12} + T_3 k_d B_{11}$
$C''_{11} = T_1 k_d B''_{01}$	$C'_{11} = T_3 k_d B'_{01} - T_1 k_d B'_{02}$	$C_{22} = B_{22}$
$C''_{12} = B''_{02} T_1 k_d - B''_{11}$	$C'_{12} = B'_1$	$C_{11} = T_3 k_d B_0$
$C''_{01} = B''_{01}$	$C'_0 = B'_{01} - B'_{02}$	$C_{12} = T_1 k_d B_0 - \left[B_{11} + B_{12} \right]$
$C''_{02} = B''_{02}$		$C_0 = B_0$

where

$$k_d \equiv \frac{b\omega_a}{V_d} = \frac{2}{r_a/b} \left[K(x_r - \frac{1}{4}) \right]^{\frac{1}{2}}$$

$$T_1 = 4.311, \quad T_3 = 7.221$$

Equation C.14. Definition of the Values of C Constants of Equation C.13 in Terms of B Constants

$$B''_4 = 1 - \frac{I_c}{I_a} \frac{x_a}{x_b} \frac{M}{m}$$

$$B''_{31} = \left(\frac{K}{x_r - \frac{1}{4}}\right)^{\frac{1}{2}} \frac{1}{4 \frac{r_a}{b}}$$

$$B''_{32} = \frac{2}{\frac{r_a}{b}} \left(\frac{K}{x_r - \frac{1}{4}}\right)^{\frac{1}{2}} \left(\frac{3}{4} - x_r\right) \left[2\left(x_r - \frac{1}{4}\right) + \frac{\frac{r_c^2}{b^2}}{\frac{x_\beta}{b}}\right]$$

$$B''_{21} = \frac{U_4}{4\pi} \frac{x_a}{x_\beta} \frac{M}{m} \frac{1}{\left(x_r - \frac{1}{4}\right)}$$

$$B''_{22} = \left(U_1 \frac{x_a}{x_\beta} \frac{M}{m} - 1\right) + \frac{U_1 \frac{r_a^2}{b^2} \frac{M}{m} - \frac{r_c^2}{b^2}}{2 \frac{x_\beta}{b} \left(x_r - \frac{1}{4}\right)}$$

$$B''_{11} = \left[\frac{U_1}{8} - U_4 \frac{\left(\frac{3}{4} - x_r\right)}{2\pi}\right] \left(\frac{K}{x_r - \frac{1}{4}}\right)^{\frac{1}{2}} \frac{1}{\left(x_r - \frac{1}{4}\right)} \frac{r_a}{b} \frac{M}{m}$$

$$B''_{01} = \frac{U_1}{2\left(x_r - \frac{1}{4}\right)} \frac{M}{m} \frac{\frac{r_a^2}{b^2}}{\frac{x_\beta}{b}}$$

$$B''_{02} = \frac{U_4}{8\pi} \frac{1}{\left(x_r - \frac{1}{4}\right)^2} \frac{M}{m} \frac{\frac{r_a^2}{b^2}}{\frac{x_\beta}{b}}$$

Equation C.15a. Definition of B'' Constants of Equation C.14

$$B_4' = 1 - \frac{x_a x_\beta}{r_c^2}$$

$$B_3' = \frac{r_a}{b} \left(\frac{K}{x_r - \frac{1}{4}}\right)^{\frac{1}{2}} \left[1 + 2(x_r - \frac{1}{4}) \frac{\frac{x_\beta}{b}}{\frac{r_c^2}{b^2}}\right]$$

$$B_{22}' = U_1 \frac{I_a}{I_c} \left(1 + \frac{\frac{x_a}{2b}}{x_r - \frac{1}{4}}\right)$$

$$B_{21}' = \frac{I_a}{I_c} \frac{U_4}{4\pi} \frac{1}{(x_r - \frac{1}{4})}$$

$$B_1' = \frac{U_4}{4\pi} \frac{I_a}{I_c} \frac{r_a}{b} \left(\frac{K}{x_r - \frac{1}{4}}\right)^{\frac{1}{2}} \frac{1}{(x_r - \frac{1}{4})}$$

$$B_{01}' = \left(\frac{\omega_h}{\omega_a}\right)^2 \frac{I_a}{I_c} \frac{U_4}{4\pi} \frac{1}{x_r - \frac{1}{4}}$$

$$B_{02}' = \left(\frac{\omega_h}{\omega_a}\right)^2 \frac{I_a}{I_c} U_1$$

where

$$\frac{r_c^2}{b^2} \equiv \frac{r_\beta^2}{b^2} + (c - a)\left(\frac{x_\beta}{b}\right)$$

and

$$\frac{I_a}{I_c} \equiv \frac{r_a^2 M}{r_c^2 m}$$

Equation C.15b. Definition of B' Constants of Equation C.14

$$B_4 = 1 - \frac{x_a^2}{r_a^2}$$

$$B_{32} = \frac{2}{\frac{r_a}{b}} \left(\frac{K}{x_r - \frac{1}{4}}\right)^{\frac{1}{2}} \left[\frac{r_a^2}{2b^2} - 2\left(x_r - \frac{1}{4}\right)\left(\frac{3}{4} - x_r\right) + \frac{x_a}{b}\left(2x_r - 1\right)\right]$$

$$B_{31} = \frac{1}{4} \frac{1}{\frac{r_a}{b}} \left(\frac{K}{x_r - \frac{1}{4}}\right)^{\frac{1}{2}}$$

$$B_{21} = 1 + \left(\frac{\omega_h}{\omega_a}\right)^2$$

$$B_{22} = 1 + \frac{\frac{x_a}{2b} - \frac{K}{4}}{x_r - \frac{1}{4}}$$

$$B_{12} = \frac{r_a}{b} \left(\frac{K}{x_r - \frac{1}{4}}\right)^{\frac{1}{2}} \left[1 - \frac{4\left(\frac{3}{4} - x_r\right)\left(x_r - \frac{1}{4}\right)\left(\frac{\omega_h}{\omega_a}\right)^2}{\frac{r_a^2}{b^2}}\right]$$

$$B_{11} = \frac{1}{4}\left(\frac{\omega_h}{\omega_a}\right)^2 \frac{1}{\frac{r_a}{b}} \left(\frac{K}{x_r - \frac{1}{4}}\right)^{\frac{1}{2}}$$

$$B_0 = \left(\frac{\omega_h}{\omega_a}\right)^2$$

Equation C.15c. Definition of B Constants of Equation C.14

APPENDIX D

INVESTIGATION OF THE POLES OF Δ, $\Delta_{\beta\alpha}$, $\Delta_{\beta\beta}$ AND $\Delta_{\alpha\alpha}$, AND THE ZEROS AT INFINITY

The force vs. displacement matrix of the aeroelastic system for n degrees of freedom is an obvious extension of the $[A]$ matrix of equation 3.1, which describes a three degree of freedom system. Δ is a sum of $n!$ terms, each containing n factors of different A_{ij} elements. A_{ij} is the general element of the $[A]$ matrix, located in the i^{th} row and j^{th} column. Therefore Δ can have only such poles as exist in the most general A_{ij} term. A_{ij} can be approximated as follows.

$$A_{ij} = M_{ij}s^2 + G_{ij}s + K_{ij} + C(k)\left[G_{ij}'s + K_{ij}'\right] + D(s) \qquad (D.1)$$

The first three terms in equation D.1 are the usual passive force terms, the mass, damping, and spring forces, respectively. The Theodorsen function of subsonic aerodynamics, C(k), weights the damping and spring aerodynamic forces, $G_{ij}'s$ and K_{ij}'. A similar lag term exists for supersonic aerodynamics, represented by D(s) in equation D.1.

It can be shown that the Theodorsen function has poles only on the negative real axis. In particular, the ratio of 2nd degree polynomials, often used as an approximation to the Theodrosen function, has two poles on the negative real axis. It is thereby seen from equation D.1 that, for subsonic speeds, A_{ij} will contain

only poles in the left half plane, those due to the Theodorsen function. A similar result holds for the usual polynomial approximation of D(s) for supersonic flow. Therefore for Δ, or any of its cofactors, left half plane poles are the only poles that exist, these due to the aerodynamic lag functions.

It is instructive to note the behavior of Δ, or any of its cofactors, as $s \to \infty$. The A_{ij} term varies as s^2 as $s \to \infty$, since the lag function becomes a constant for large s. Hence Δ varies as s^{2n}. Also, any cofactor of Δ, such as Δ_{ij}, varies as s^{2n-2}. Therefore, in the basic aeroelastic servo feedback system of figure 3.2, whose characteristic equation is equation 3.4, the order of the zero at infinity is 2 for the case G(s) equal to a constant. From the theory of part II, H(s) must be a first degree polynomial in s in equation 2.9, in order that the zero at infinity exist at π radians.

APPENDIX E

TECHNIQUES OF REDUCING THE LAG IN G(s)

The time delay in the control surface actuator or jet reaction actuator described in this study, was represented by G(s) in the basic block diagrams, figures 3.5 and 6.2, respectively. In subsequent analyses, these delays were considered small enough to be ignored. An extremely small effective delay can be produced in practice from two considerations.

a) The basic delay is itself small.

b) In addition, a feedback loop can be used around the actuator, such as the flap servo in figure 3.5, to compensate for the delay.

Relative to the first point, it is to be noted that the servo output is a torque, T_β or T_a, not a motion. Hence the time delay is primarily the delay associated with opening the valve, a very small delay. This is different than the usual servo actuator delay associated with the inertia of the output mass (here the control surface). In our problem this inertia is lumped with the aeroelastic matrix, and not with the G(s) operator. Typical delay times of milliseconds can be achieved.

Regarding the second point, this is a standard technique of reducing the delay of some element. It is not uncommon to achieve a reduction by a factor of 10 in delay time by such techniques.

From these two considerations, the effective delay time of the servo is made very small. In addition $H_a(s)$ is made a lead

network, as previously described, to further compensate for the lags in G(s). Thus the performance of the actual system is closely that predicted by the theory of parts IV, V and VI.